TU Delft Delft University of Technology

Potential of polymer sewage heat exchangers with enhanced thermal properties

Maneesh Avadhani

Potential of polymer sewage heat exchangers with enhanced thermal properties

by

Maneesh Avadhani

in partial fulfillment of the requirements for the degree of

Master of Science

in Mechanical Engineering

at the

Faculty of Mechanical, Maritime and Materials Engineering

Delft University of Technology

to be defended on Thursday, August 22, 2019 at 10 AM

Student number:	4744934	
Project duration :	December 2018 - August 2019	
Supervisor :	Dr. ir. C. A. Infante Ferreira,	TU Delft, P&E (ETh)
Thesis committee :	Prof. dr. ir. T.J.H. Vlugt,	TU Delft, P&E (Eth) : **Chair**
	Dr. ir. C. A. Infante Ferreira,	TU Delft, P&E (Eth)
	Dr. ir. I. W. M. Pothof,	TU Delft, P&E (ET)
	Ir. R. T. A. van Rooyen,	Gemeente Rotterdam (Guest Expert)

TU Delft Delft University of Technology

Gemeente Rotterdam

Abstract

Buildings contribute to 30% of global CO_2 emissions and consume 40% of the global energy supply (Yang et al., 2014). Heating and cooling requirements of the buildings form the major part of the energy consumption in buildings (Culha et al., 2015). Thus to solve this problem, one of the solutions currently being looked at is to recover heat from the sewage. Cities have large sewage flows and in the winter the sewage is warmer than ambient and in the summer it is colder than the ambient, thus making it a good heat source and sink respectively. This work involves the integration of waste water heat exchanger with heat pump to form a Waste Water Source Heat Pump (WWSHP). This system was further integrated with Aquifer Thermal Energy Storage (ATES) system. The WWSHP system was modeled in Matlab and the aquifer was modeled in COMSOL. COMSOL Live-link Matlab feature was used to integrate the two models.

Polymers were chosen as heat exchanger material due to their low cost, low weight (lower CO_2 emissions during transportation), flexibility, non corrosive nature and low energy requirement in manufacturing (Hussain et al., 2017). Two systems were proposed to support the heating and cooling demands of the concert venue and convention centre of the Rotterdam, the 'Doelen'. The objective of this work was to illustrate the potential of polymer sewage heat exchangers. The first system was called the WWSHP system. In this system, heat was recovered from the sewage in the winter through polymer heat exchangers and was upgraded in a heat pump for use in the heating network of the 'Doelen'. The heat pump was a reversible one, thus, in the summer, heat was extracted from the cooling network of the 'Doelen' and rejected to the sewage through the same polymer heat exchangers. To obtain more heat in the winter, a second system was proposed. This system was called WWSHP + ATES system. In this system, heat was extracted from the sewage and an aquifer. This extracted heat was upgraded in a heat pump for supply to the 'Doelen'. In the summer, the heat extracted from the 'Doelen' along with the heat recovered from the sewage were used to refill the warm well of the aquifer to maintain thermal balance. The scope of the work also included optimizing the dimensions, material and cost of the waste water heat exchanger. In both the systems, the summer and the winter models were different, hence they were simulated separately.

The heat recovery model was built based on a sewage channel near the 'Doelen'. The sewage channel data and the sewage flow and temperature data were provided by the Gemeente of Rotterdam. The waste water heat exchanger was chosen to be a multi row tube polymer heat exchanger. Various polymer options were available, among which the option with the highest thermal conductivity, High Density Poly-ethylene (HDPE) was chosen. Among six combinations of standard HDPE tube lengths and diameters, tube length of 30 m and tube inner diameter of 29 mm were found to be the most optimum in terms of economics and heat recovery. Based on the optimized tube dimensions, heat delivered by the system to the 'Doelen' per unit cost was compared for different materials and the results confirmed that HDPE with a cost of 0.54 €/kg was the best choice. Thus, using the optimized combination of tube dimensions and HDPE as tube material, 374 MWh of heat was recovered from the sewage in the winter and 486 MWh of heat was supplied to the heating network of the 'Doelen' through the heat pump. In the summer, 23 MWh was removed from the 'Doelen' by the heat pump and 26 MWh was rejected to the sewage using the same HDPE heat exchangers. Among the different polymer and filler combinations, PE (Polyethylene) with 30% graphite filler was found to be the best choice. Using PE with 30% graphite resulted in 32% higher heat recovery from the sewage in the winter and 15% higher heat rejection to the sewage in the summer when compared to HDPE with no fillers. Thermal enhancement of polymer tubes, although increased the amount of heat exchanged with the sewage in the winter and the summer, it reduced the system economic performance (kWh/€) in the winter.

The WWSHP + ATES system supplied 1244 MWh of heat to the 'Doelen' in the winter and removed 388 MWh of heat from the 'Doelen' in summer. Furthermore, thermal enhancement of polymers of the waste water heat exchangers reduced the performance (kWh/€) of the WWSHP+ATES system in both the summer and the winter. WWSHP + ATES system proved to be capable of handling higher heating and cooling demand than the WWSHP system. The costs of heat exchangers and electricity were also much higher for this option, thus making it less economical. For instance, the WWSHP model supplied 66 kWh to the 'Doelen' per € spent, as opposed to the WWSHP + ATES system which supplied only 34 kWh/€. Thus, only high heating and cooling requirements would justify the use of WWSHP + ATES system.

Acknowledgements

First of all, I would like to thank Dr. Carlos Infante Ferreira for providing me the opportunity to work on this thesis. I am grateful for his continuous support and guidance throughout this thesis. His inputs were invaluable for my work. I truly enjoyed working with him.

I would like to thank the Gemeente of Rotterdam, especially Mr. Roland van Rooyen & Mr. Jason Zondag for providing all the necessary data. Your interest in making Rotterdam more sustainable is truly commendable.

I would like to thank my parents for always believing in me and supporting me. I would like to also thank my friends Anmol, Palash, Nihal, Chinmay for making my stay at home fun and relaxing which helped me to focus on my work better. Special thanks to Vadiraj Patil and Karthick Sriram for helping me make my report better.

Last but not the least, I would like to thank all my friends at crows nest for providing me company during lunch and coffee breaks. Time flew by much faster because of you guys.

Maneesh Avadhani
12th August, 2019

Contents

List of abbreviations

AlN	: Aluminium Nitride
ATES	: Aquifer Thermal Energy Storage
COD	: Chemical Oxygen Demand
COP	: Coefficient of Performance
GWP	: Global Warming Potential
HDPE	: High Density Polyethylene
HEX	: Heat Exchanger
LDPE	: Low Density Polyethylene
LHS	: Left Hand Side
MEG	: Mono-Ethylene Glycol
NA	: Not available
PC	: Polycarbonate
PE	: Polyethylene
PEEK	: Polyether Ether Ketone
PP	: Polypropylene
PPS	: Polyphenylene Sulphide
PS	: Polystyrene
PVDF	: Polyvinylidene Fluoride
RHS	: Right Hand Side
SHB	: Spherical Hexagonal Boron
UTES	: Underground Thermal Energy Storage
YTS	: Yield Tensile Strength
WW	: Waste Water
WWSHP	: Waste Water Source Heat Pump
WWTP	: Waste Water Treatment Plant

List of symbols

A	: Area, m^2
b	: Thickness of aquifer, m
B	: Transmissivity, m^2/s
c	: Specific heat capacity, J/kg K

$Cost$: Cost, €

d : Diameter

f : Friction factor

F : Function

g : Acceleration due to gravity, m/s^2

h : Enthalpy, J/kg K

H : Hydraulic head, m

k : Thermal conductivity, W/m K

k' : Permeability, m^2

K : Hydraulic conductivity, m/s

l : Length, m

L : Cost constant

lev : Level, m

$LMTD$: Logarithmic Mean Temperature Difference, K

$\dot{m}$: Mass flow rate, kg/s

M : Cost constant

n : Cost exponent

N : Number (quantity)

Nu : Nusselt number

p : Pressure, bar/Pa

P : Perimeter, m

Q : Heat, J

$\dot{Q}$: Heat flow, W

r : Radius, radial ordinate m

$rate$: Cost per kg, €/kg

Re : Reynolds number

Pr : Prandtl number

s : Entropy, J/kg K

S : Source term (flow or heat), kg/(m^3.s) / J/(kg.s)

t : Time, s

thk : Thickness, mm

T : Temperature, °C or K

U : Overall heat transfer coefficient, W/m^2 K

v : Velocity, m/s

V : Volume , m^3

$\dot{V}$: Volumetric flow rate, m^3/s

w : Pitch, mm

W : Work, J

$\dot{W}$: Power, W

$Weight$: Weight, kg

x : Freezing temperature, °C

X : Sizing factor for cost calculation

y : Secondary water temperature, °C

z : Vertical ordinate (cylindrical), m

List of Greek symbols

α : Convective heat transfer coefficient, W/m^{2}K

Δ : Difference

μ : Dynamic viscosity, Pa s

ϕ : Aquifer porosity, filler volume fraction in polymer composites

φ : Angular ordinate (cylindrical), radian

η : Efficiency

ρ : Density, kg/m^3

σ : Allowable stress, Pa

List of subscripts

act : Actual

aq : Aquifer

c : Cross sectional

ch : Sewage channel

cl : Clay

comp : Compressor

cond : Condenser

darcy : Darcy

dyn : Dynamic

elb : Elbows

elec : Electrical

eq : Equivalent

evap : Evaporator

ext : Extraction

f : Flow

foul : Fouling

gw : Ground water

h : Heat

hd : Header

hex : Heat exchanger

hyd : Hydraulic

i : Inner

in : inlet

ini : initial

inj : Injection

is : Isentropic

m : Mean

max : Maximum

o : Aquifer reference point / initial/ outer

out : Outlet

p : at constant pressure

poly : Poly

pump : Pump

r : Radial

ref : Refrigerant

s : Surface of single tube

sand : Aquifer sand

sat : Saturated

sub : Submerged

sw : Secondary water

t : Tube

th : Thermal

tot : Total

v : Voids in aquifer

w : Water

ww : Waste water

1 Introduction

Buildings consume about 40 % of the total global energy and contribute to over 30 % of the CO_2 emissions (Yang et al., 2014). Space heating and cooling and domestic hot water supply form the largest part of the energy consumed in residential buildings (Culha et al., 2015). Use of fossil fuels to cope with heating and air-conditioning demands of buildings will lead to a series of critical problems such as pollution, climate change and energy shortage (Liu et al., 2013). Thus, it is vital to develop sustainable technology that would assist in reducing this energy consumption.

One of the major research avenues considered for reducing energy consumption in buildings is heat recovery from waste water. According to Swiss researches more than 15 % of the thermal energy supplied to buildings is lost through the sewer system. Thus, heat recovery from sewage has immense potential in reducing the energy consumption in buildings. Waste heat recovery from waste water plays an important role in conservation of energy and protection of environment (Hepbasli et al., 2014).

Use of heat pumps for the heating and cooling system of buildings is a well known technology. Heat pumps have been widely used in developed countries for years due to their higher energy utilization efficiencies (Hepbasli et al., 2014). Based on the type of heat source, heat pumps can be classified as air source, water source and ground source. Heat from these relatively low temperature sources is recovered and upgraded in the heat pump for use in heating and cooling system of buildings.

Waste water is used as a renewable energy source for heat pumps. Water that has been affected in quality due to anthropogenic influence is called waste water. Waste water provides concentrated source of energy due to its high heat capacity and density. The characteristics of waste water that make it very suitable for use in heat pump systems are (i) large amount of sewage produced in cities every year. To get a sense of magnitude, about 1928 Mm^3 of waste water was produced in 2008 according to Dutch communal water sector data (Frijns et al., 2013). For a 4 K ΔT, this flow represents energy of about 32 PJ. (ii) temperature of sewage is lower than ambient in the summer and higher than ambient in the winter. The variation in sewage temperature across a season is minimal (iii) large heat content (Hepbasli et al., 2014).

Germany, Switzerland and other Scandinavian countries have been utilizing the heat from waste water in heat pumps since the 1980s. Currently about 500 Waste Water Source Heat Pumps (WWSHP) are estimated to be in operation with thermal rating in the range of 10 - 20,000 kW. Studies suggest that about 3% of the buildings in Switzerland and Germany could be supplied with heat recovered from waste water (Hepbasli et al., 2014). Installation of waste water source heat pump systems can be either in the sewer system or after the waste water treatment plant. Although recovering heat after waste water treatment plant would eliminate the risk of bio-film growth in the heat exchanger, the maximal temperature of waste water is usually at the initial stages of the sewer system. Moreover, heat recovery location in the sewer is closer to the consumers than waste water treatment plants (Wanner et al., 2005).

A waste water source heat pump consists of three components (i) Waste Water Heat Exchanger - Heat is recovered from waste water in this part (ii) Heat pump - The heat recovered is upgraded to be used in the heating system of buildings (iii) Distribution system of heating and cooling in buildings.

During the heating period, heat is recovered from waste water through evaporator and supplied to the building through the condenser of the heat pump. During the cooling period the heat pump can be reversed and heat removed from the building can be rejected to waste water (Hepbasli et al., 2014).

A special consideration is needed for the choice of material during the design of waste water heat exchangers, as one of the working fluids is waste water. Waste water can lead to the fouling of the waste water heat exchanger. Fouling occurs when fluid degrades near heat transfer surface or solids deposit on surface and sometimes, microorganisms create bio-film matrices on heat exchange surface which will result in reduced heat transfer performance of the heat exchanger (Culha et al., 2015). In the work of Liu et al. (2013), it was found that the convective heat transfer resistance and fouling resistance on the sewage side of the waste water heat exchanger accounted for 80% of the total thermal resistance.

In order to reduce the net energy demand of buildings, using ATES system with heat pump is a good option. A 20 to 40% reduction in energy required for cooling and heating of buildings has been observed due to the

use of Aquifer Thermal Energy Storage (ATES) system. In the ATES system, the energy in the underground water is utilized to exchange heat or cold with the buildings. Temperature of the ATES system changes all through the year based on amount of removal or addition of heat or cold and heat loss to surroundings (Bozkaya et al., 2017). Thus, it is important to have a well defined dynamic model to simulate the ATES system behaviour.

In this project, sustainable and economic system design is looked at to recover waste heat from sewage for heating/cooling of buildings to reduce their carbon footprint. The ”Doelen” case in Rotterdam is considered to illustrate the benefits of heat recovery in terms of renewable energy, economics and sustainability of installed sewers. The Doelen is a concert venue and convention centre in Rotterdam, Netherlands. The heat recovered from sewage will partially cater to the heating requirements of ’Doelen’. Utilization of energy in the ATES to reduce the heating and cooling load of the building is also evaluated in this project.

Furthermore, polymer sewage heat exchangers are considered over metallic ones for heat recovery due to their advantages such as low cost, lesser weight, lower fouling and corrosion resistances. It is estimated that the energy required to produce unit mass of polymers is two times lower than common metals, which makes polymer heat exchangers more environmentally friendly (Chen et al., 2016).

1.1 Problem statement

The objective of the project was to develop technology that would provide a strong basis for scaling up of sewage waste heat recovery systems for large urban areas. The scope of the project includes designing, modeling and validation of the most suitable polymer heat exchangers for heat recovery from sewage systems. The design of the waste heat recovery system was based on the following considerations,

- Reduce the energy consumption of heating and cooling systems of buildings by utilizing the waste heat recovered from sewage flows
- Adaptability of system and heat exchanger designs to sewage conditions
- Ensure economic feasibility of waste water heat exchangers

1.2 Deliverables

The following deliverables were expected as the outcome of the project

- A Matlab model for the optimization of polymer heat exchangers for implementation in the sewage pipes around ”Doelen” and integration with heating and cooling systems of the building.
- Model for integration of ATES with the heat pump system

1.3 Methodology

To achieve the aforementioned objectives, the following methodology (Figure 1) was followed.

- **Literature Study**

  The focus of literature review was to acquire all relevant data required to develop a waste water heat recovery model and an aquifer model. The expected outcomes from this stage of the research were, location of heat recovery, type of waste water source heat pump system to be used, choice of polymer for waste water heat exchanger and published data on ATES models required for validation.

- **Modeling**

  Based on the outcomes of the literature review, a Matlab model was developed to simulate waste water source heat pump system, consisting of a polymer heat exchanger model and heat pump model. An ATES model was developed in COMSOL Multiphysics and was then integrated with the waste water source heat pump model using COMSOL Livelink Matlab feature. Summer and winter situations were modeled separately.

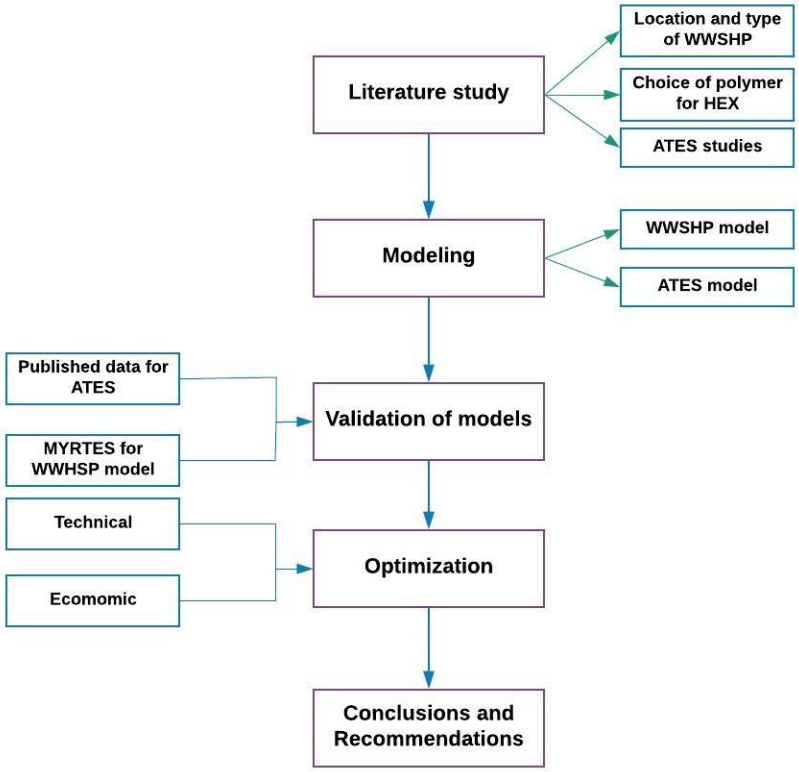

Figure 1: Research Methodology

- **Validation of Models**

  The waste water source heat pump system built for the Myrtes project was used as a reference to validate the waste water source heat pump model. Published data on ATES system was used as reference for the validation of the ATES temperature profile obtained.

- **Optimization**

  The waste water heat exchanger model was optimized with respect to material and cost. The choice of heat recovery system was optimized by comparing the economic performance of different heat recovery options.

- **Conclusions and Recommendations**

  Based on the results of the study, conclusions were obtained about the different heat recovery systems. Recommendations were provided for future research in similar domains.

1.4 Literature Study

The objective of this project was to develop a Matlab model to simulate the heat recovery from sewage through a waste water source heat pump system. With this in mind, a review of relevant published literature was done to obtain a thorough overview of different aspects of the waste water source heat pump systems.

First, the potential of heat recovery from waste water was looked at to obtain an estimate of the scale of recoverable energy. Next step was to ascertain the location of heat recovery from the sewage network. Then based on the choice of location of the system, relevant waste water source heat pump systems were reviewed. This was followed by an overview of types of waste water heat exchangers, comparison of polymers and metals for heat exchanger material and a comparison of different polymers. One of the objectives of the project was also to integrate ATES system with the waste water source heat pump system, thus relevant data necessary to model and validate the behaviour of ATES system was reviewed. The expected outcomes of literature review were choice of waste water source heat pump system, waste water heat exchanger and its materials and published data to model the ATES system.

1.4.1 Sewage heat recovery potential

- **Waste water heat recovery potential in Netherlands**

  Total water consumption and the corresponding sewage flow data were obtained from literature to get an estimate of the heat recovery potential. The water cycle of Amsterdam is described to elucidate the different components of a city's water cycle and understand which components might have a greater impact on sewage temperature.

  Netherlands, with a population of 17 million has about 7 million households. It was estimated that about 70 % of the total drinking water produced is used for domestic purposes (Hofman et al., 2011). In the year 2007, the Dutch households consumed 789 million m^3 of water while the industries consumed 300 million m^3 of water. The total sewage flow in the Netherlands added up to 1,139 million m^3 in 2007, which was inclusive of industrial water, storm water and groundwater infiltration in addition to domestic water. While, in 2008, the total sewage flow in the Netherlands increased to 1928 million m^3 (Frijns et al., 2013).

  To provide a perspective of water utilization of a single city, the water cycle flow estimates of Amsterdam are provided. Authors Van Der Hoek et al. (2016) in their work, estimated the total wastewater flow in Amsterdam in the year 2013 to be 74.9 million m^3/year. A breakdown of different components of the water cycle of Amsterdam and their respective flows is provided in Figure 2.

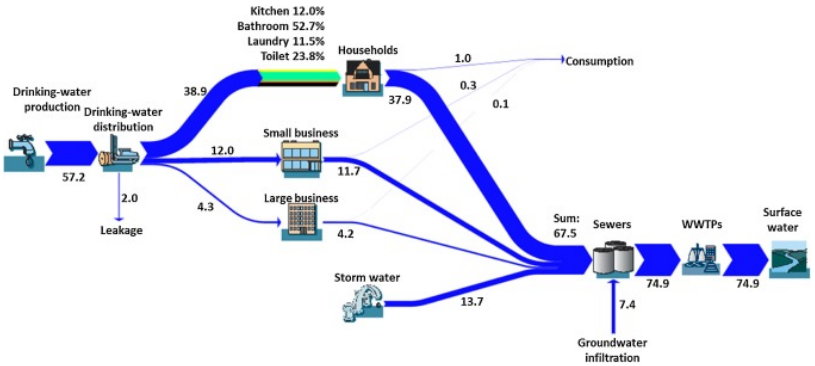

Figure 2: Amsterdam's water cycle in 2013 in million m^3 (Van Der Hoek et al., 2016)

As seen in Figure 2, domestic water usage represented 70 % of the total water demand. Thus a knowledge of the temperature of domestic sewage was considered important considering that it formed the majority of the sewage flow. Roest et al. (2010) in their study, found that drinking water from the household left at around 27 °C, water from bathing and showers left at a temperature of 38-40 °C. Tap water and water from the dish washer and washing machine had a temperature of approximately 40 °C. If this heat is not utilized then it would account for 40 % of the total energy losses in the modern Dutch houses (Hofman et al., 2011).

Roest et al. (2010) estimated that if every Dutch household had a shower heat exchanger a total of 15.9 PJ of primary energy could be recovered (in 2008). The temperature of the effluent (consisting of all sewage flows) leaving the WWTP was found to be roughly 15 °C, which would represent a large quantum of energy due to huge mass flow of sewage. A 5 K ΔT from 15 °C to 10 °C and annual sewage flow of 1,928 million m^3 (in 2008), contained about 40.4 PJ primary energy, which could provide each Dutch resident with approximately 2.35 GJ of energy per year.

Frijns et al. (2013) presented an energy input and heat recovery potential schematic for the Dutch water cycle, as shown in Figure 3. They predicted a potential heat recovery capacity of 56 PJ/ year.

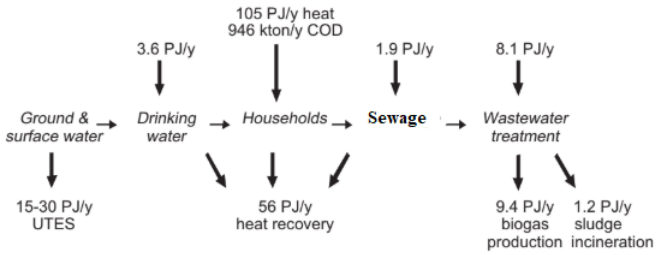

Figure 3: Energy input and output potential of Dutch water cycle (Frijns et al., 2013)

In the year 2006, the total heat demand in the Netherlands was 1093 PJ. Out of the total heat demand, 280 PJ and 206 PJ were the heat demands of residential and non-residential buildings (Menkveld and Beurskens, 2009). Thus, recovering 40.4 PJ/year of heat from waste water would contribute to 19% (for COP = 4) of residential buildings heat demand.

Furthermore, it was important to know the typical waste water temperatures to assess the potential of waste water for heat recovery. Cipolla and Maglionico (2014) in their work studied the variability of flow rate and temperature in the sewer of Bologna, Italy. The results they obtained indicated that the waste water temperature varied between 11-16 °C in the winter, 14-18 °C in autumn and 18-22 °C in the summer. The sewage temperature was higher than ambient in the winter and lower than ambient in the summer, thus making it convenient for heat recovery and heat rejection respectively. Typically the waste water temperature variation was found to be between 2 to 3 °C. At night when the waste water flow rate was lower, the temperature of waste water was found to be 2-4 °C lower than during the day. Thus it was noted that the variation of waste water temperature in any given season was not drastic.

The authors also estimated the magnitude of recoverable heat based on waste water flow of 2 l/s (corresponding to 800-1000 inhabitants), ΔT of 6.9 K (waste water cooled from 14.9 °C to 8 °C) to be 58 kW.

1.4.2 Possible sewage heat recovery locations

Heat recovery from sewage can be done in three locations of the sewage network as explained by Culha et al. (2015). Heat can be recovered at the source of sewage (buildings), or in the sewage line or after the treatment of sewage. Each of these locations are further described below.

- **Domestic**

  Used water from appliances such as washer, dishwasher, sink, shower etc is used for heat recovery. The recovered heat is typically used to pre-heat the fresh water to be used as domestic hot water. Generally, gravity film, spiral helical, plate and shell and tube heat exchangers are used for this application. Average temperature of domestic sewage is around 27 °C and about 15.9 PJ/year can be recovered with the installation of shower heat exchangers in every Dutch household (Roest et al., 2010). According to Chapin et al. (1984), the major obstacle for implementation of domestic waste water heat recovery was the pre-existing infrastructure in buildings.

- **Sewage**

  In this case heat is recovered from the urban sewage network. The system operates fairly continuously due to large and continuous sewage flow. The sewage contains relatively high energy when compared to the domestic systems (but lower exergy).

- **After treatment**

  Waste water temperature affects the water treatment process. Nitrification, one of the steps of water treatment is a temperature dependent process. Growth of nitrifying bacteria is impeded at lower waste water temperatures (Wanner et al., 2005). Thus, to avoid problems related to water treatment, heat can also be recovered after water treatment plant. The only disadvantage is that the water treatment plants are located far away from the consumers, which leads to heat losses and requires more piping and power for pumping.

- Comparison of the different locations of heat recovery

  All the three locations of heat recovery were qualitatively compared as shown in Table 1.

Table 1: Advantages and disadvantages based on heat recovery location (Culha et al., 2015)

Location	Advantages	Disadvantages
Domestic	1. Relatively high water temperature 2. Short heat transport distance 3. Impact of rainwater is less 4. Can be used for domestic hot water	1. Time dependent outflow 2. Flow distorted by materials in WW 3. Decentralized and expensive
Sewage	1. Large WW flows 2. Relatively short heat transport route	1. Depends on sewage network 2. WW temperature change has impact on WW treatment
Treatment	1. No impact on WW treatment 2. Relatively large effluent flow 3. Purified WW, thus no fouling	1. WWTP are far away from consumers 2. Amount of heat recovered depends on the location of WWTP

Funamizu et al. (2001) described the implementation example of reuse of heat energy from waste water. The authors presented a flow diagram with material and heat flows as shown in Figure 4. The analysis was done for the water system of Sapparo, Japan. The supply temperature of raw water was 3 °C and tap water was 3.8 °C. After usage, the waste water temperature went up to 13.1 °C, which was the influent of WWTP. Post water treatment, the temperature of waste water further increased by 0.7 °C to 13.8 °C. Based on the flows and temperatures, the energy carried by influent waste water was estimated to be 670 MW while, the effluent had 700 MW of heat energy. Thus, the energy in the waste water effluent was only about 4.5 % higher than that of influent waste water .

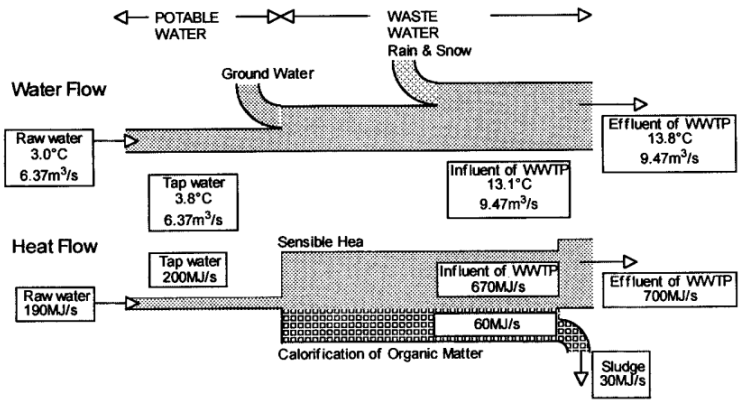

Figure 4: Comparison of energy flow before and after WWTP (Funamizu et al., 2001)

Looking at the pros and cons of each location, it was clear that recovering heat from sewage would be more advantageous since waste water flow is higher and continuous in comparison to the decentralized domestic sewage system. The problem with recovering heat after treatment is that the WWTPs are located far away from residential buildings, which necessitates additional investment on pipelines and insulation.

1.4.3 Overview of Waste Water Source Heat Pump Systems

- **Waste Water Source Heat Pump**

  Waste water source heat pump systems recover heat from the waste water and supply it to buildings to reduce heating demand. Although waste water temperature is higher than ambient temperature in the winter, it is not high enough for direct supply to the heating network of buildings. The residential heating systems require a temperature of about 55°C whereas the waste water temperature is about 10°C to 15°C in the winter. Thus, to improve the exergy of heat recovered from waste water, a heat pump system is used.

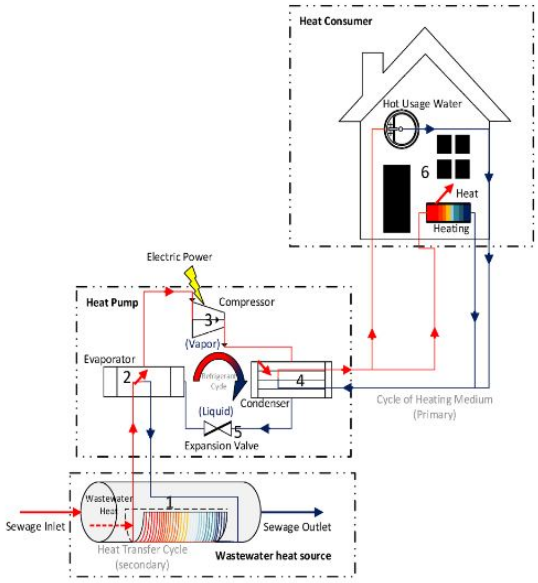

Figure 5: Schematic of WWSHP (Culha et al., 2015)

In the winter, waste heat is removed from the sewage flow and supplied to the buildings, while in the summer, waste water is used as a low temperature sink (Hepbasli et al., 2014). In the summer, the waste water temperature is lower than ambient and is about 18°C to 22 °C. Typically, the heat pump is operated in reverse mode in the summer to reject the heat from the buildings to the waste water. Figure 5 provides a schematic of the waste water source heat pump system. The waste water heat exchanger recovers heat from the sewage and transfers it to the secondary fluid (water-glycol mixture). The secondary fluid transfers heat to the refrigerant in the evaporator of the heat pump. The upgraded heat is rejected through the condenser of the heat pump system. In the condenser, the heat is transferred to water that is used for space heating in the buildings. Thus the waste water source heat pump has two systems coupled together. A waste water heat exchanger between sewage and secondary water and a heat pump that has a refrigerant as the working fluid.

- **Typical waste water source heat pump systems**

  Two typical waste water source heat pump systems are briefly described to provide an understanding of waste water source heat pump systems. The underlying principle of operation (indirect heat exchange) of both systems is the same. It can be seen from Figure 6 and Figure 7 that heat is recovered from waste water by a secondary flow. Heat from secondary flow is upgraded in the heat pump system and it is then supplied to the buildings.

  1. **Urban Sewage Source heat pump in Dalian China (2014)**

     The waste water source heat pump system as shown in Figure 6 was designed for partial heating supply of a residential building with 10,000 occupants in Dalian, China. The system was reversible and hence could be used for heating and cooling. Authors Liu et al. (2013), in their work analyzed test data obtained from the installation to evaluate the COP of the system.

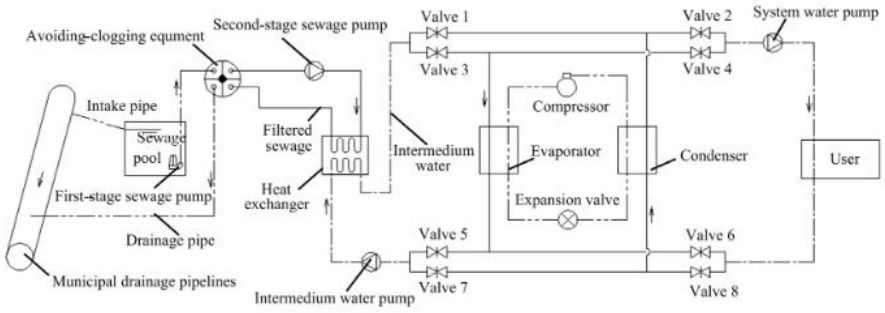

Figure 6: Schematic of the WWSHP system (Liu et al., 2013)

Points to note :

- Heat recovery was of the indirect type. It is clear from Figure 6 that waste water exchanged heat with secondary flow (intermediate water) in a heat exchanger, after which it was sent back to the municipal sewage pipelines.
- Three distinct systems can be found in Figure 6. First the waste water heat recovery section which included the sewage pool, avoid-clog equipment and a waste water heat exchanger. Second, the heat pump system and third the heating/cooling system of the buildings (user).
- Avoid clogging equipment was used for the defouling of the waste water so as to enhance the heat transfer performance of the heat exchanger. Defouling equipment has been described in detail in the section to follow.
- Shell and tube heat exchanger was the type of waste water heat exchanger used in this system.
- The system was found to have an overall COP of 3.6 for a building heat load of 700 kW.

2. **Myrtes in Brussels, Belgium**
   Spriet and Hendrick (2017) developed a simulation to evaluate the potential of heat recovery from waste water. They validated their model with the experimental results of an existing installation called Myrtes in Brussels, Belgium. The schematic of the system installed is as shown in Figure 7. Sewage heat exchanger was placed in the sewer while the heat pump was placed in a technical room. The recovered heat was used for heating of the conditioned space.

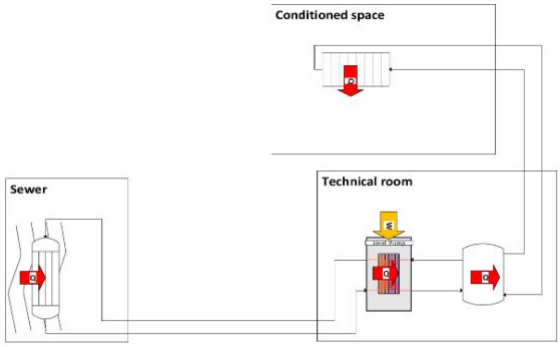

Figure 7: Myrtes Heat recovery system (Spriet and Hendrick, 2017)

– **Waste water heat exchanger**
  The waste water heat exchanger used in Myrtes was multi-row tube type. HDPE tubes were connected in series in multiple tube rows. The tubes were installed inside the sewage channel to recover heat from waste water as shown in Figure 8. Glycolated water (MEG 33 %) was used as the heat transfer medium inside the tubes to recover heat from waste water .

Figure 8: WWHEX in Myrtes facility (Spriet and Hendrick, 2017)

The specifications of the heat exchanger were as given in Table 2. The number of tubes submerged in sewage flow depended on the sewage level and that in turn affected the amount of heat recovered.

Table 2: Heat exchanger details (Spriet and Hendrick, 2017)

Parameter	Description
Type	Multi-pass
Material	HDPE
Length	6 m
Area	10.3 m^2
d_i	32 mm
d_o	36.3 mm
thk_t	2.1 mm
N_t	30

– **Experimental data and results**

Temperature and flow of sewage were measured at the site using probes. The measurements showed that the waste water temperature varied from 8 °C to 16 °C. Correspondingly, the flow of waste water was found to vary between 5 - 60 m^3/h. The heat recovered from sewage was found to vary between 2.5 to 5.5 kW. Using this heat, the heat pump delivered 3.2 to 7 kW to the building for heating. The measured COP varied between 3.7 to 5. The experimental data indicated that the maximum heat recovery occurred when the sewage flow was maximum and the sewage temperature was minimum. According to Spriet and Hendrick (2017), the likelihood of high sewage flow and high sewage temperature occurring at the same time is low and even if it occurred, the increase in sewage level might be due to rainfall which actually reduces the sewage temperature leading to lower heat recovery rate.

– **Heat recovery simulation model**

Spriet and Hendrick (2017), developed a simulation model based on the measured ambient and sewage temperature and sewage flow rate.

– **Results of the simulation**

* It was observed that a heating power of 6.3 kW was available in 99.3 % interval of the normally distributed resultant heating values.
* COP of 3.5 was obtained through the simulation which was lower than the COP obtained through experimentation (3.7 to 5).
* From the environmental model it was seen that the implementation of wastewater heat recovery system could reduce CO_2 emissions by 49 % over its lifetime of 20 years.

Thus, among the two waste water source heat pump systems described, the first one used a metallic shell and tube heat exchanger for heat recovery from waste water. The use of shell and tube was only possible if sewage was cleaned off of the fouling elements using a complex anti-clogging equipment. The anti-clogging system requires regular maintenance and adds to the overall cost of the system. Thus, considering the overall system complexity, space requirements and the cost of metallic heat exchangers, the system used in Myrtes was chosen in this work. The waste water heat exchanger was of the indirect type as in the case of all three systems. The experimental and simulation results of the Myrtes were used for the validation of the model developed in this work.

1.4.4 Waste Water Heat Exchangers

Heat exchangers used to extract the heat from waste water are called waste water heat exchangers. As described in the previous section, the multi-row tube type, indirect heat exchanger was chosen as the type of waste water heat exchanger. More details on the classification, terminologies, materials used are provided in this section.

- **Classification of waste water heat exchangers**

  In broader terms, waste water heat exchanger systems are divided as direct and indirect.

  - **Indirect (Waste water to water)** : In this group of waste water heat exchangers, heat from waste water is recovered by an intermediate fluid first and is then transferred to the refrigerant in the heat pump cycle. In this project, indirect heat exchange was chosen to reduce the problem of fouling and leakage of waste water into heat pump system.
  - **Direct (Waste water to refrigerant)** : In this group of waste water heat exchangers, heat from waste water is directly recovered by refrigerant in the heat pump cycle. These type of heat exchangers typically require equipment that prevent clogging in the heat exchanger.

  Furthermore, sewage heat exchangers are classified based on their construction as described by Culha et al. (2015). The three prominent types are external, integrated and modular.

  - **External** - In this type, the waste water heat exchangers are installed outside the sewage channels. Bypass piping system is used to transfer heat to fresh water. These HEXs prevent biofouling and increase heat transfer efficiency from waste water to fresh water.
  - **Modular** - These waste water heat exchangers are designed specifically according to the channel size and geometry and can be installed inside the channels. Heat transfer surface and position, length and diameter of tubes mainly depend upon the sewage flow rate.

    The waste water heat exchanger designed in this work was of the modular type since it was designed specifically for the 'Doelen' sewage channel.

- **Comparison of metal and polymer heat exchangers**

  The following aspects were considered for the choice of polymer as the material for heat exchanger over metals (Chen et al., 2016).

  - Although the thermal conductivity of metals is around a hundred times more than that of polymers, the alloys used for heat exchangers with corrosive fluids (ex. - Cu-Ni) have lesser thermal conductivity values in the range of 17-50 W/m K. Generally, polymers without any fillers have thermal conductivity values lesser than 1 W/m K but, making use of fillers, the thermal conductivity of polymers can be enhanced many folds based on the type of polymers and fillers used.
  - For the same heat transfer rate, it was found that a heat exchanger made of PVDF would cost 2.5 times less than that of Ni-Cr-Mo alloy. The cost benefit of polymer heat exchangers is very evident when the comparison is made between polymers and expensive corrosion resistant metal alloys. Thus, reducing the thickness of the polymer heat transfer surfaces and increasing surface area can increase the heat transfer performance of polymers significantly.
  - When yield strengths of polymers were compared with that of corrosion resistant alloys, it was found that the maximum yield strength of 99 MPa was for PEEK which was low when compared to 517 MPa for titanium and 140 MPa for Cu-Ni alloy. This would mean that the minimum wall thickness achievable for polymer heat exchangers would be limited due to low yield strengths.
  - Although metals have very high melting points ($>$1000 °C) compared to polymers ($<$300 °C), it does not matter since the heat exchanger operating temperatures for waste water applications are generally much lower.
  - Polymers are easier to mould than metals and hence the energy required to mould polymers is much lower. Most polymers are recyclable and can be re-built into a different product. Because of the low weight of polymers, the emissions due to handling and transportation are lower than that of metals.

  Thus, due to low cost. ease of manufacturing, lower weight and hence lower emissions, polymers were chosen as waste water heat exchanger material over metals.

- **Polymer Heat Exchangers**

  Polymer heat exchangers hold several advantages over metals for use in heat exchangers as described in the previous section. Low cost, light weight , corrosion and fouling resistance are some of the important advantages of polymers over metals (Hussain et al., 2017). Although, a large difference can be observed in the thermal conductivity values of polymers and metals, the cost benefit of polymer heat exchanger is high when the comparison is made with corrosion resistant metal alloys.

  Commonly used polymers

  Polymers are large molecules that are made of repeating sub units. Polymers can be broadly classified into thermoplastics and thermosets. Thermoplastics soften when heated and become hard on cooling and this process can be repeated. Thermosets become soft on heating and can be molded into required forms, but the hardening is permanent. PC, LDPE, PP, PS, Ionomer etc all fall under thermoplastics category. Epoxy, phenolic resins and polyester resins are of the thermosets type. Table 33 of Appendix B summarizes the mechanical and thermal properties of commonly used polymers.

  Polymer matrix composite materials

  Thermal conductivity values of polymers vary between 0.11 - 0.46 W/m K (Table 33), whereas, for metals such as aluminum or copper it varies between 200 - 400 W/m K. To enhance the thermal conductivity of composites, polymer matrix composites are formed. A composite is made of a constituent that is continuous and often in large quantity called matrix and filler that is used to improve certain properties of the polymer.

  The fillers used in polymer composites are particles, fibers, flakes and laminas. Figure 9 illustrates the different types of fillers used in composites. In particulate composites the particles within the matrix are either randomly dispersed or arranged in parallel like flakes. Fibers are either long or short. Laminate composites have different layers of fiber orientation. Thus, particulate composites are isotropic while laminate composites are anisotropic. In this work, particulate composites were considered to study the effect of thermal conductivity enhancement of polymers on the heat transfer performance of the waste water heat exchanger.

  Chen et al. (2016) have provided a list of some composites with their matrix material, filler material, filler volume and the resultant thermal conductivity values. Those values are tabulated in Table 3 and were used to study the effect of enhancement of thermal conductivity of polymers in this work.

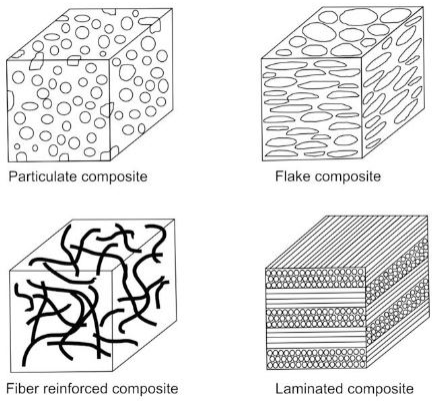

Figure 9: Types of fillers used in composites (T'Joen et al., 2009)

Table 3: 'k' values of thermally enhanced polymers Chen et al. (2016)

Matrix	Filler	Filler (%)	k_t (W/m K)
PE	Graphite	10	0.65
		30	1.8
PS	Graphite	10	0.25
		30	0.9
PPS	Spherical hexagonal Boron	10	1.83
		30	1.89
LDPE	AlN	30	1.08

- **Ranking of polymers based on thermal conductivity**

  Different polymers were compared based on the values of three of the most important features : thermal conductivity, yield strength and cost. Polymers were ranked on the basis of decreasing order of thermal conductivity (top five). PP with the lowest k value was also compared, to understand why it is commonly used in heat exchangers. The comparison is presented in Table 4.

Table 4: Ranking of polymers based on k_t values

Rank	k_t(W/m K)	YTS (MPa)	Cost (€/kg)
1 - HDPE	0.46	25.9	0.54
2 - LDPE	0.30	10.8	0.57
2 - PPS	0.30	68.9	1.10
3 - PC	0.20	62.0	1.10
4 - PS	0.14	43.9	0.90

Note : The cost of polymers mentioned in Table 4 are the cost of polymer as raw materials and not polymer tubes. Cost of polymers were chosen from [1].

The advantage of having high yield strength is that the thickness required to withstand pressure can be low. Low thickness leads to higher U_o values. When compared to metals, the benefit of low cost of polymers far outweighs that of high thermal conductivity of metals. Among the remaining options, HDPE had the highest k value with a relatively high yield strength. HDPE was shortlisted as one of the materials for heat exchangers. Choice of HDPE also ensured similarity in comparison with Myrtes model.

1.4.5 Studies on ATES modeling

- **Fundamentals of ATES**

  Aquifers contain water in underground porous formations. If an aquifer is located in between two impermeable layers of cap rock and bed rock (or clay) then the aquifer is a confined aquifer (Ghaebi et al., 2014). Aquifers used for storage and retrieval of thermal energy are called Aquifer Thermal Energy Storage (ATES) systems. Thermal energy recovery and storage is done by extraction and injection of ground water respectively from the aquifers. Figure 10 illustrates the cyclic operation of an ATES system. During summer, water is extracted from the cold well, and is then used as a sink to remove heat from buildings and is then injected back into the hot well. During the winter, water flow is opposite to that of summer and groundwater acts as a heat source.

[1] New Media Publisher

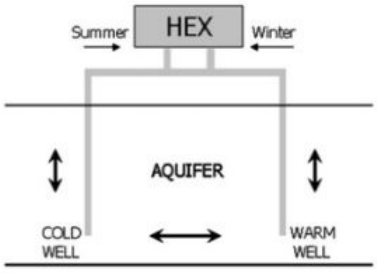

Figure 10: General operation of ATES system (Kim et al., 2010)

- **Modeling of the ATES system**

  Bozkaya et al. (2017), in their work developed a building integrated ATES model which was validated using data from a building integrated ATES in Amsterdam, Netherlands. Bozkaya et al. (2017) linked Matlab with COMSOL Multiphysics to model the ATES system. The results of their model were compared with the results of the model developed in this work for validation. The approach to modeling considered by the authors is described in this section.

  To model flow and heat transfer phenomena in aquifers in COMSOL Multiphysics, the authors coupled the physics of heat transfer through porous media with Darcy's flow. The sandy aquifer layer was modeled as a porous medium with a defined porosity, while the upper and lower impermeable clay layers were modeled as solids with no groundwater flow through them. The behaviour of hot well and cold well was studied in two separate models. The aquifer models were simulated as 2D axi-symmetric models as with injection/extraction on one side. The computational domain used by the authors is as shown in Figure 11. Finite element method was used with quadratic meshing to model the ATES system. The simulation time step chosen was 1 hour. The following assumptions were made to develop the ATES model :

  1. The aquifer is homogeneous and isotropic. Thus the flow of water is uniform in all dimensions.
  2. Since the ATES is confined, there is no vertical flow of water. Water flows only radially.
  3. As there is no vertical flow of water, there is no thermal interaction of wells.
  4. Ground water flow in the Netherlands is negligible (few meters / year). Thus model was simplified into a 2D axis-symmetrical one.
  5. Dispersion and buoyancy effects were neglected.

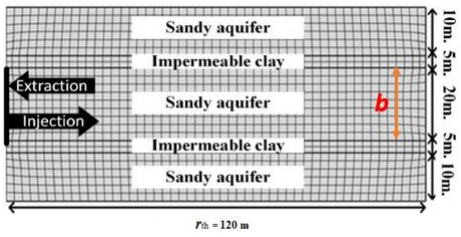

Figure 11: 2D axis-symmetrical computational domain of ATES (Bozkaya et al., 2017)

COMSOL makes use of the following equations to model heat transfer and flow through porous media and heat transfer through solids.

1. **Flow through porous media - Darcy's equation**

   - **Porosity of aquifer, ϕ**

     It is the ratio of volume of voids (V_{v}) to the total volume (V_{aq}). For a saturated aquifer, volume of voids would be equal to volume of water. Aquifer porosity generally lies between 10 % - 45 % (Bozkaya et al., 2017).

     $$\phi = \frac{V_{\mathrm{v}}}{V_{\mathrm{aq}}} \tag{1}$$

   - **Density of an aquifer, ρ_{aq}**

     Based on the definition of porosity, the following expression is used to evaluate the density of an aquifer,

     $$\rho_{\mathrm{aq}} = \rho_{\mathrm{w}} \ \phi + \rho_{\mathrm{sand}} \ (1 - \phi) \tag{2}$$

   - **Darcy's flow equation for flow through an aquifer**

     $$\vec{v} = \frac{-k'}{\mu_{\mathrm{w}}} \ \vec{\nabla} p \tag{3}$$

     where, k' is the permeability of aquifer, μ is the dynamic viscosity of water, $\vec{\nabla} p$ is the pressure gradient in the aquifer. Hydraulic conductivity (K) and permeability (k') are related as follows

     $$K = \frac{k' \ \rho_{\mathrm{w}} \ g}{\mu_{\mathrm{w}}} \tag{4}$$

     Thus Equation 3 can be re-written as

     $$\vec{v} = -K \ \vec{\nabla} H \tag{5}$$

     where, $\vec{\nabla} H$ is the hydraulic head difference between the point of injection/extraction and any point considered. Assuming that the flow pattern is symmetrical in $\vec{z}$ and that there is no variation in flow in $\vec{\varphi}$

     $$\vec{v}_{\mathrm{r}} = -K \frac{\partial H}{\partial r} \tag{6}$$

   - **Equation of continuity in porous media**

     Differential form of continuity equation

     $$\left[\frac{\partial \rho}{\partial t} + \vec{\nabla} \cdot (\rho v)\right] = S_{\mathrm{f}} \tag{7}$$

     Continuity equation for flow in porous media

     $$\left[\frac{\partial (\rho_{\mathrm{aq}} \phi)}{\partial t} + \vec{\nabla} \cdot (\rho_{\mathrm{aq}} \vec{v})\right] \ dV = S_{\mathrm{f}} \tag{8}$$

     Since porosity and density of the aquifer are time independent, Equation 8 can be written as

     $$\left[- K \ \rho_{\mathrm{aq}} \ \nabla^2 H(r)\right] \ dV = S_{\mathrm{f}} \tag{9}$$

2. **Heat transfer in porous media**

The following equations are used by COMSOL to model heat transfer through porous media.

- **Heat capacity and thermal conductivity of porous media**

  * Specific heat capacity, c_{aq}

$$c_{\text{aq}} = c_{\text{p,w}}\ \phi + c_{\text{p,sand}}\ (1-\phi) \tag{10}$$

  * Thermal conductivity of aquifer, k_{aq}

$$k_{\text{aq}} = k_{\text{w}}\ \phi + k_{\text{sand}}\ (1-\phi) \tag{11}$$

- **Energy balance of the aquifer**

Heat in the aquifer is conducted through the porous media, carried away by water due to flow (convection) and is added or removed due to injection / extraction. Based on that, the following equation for variation of internal energy of aquifer was written as follows. COMSOL solves the heat equation for the variable T (aquifer temperature). First term on the RHS indicates the conduction of heat through the aquifer, the second term indicates the heat carried away by ground water flow and the last term is the heat source/sink term based on injection/extraction of ground water.

$$c_{\text{aq}}\frac{\partial T}{\partial t} = \nabla^2(k_{\text{aq}}T) - (\rho_{\text{w}}c_{\text{w}})\ \vec{v}\ .\ \vec{\nabla}T + S_{\text{h}} \tag{12}$$

- **Energy balance of the impermeable layers above and below the aquifer**

Since impermeable clay layers have very low porosity, it was assumed by Bozkaya et al. (2017) that conduction was the only heat transfer mode in those layers. Heat equation for clay layers can be written as follows,

$$\frac{\partial T}{\partial t} = \frac{k_{\text{cl}}}{(\rho_{\text{cl}} \times c_{p,\text{cl}})}\ \nabla^2 T \tag{13}$$

- **Radius of the aquifer**

Radius of the aquifer required is calculated keeping in mind that no thermal interaction should occur with the adjacent well. Bozkaya et al. (2017), calculated that a radius of 120 m was enough to prevent thermal interaction between the hot and cold wells based on the maximum injected volume of V_{w} = 176,000 m^3. The equation used to calculate the thermal radius of the aquifer (r_{th}) is as follows,

$$r_{\text{th}} = \sqrt{\frac{c_{\text{w}}\ V_{\text{w}}}{c_{\text{aq}}\ \pi\ b}} \tag{14}$$

Thus for modeling, at $r = r_{\text{th}}$, heat flux = 0.

- **Hydraulic head calculation**

The injection/extraction head of groundwater at the borehole was calculated based on Darcy's law. The head required at injection/extraction is a function of the ground water flow rate ($\dot{V}_{\text{w}}$).

During injection

$$H_{\text{inj}} = \frac{\dot{V}_{\text{w}}}{2\pi K b} \; log\frac{r}{r_{\text{o}}} \tag{15}$$

During extraction

$$H_{\text{ext}} = \frac{-\dot{V}_{\text{w}}}{2\pi K b} \; log\frac{r}{r_{\text{o}}} \tag{16}$$

Both the equations convert water flow rate of injection / extraction to hydraulic head at inlet. In the equations, r is the radial distance from the point of injection and r_{o} is the radius of the aquifer bore hole. The hydraulic head at the end of the well ($r = r_{\text{th}}$) was set to 0. Thus, the aquifer pump would have to also produce head to offset the Darcy pressure drop in the aquifer.

3. **Initial and Boundary conditions**

The following initial and boundary conditions were set by Bozkaya et al. (2017) to run the simulation. The conditions for the heat transfer through the porous media module and Darcy's flow module are described separately.

- **Heat transfer through porous media**

  The initial temperature (T_{o}) of the warm well and cold well were set as described in Table 5. The injection temperature of the ground water, T_{inj} or T_{ext} was set as the temperature at the edge of the borehole ($r = 0$). It was assumed that there was no heat transfer beyond the domain, thus at $r = r_{\text{th}}$, $\nabla^2(k_{\text{aq}}T) = 0$

- **Flow through porous media**

  As described before, at the active boundary ($r = r_{\text{o}}$), the head was calculated based on injection/extraction flow rate ($\dot{V}_{\text{w}}$). The head at the end of the domain $H_{\text{r=r}_{\text{th}}} = 0$.

- **Parameters of the model**

  The COMSOL model was run on the following parameters of the ATES model. The injection flow rates and temperatures were varied in the model by Bozkaya et al. (2017). But the validation case was developed for the parameters mentioned in Table 5.

Table 5: Input parameters for the COMSOL model

Parameter	Value	Unit
K	5×10^{-4}	m/s
k_{aq}	2.5	W/(m K)
ϕ	0.35	-
$c_{p,\text{aq}}$	1529	J/(kg K)
$c_{p,\text{cl}}$	1880	J/(kg
Warm well		
b	60	m
T_{ini}	12.5	°C
T_{inj}	16	°C
$\dot{V}_{\text{w}}$	40	m^3/h
Cold well		
b	20	m
T_{ini}	11.5	°C
T_{inj}	8	°C
$\dot{V}_{\text{w}}$	40	m^3/h

Note : The thickness of the warm well and cold well were chosen to be different to match the actual thickness data of the aquifer in Amsterdam based on which Bozkaya et al. (2017) validated their model.

4. **Results**

For the conditions mentioned in Table 5, the following results were obtained. Variation of the aquifer temperature due to injection of groundwater is depicted using temperature plots as shown in Figure 12 and Figure 13. These temperature plots were used as reference to validate the ATES model developed in this work. The warm well and cold well models were simulated for one season each to verify if the size of the aquifer was sufficient to prevent thermal interaction of the adjacent aquifers. It was concluded from the results that the aquifer radius of 120 m was good enough to make the 'no heat transfer beyond the domain' condition realistic.

– **Effect of groundwater injection on warm well temperature**
At the end of one season, injection of groundwater into the warm well at 16°C was found to have a noticeable thermal impact up to a distance of 60 m. The rest of the aquifer was found to be still at 12.5°C.

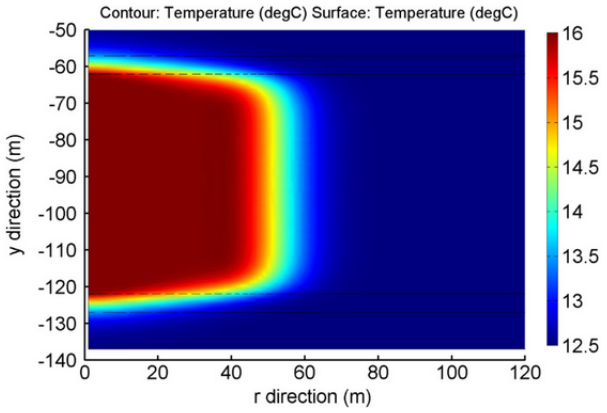

Figure 12: Warm well temperature profile after one injection season Bozkaya et al. (2017)

– **Effect of groundwater injection on cold well temperature**
Similar to the warm well, noticeable thermal impact on the cold well was observed up to a distance of 60 m. Up to a distance of 60 m the cold well temperature was found to be around 8°C, but the rest of the aquifer was found to be still at 11.5°C, the initial aquifer temperature.

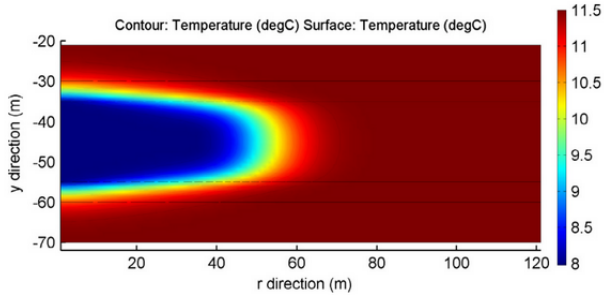

Figure 13: Cold well temperature profile after one injection season Bozkaya et al. (2017)

5. **Integrating Matlab with COMSOL**

Figure 14 illustrates the flowchart followed by Bozkaya et al. (2017) to integrate Matlab with COMSOL using the COMSOL Livelink Matlab feature. The initial conditions, flow rates and boundary conditions were set by the Matlab model and the results obtained were stored using Matlab as shown in figure. Based on the initial and boundary conditions, the aquifer model in COMSOL was solved using the subsurface flow and heat transfer in porous media modules. Similar approach was also followed in this work to integrate the WWSHP system with ATES system.

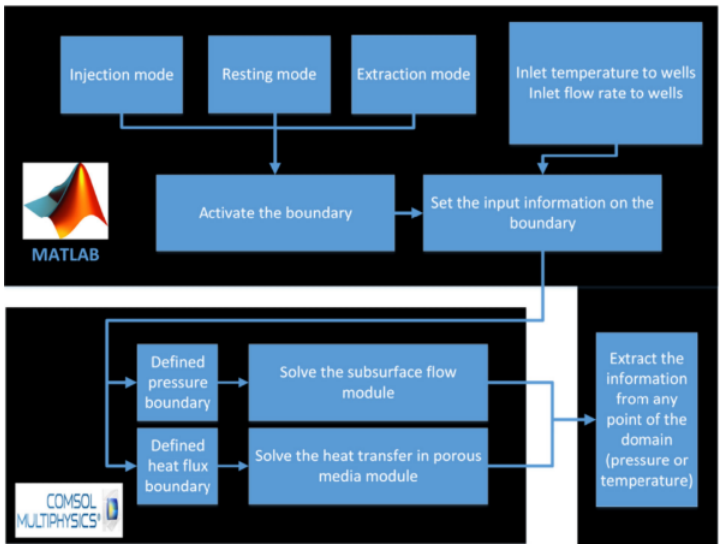

Figure 14: Matlab and COMSOL integration scheme used by Bozkaya et al. (2017)

2 Modeling

This section includes the modeling approaches of waste water source heat pump system, ATES system and their integration. Waste water source heat pump model was developed in Matlab and the ATES model was developed in COMSOL Multiphysics. To integrate waste water source heat pump model with the ATES model, COMSOL Livelink Matlab feature was used. Two systems of heat recovery were considered. One was to only make use of heat from sewage through a waste water source heat pump. Second was to integrate waste water source heat pump with ATES to recover more heat. For both of these options, summer and winter models were designed separately. Months of the year where 'Doelen' required heating were categorized as winter, whereas the rest of the months where cooling was required were considered to be summer. Winter models aimed at recovering heat from sewage, or both sewage and aquifer, to produce hot water for the heating system of 'Doelen'. Summer models aimed at removing heat from 'Doelen' to produce chilled water for its cooling network and at the same time replenish the extracted heat from the aquifer if it was used in the winter. Each of these systems are explained in detail in this section.

2.1 Input data

The model developed in this work was for a particular sewage channel in the center of Rotterdam. Thus, the data required for modeling of the sewage heat recovery system such as sewage temperature, sewage flow and sewage channel dimensions were provided by the Gemeente of Rotterdam.

2.1.1 Sewage Temperature

Sewage temperature values were obtained for the year 2018. Temperature values were available in intervals of 5 minutes for each day of the year 2018. Since the daily variation of sewage temperature was not significant, daily average was calculated for each day of the year and was considered to be the sewage temperature for that day. Figure 15 is a box plot of sewage temperature variation for the month of January. 288 temperature values measured at intervals of 5 minutes each, were available for each day of the month. Using these data a box plot was made for a whole month. It is clear from the box plot that 50% of the temperature values (in 2nd and 3rd quartile) for each day lie within a range of 2 K for most of the days. Thus, mean sewage temperatures were calculated for each day and have been indicated in the box plot.

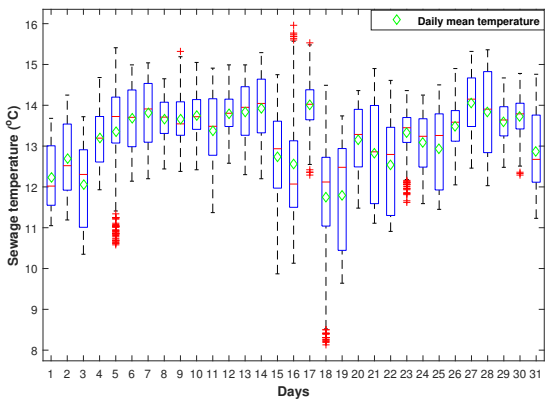

Figure 15: Box plot of sewage temperature for January, 2018

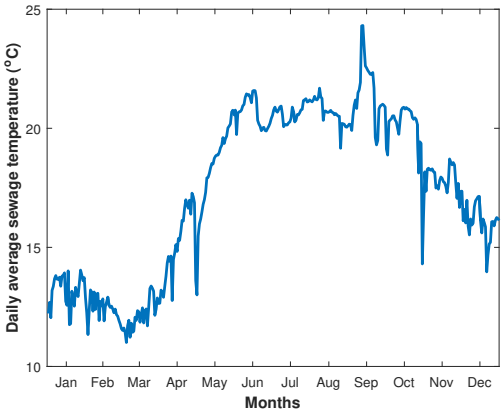

Figure 16: Variation of daily average sewage temperature

Variation of daily average sewage temperatures throughout the year is plotted in Figure 16. Sewage temperature was found to vary between a maximum of 24.3 °C to a minimum of 11 °C. It can be seen that sewage temperatures are higher in the summer (June, July and August) and lower in the winter.

2.1.2 Sewage flow

Sewage flow data of the year 2018 was obtained in the form of total sewage flow per day. Thus, daily average sewage flow was evaluated per second and that was considered to be the same flow throughout the day. The flow was found to vary between a maximum of 606.8 l/s to a minimum of 41.5 l/s. Figure 17 shows sewage flow variation in 2018.

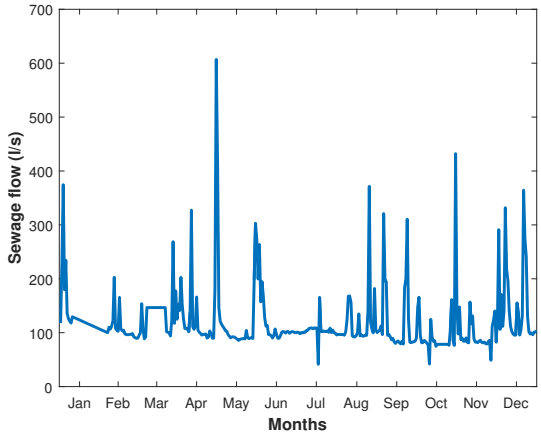

Figure 17: Variation of daily average sewage flow

2.1.3 Sewage channel dimensions

The dimensions of the sewage channel considered for the placement of waste water heat exchanger are as shown in Figure 18. This sewage channel is located close to the center of Rotterdam near the 'Doelen'. The sewage channel is approximately oval shaped with the flow passage area spanning 1.5 m in width and 1.44 m in height.

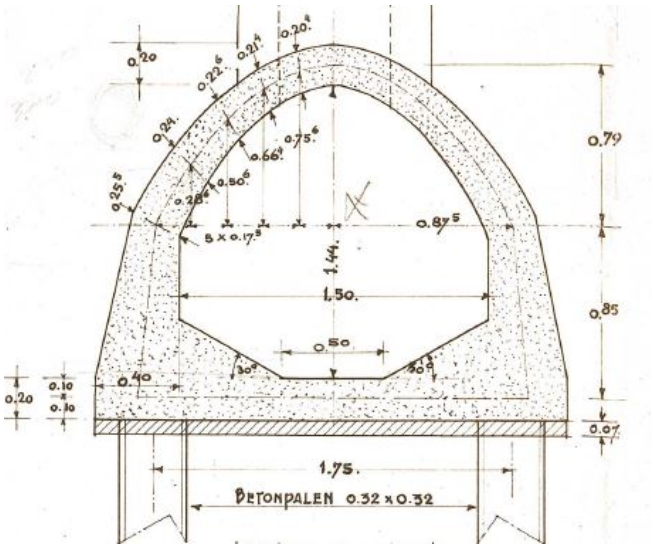

Figure 18: Sectional view of the sewage channel

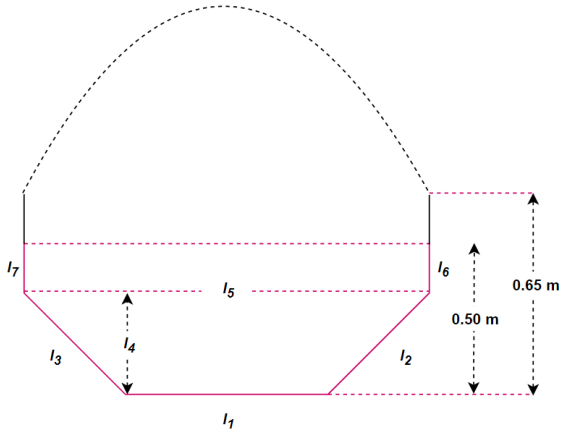

Figure 19: Channel sides for calculation

The sides of the inner profile of the sewage channel necessary for modeling are marked in Figure 19. Number of tubes of heat exchanger actually submerged in sewage flow, hydraulic diameter of the channel, flow

cross-sectional area, sewage flow velocity are all dependent on the sewage level. Thus, each of these parameters were dynamically evaluated for each sewage level. The angle between the horizontal and l_2 is 30°as seen in Figure 18. When the sewage level was higher than l_4, the flow area was divided into a trapezium with sides l_1, l_2, l_5, l_3 and a rectangle with area $l_5 \times l_6$. In that case, the length of the sides l_6/l_7 was calculated as the difference in sewage level and l_4. For sewage level lower than l_4, the flow area was just a trapezium and length of sides l_6/l_7 was 0. From a measurement done in 2018, it was seen that the highest sewage level was 0.5 m. Thus, the maximum possible value for $l_4 + l_6$ was considered to be 0.5 m. Calculation of sewage channel dimensions is described in detail in Appendix A. Dimensions of the sewage channel calculated for the sewage level of 0.5 m are provided in Table 6.

Table 6: Dimensions of sewage channel for sewage level = 0.5 m

Channel dimensions	
l_1	0.50 m
l_2	0.58 m
l_3	0.58 m
l_4	0.29 m
l_5	1.50 m
l_6	0.21 m
l_7	0.21 m
$P_{\text{tot,ch}}$	3.58 m
P_{ch}	2.08 m
$d_{\text{hyd,ch}}$	0.68 m
$r_{\text{hyd,ch}}$	0.17 m
$A_{\text{c,ch}}$	0.61 m^2

2.1.4 Sewage level and velocity

Sewage flow velocity and level were calculated based on flow data and channel dimensions. From the known data that the highest sewage level in 2018 was 0.5 m, sewage levels for all other flow rates were interpolated linearly with sewage flow. Since the interpolation is linear, the sewage level variation trend is exactly the same as that of the sewage flow and is as plotted in Figure 20. Equation 17 was used to calculate the sewage level for any given sewage flow rate,

$$lev_{\text{ww}} = \frac{0.5 \times \dot{V}_{\text{ww}}}{\dot{V}_{\text{ww,max}}} \tag{17}$$

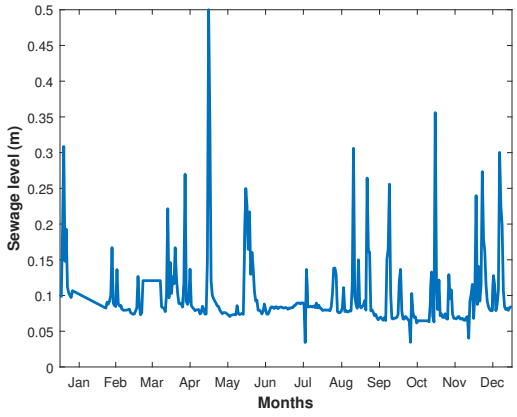

Figure 20: Variation of sewage level

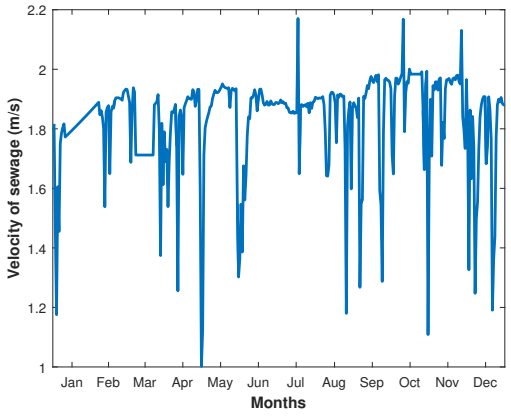

Figure 21: Variation of sewage velocity

Velocity of sewage flow was estimated from sewage flow rate, sewage level and the corresponding channel dimensions. Flow area is dependent on the sewage level and sewage level is dependent on flow. Figure 21 describes the variation of sewage velocity on different days of the year. It can be observed that on the day of the highest sewage level, flow velocity is the lowest. Sewage velocity was found to vary between a minimum of 1 m/s to a maximum of 2.17 m/s. The corresponding Re number was found to vary between 1.5 $\times 10^4$ to 7.6 $\times 10^4$. Thus, the flow was turbulent. Sewage velocity was estimated using Equation 18.

$$v_{\mathrm{ww}} = \frac{\dot{V}_{\mathrm{ww}}}{A_{\mathrm{c,ch}}} \tag{18}$$

2.2 WWSHP system

The waste water source heat pump systems used in this work are depicted in Figure 22 and Figure 23. Heat was recovered from sewage in the winter and heat was rejected to sewage in the summer. Thus, a reversible heat pump was used. Heat exchange with sewage was done with waste water heat exchangers. Four heat exchangers were placed in parallel inside the sewage channel as shown in the figures. Secondary water (mixture of water and glycol) was used as an intermediate fluid between the heat pump and the waste water heat exchanger. During the winter, secondary water transferred the heat recovered from the sewage to the refrigerant in the evaporator. The hot secondary water was cooled to a temperature 2 K higher than the evaporation temperature of the heat pump to prevent temperature cross-over. The heat required by 'Doelen' was supplied by the condenser. The condensation temperature was set at 55°C. The water used for heating in 'Doelen' was heated from 25°C to about 53°C in the condenser and then supplied to the heating network of 'Doelen'. In the summer, the heat pump was operated in reverse. Chilled water from the cooling network of 'Doelen' was cooled from 14°C to 10°C in the evaporator whose evaporation temperature was set as 8°C. The condensation temperature of the heat pump was varied such that the secondary water inlet temperature to the waste water heat exchanger was higher than the sewage temperature.

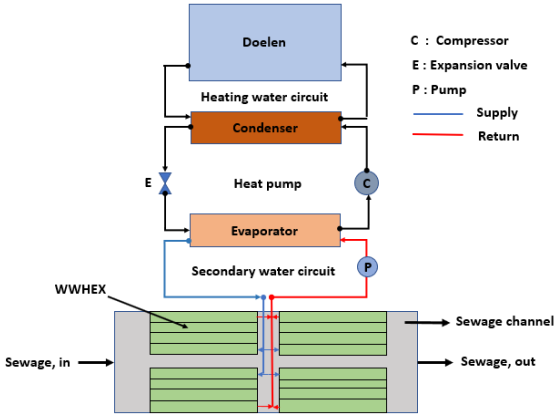

Figure 22: WWSHP : Winter model

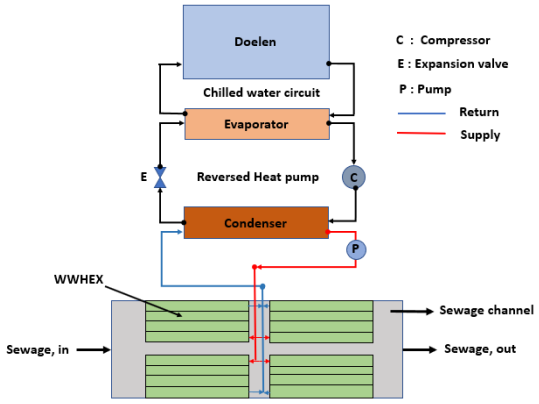

Figure 23: WWSHP : Summer model

Winter and summer situations were simulated separately due to their inherent differences in operation. A flowchart of the winter model is provided in Figure 24. For each combination of tube length and diameter of the waste water heat exchanger, the winter model was simulated on a daily basis for nine months of winter. Thus for each tube dimension combination, the winter model had an outer loop iterating over 9 months of winter. In the heat recovery system, sewage temperature and condensation temperature of the heat pump were the only known values while all other temperatures were unknown. Based on sewage temperature secondary water outlet temperature ($T_{\mathrm{sw,out}}$) was set. The secondary water inlet temperature ($T_{\mathrm{sw,in}}$) was varied from 0°C to a temperature 2 K lower than $T_{\mathrm{sw,out}}$. The evaporation temperature of the heat pump was set 2 K lower than $T_{\mathrm{sw,in}}$. For each of the 9 months, a primary inner loop was run for the number of days of that month while a secondary inner loop ran over all combinations of temperatures until the increase in

COP of the system was less than 5% (convergence criterion). Once the combination of temperatures with the optimized COP was found, the secondary inner loop was terminated and the calculations for the next day started. After the winter model was simulated for 9 months, the total heat recovered, heat supplied, pump and compressor power required were calculated and seasonal COP was calculated. After that, the same calculations were repeated for the next combination of tube dimensions. At the end, all the seasonal performance parameters were compared to find the most optimum heat exchanger tube dimensions.

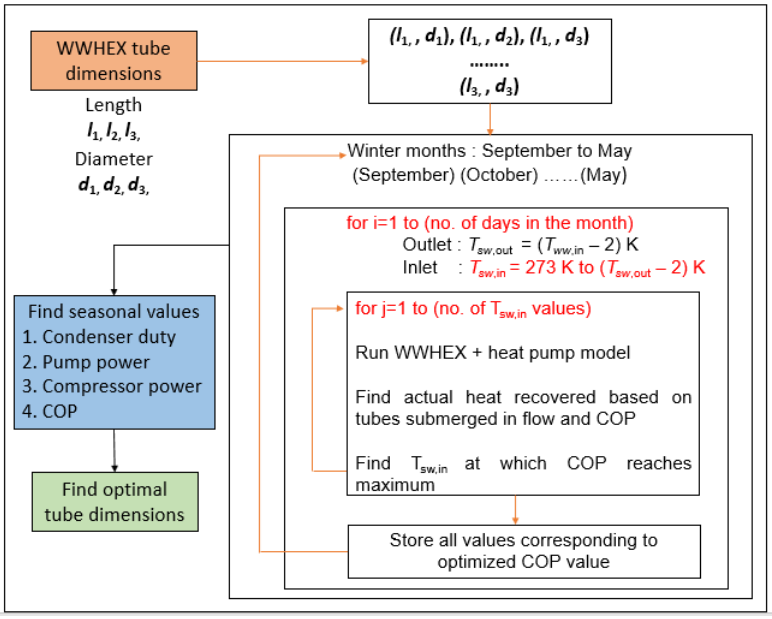

Figure 24: Winter : Flowchart of WWSHP model

The same set of optimized tube dimensions were used for the summer model since the waste water heat exchanger installation would still be the same in the summer. In the summer, the secondary water rejected heat to the sewage, thus its temperature was set higher than sewage temperature. The extent of increase in secondary water temperature ($T_{\text{sw,in}} + \Delta T$) at the inlet of waste water heat exchanger over $T_{\text{ww,in}}$ was varied from 10 K to 50 K to study the effect on system performance. Thus, the summer model was simulated for different secondary water inlet ($T_{\text{sw,in}}$) temperatures. For each $T_{\text{sw,in}} + \Delta T$, a primary inner loop iterated over all the months of the summer. A secondary inner loop iterated over all the days of the summer where the condensation temperature was set to be equal to $T_{\text{sw,in}}$ and the secondary water outlet temperature ($T_{\text{sw,out}}$) was set 1 K higher than the daily average sewage temperature. Similar to the winter model, all the seasonal values of the system performance indicators were calculated to find the most optimum value for $T_{\text{sw,in}}$.

2.2.1 Waste Water Heat Exchanger

The waste water heat exchanger had sewage on the hot side and secondary water on the cold side in the winter and vice-versa in the summer. As discussed in Chapter 2, multi-row polymer tube heat exchanger was chosen as the type of waste water heat exchanger. As in the case of Myrtes in Brussels, Belgium, the polymer tubes were modeled to be arranged in series. To reduce the pressure drop, the total secondary water flow required was distributed among 4 heat exchangers which had tubes arranged in series. As in Myrtes, all the tube rows were located on the surface of the sewage channel, such the the sewage flow was directly over the polymer tubes. From initial analysis, it was inferred that due to low thermal conductivity of polymer tubes, large number of tubes would be required. Thus the tubes were closely packed. The hot and cold streams of the waste water heat exchanger are indicated in Figure 25 and Figure 26.

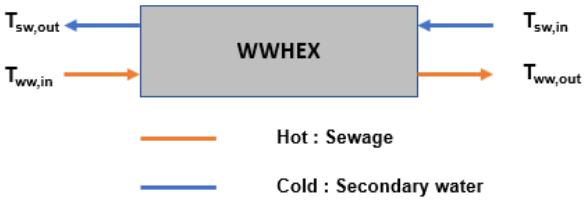

Figure 25: Hot and cold streams of WWHEX in the winter

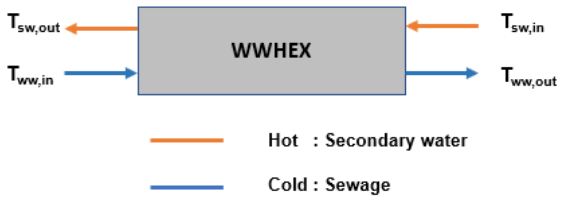

Figure 26: Hot and cold streams of WWHEX in the summer

Figure 27 illustrates the cross sectional view of an indicative tube arrangement system to assist the understanding of modeling of the heat exchanger. All the dimensions in the diagram are in mm. Figure 27 indicates the tube arrangement for a sewage level of 0.5 m and depicts two heat exchangers placed symmetrically. In each heat exchanger, the tubes were connected in series. One heat exchanger is on the RHS and another on the LHS. A small separation between the two can be seen on the bottom edge of length 500 mm. Two more heat exchangers were placed along the channel adjacent to these two heat exchangers. A common header was used to carry the total secondary water flow, which was split into 4 branches of the 4 heat exchangers.

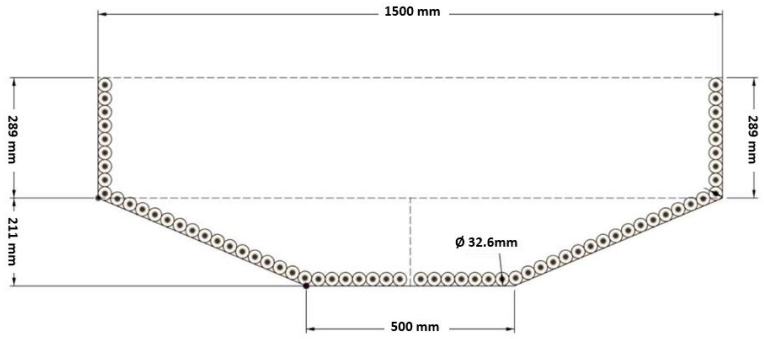

Figure 27: Cross sectional view of the planned arrangement of the WWHEX polymer tubes

- **Heat duty of the waste water heat exchanger in the winter and summer ($\dot{Q}_{ww}$)**

  The aim was to design a heat exchanger capable of exchanging (recovering/rejecting) 180 kW from sewage. On the day with the lowest temperature in the winter, the heat exchanger was designed to recover 180 kW. While on the hottest day in the summer, 180 kW was to be rejected to the sewage. The months of September, October, November, December, January, February, March, April and May were considered as the months that required heating (winter). The rest of the months, June, July and August were considered to require cooling, (summer). Heat duty of the waste water heat exchanger was considered to linearly scale with the ambient temperature. Thus, 180 kW would be recovered from sewage for lowest outside temperature while no heat would be recovered ($\dot{Q}_{ww}$ = 0 kW) when the ambient temperature was more than 20°C in the winter. In the summer, 180 kW was rejected to sewage on the hottest day and cooling was not required on those days when ambient temperature was lower than 20°C. Heat recovered from the sewage was considered to be equal to the duty of the evaporator in the winter and the heat rejected to sewage to be equal to condenser duty in the summer. Figure 28 depicts the variation of ambient temperature in 2018 and the required heat exchange with sewage in the winter and Figure 29 indicates the heat to be rejected to the sewage in the summer. A horizontal line marking 20 °C can be seen in both the plots. It can be seen that in the winter when the ambient crosses 20°C line, the heat duty goes to zero and in the summer, the heat duty goes to zero when the ambient is below the 20°C mark.

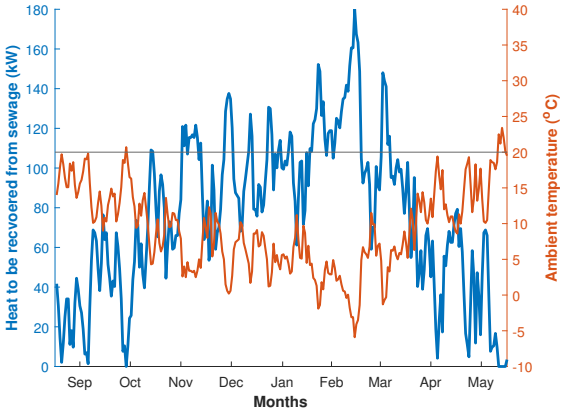

Figure 28: Heat to be extracted from the sewage in the winter

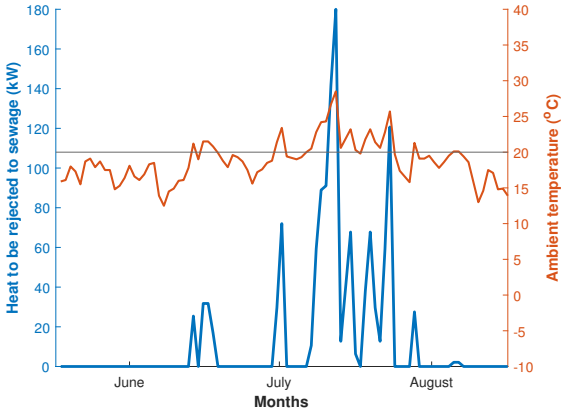

Figure 29: Heat to be rejected to the sewage in the summer

In the summer, it is clear that the heat to be rejected to the sewage is minimal in June and higher in July and August. It can also be seen that it is intermittent. At the point of highest temperature, cooling load peak of 180 kW is seen.

- **Mass flow rate of sewage**

  Mass flow rate of sewage was calculated based on velocity, v_{ww} , as follows,

$$\dot{m}_{\text{ww}} = \rho_{\text{ww}} \times A_{\text{c,ch}} \times v_{\text{ww}} \tag{19}$$

- **Physical properties of sewage**

  Due to the large sewage flow, reduction in sewage temperature was negligible after heat extraction. Thus, the physical properties of sewage at inlet and outlet of waste water heat exchangers were considered to be the same. Due to the fact that exact data indicating the quantitative and qualitative analysis of the sediments in the sewage of Rotterdam was not available, properties of water were considered for sewage water calculations. It was also found in one of the measurements done by the Gemeente that the sediments were really low in the sewage channel considered. Properties of water were evaluated as a function of sewage temperature.

- **Convective heat transfer coefficient on sewage side, α_{ww}**

  Flow of sewage in the sewage channel was approximated to flow through tubes. Hydraulic diameter of the channel based on the sewage level was considered to be the diameter of the channel for Nu number calculation. Thus, the convective heat transfer coefficient on the sewage side (α_{ww}) was calculated based on sewage flow velocity (v_{ww}), hydraulic diameter of the channel ($d_{\text{hyd,ch}}$). Properties of sewage such as k_{ww}, μ_{ww}, ρ_{ww} and $c_{p,\text{ww}}$ required for the calculation of (α_{ww}) were calculated at different sewage temperatures as explained before. The calculation of convective heat transfer coefficient is explained in Appendix C.

- **Secondary water parameters**

  The intermediate heat exchange fluid flowing through the tubes of waste water heat exchanger was chosen to be a mixture of water and mono-ethylene glycol ($C_2H_6O_2$). Mono-ethylene glycol was used to prevent water from freezing either due to low operating temperatures or due to contact of heat exchanger pipe headers with cold air during extreme weather conditions. In this report, water-mono-ethylene glycol mixture is referred to as secondary water.

– **Temperature of secondary water - Winter model**

In the winter model, an approach of 2 K was chosen between waste water inlet ($T_{\text{ww,in}}$) temperature and secondary water outlet ($T_{\text{sw,out}}$) temperature, thus limiting the maximum temperature to which the secondary water could be heated. The inlet temperature of the secondary water ($T_{\text{sw,in}}$) was varied from 0°C to a temperature 2 K lower than $T_{\text{sw,out}}$. Thus the lowest ΔT between inlet and outlet of secondary water stream was equal to 2 K. The lower limit to secondary water inlet temperature was chosen to be 0°C so the the designed freezing point of MEG solution would be -20°C in the worst case scenario. Therefore, for every waste water temperature there was one secondary water outlet temperature value and multiple inlet temperature values. The ΔT at which the COP of the system was maximized was identified by the model and the mass flow rate of secondary water corresponding to that was chosen and correlated with that particular sewage temperature. The following equations describe the constraints set for the secondary water stream in the winter model.

$$T_{\text{sw,out}} = T_{\text{ww,in}} - 2 \tag{20}$$

$$T_{\text{sw,in}} = 273.15 \text{ K to } (T_{\text{sw,out}} - 2) \tag{21}$$

– **Temperatures of secondary water - Summer model**

In the summer model, heat pump was operated in reverse. Thus, heat rejected by the condenser of the heat pump was carried by secondary water and transferred to the sewage. The secondary water temperatures at inlet ($T_{\text{sw,in}}$) and outlet ($T_{\text{sw,out}}$) of waste water heat exchanger were set higher that sewage temperature to ensure that heat transfer would occur. A sensitivity analysis was done to find the effect of $T_{\text{sw,in}}$ on the system performance. ΔT is the temperature increment factor, which was varied from 10 K to 50 K to find an optimum condensation temperature.

$$T_{\text{sw,in}} = T_{\text{ww,in}} + \Delta T \tag{22}$$

The secondary water outlet temperature ($T_{\text{sw,out}}$) from the waste water heat exchanger was set 1 K higher than waste water temperature.

$$T_{\text{sw,out}} = T_{\text{ww,in}} + 1 \tag{23}$$

The condensation temperature of the heat pump (T_{cond}) was considered to be equal to $T_{\text{sw,in}}$ since that was the outlet temperature of secondary water out of the condenser. Due to some super heat at the exit of the compressor, the refrigerant temperature at the inlet of the condenser would be higher than $T_{\text{sw,in}}$ or T_{cond}. Thus, there would be no temperature cross-over in the condenser.

$$T_{\text{cond}} = T_{\text{sw,in}} \tag{24}$$

– **Physical properties of secondary water**

Physical properties of secondary water such as density, specific heat, thermal conductivity and dynamic viscosity at different inlet and outlet temperatures were evaluated using a polynomial expression (Equation 25). The values of the coefficients C_{ij} for different physical properties have been provided in the Appendix B. Averages of input and output values of all properties of secondary water were calculated to be used in calculations.

$$F = \sum C_{ij} \cdot (x - x_m)^i \cdot (y - y_m)^j \tag{25}$$

where,

* x is the required freezing point, x = -20 °C
* y is the temperature of secondary water, in °C

* Appendix B has the tabulated values of physical properties at certain mean values of freezing point and secondary water temperature
* x_m is the mean freezing point, x = -20.69 °C
* y_m is the mean temperature of secondary water, 31.73 °C
* $0 \leq i \leq 5$, $0 \leq j \leq 3$, $i+j \leq 5$
* For dynamic viscosity, the LHS of Equation 25 is log F

– **Mass flow rate of secondary water**

For the winter case, for different ΔT values of secondary water (based on $T_{\text{sw,in}}$ and $T_{\text{sw,out}}$ values), total mass flow of secondary water required was obtained using Equation 28.

$$\Delta T_{\text{sw}} = T_{\text{sw,out}} - T_{\text{sw,in}} \tag{26}$$

In the summer,

$$\Delta T_{\text{sw}} = T_{\text{sw,in}} - T_{\text{sw,out}} \tag{27}$$

Mass flow was calculated from Equation 28, where $\dot{Q}_{\text{ww}}$ was either the heat to be recovered from the sewage or heat to be rejected to the sewage (winter or summer respectively).)

$$\dot{m}_{\text{sw,tot}} = \frac{\dot{Q}_{\text{ww}}}{c_{p,\text{sw}} \cdot \Delta T_{\text{sw}}} \tag{28}$$

Then the mass flow of secondary water through each heat exchanger ($\dot{m}_{\text{sw}}$) was obtained by dividing the total mass flow by the number of heat exchangers. Total volumetric flow of secondary water flow i.e., discharge through the header was calculated as in Equation 29. Similar to mass flow through each heat exchanger, volumetric flow through each tube ($\dot{V}_{\text{sw}}$) was calculated ($\dot{V}_{\text{sw,tot}}/N_{\text{hex}}$).

$$\dot{V}_{\text{sw,tot}} = \frac{\dot{m}_{\text{sw,tot}}}{\rho_{\text{sw}}} \tag{29}$$

Them from volumetric flow rate through each tube ($\dot{V}_{\text{sw}}$), the velocity of secondary water through each tube was calculated using Equation 30

$$v_{\text{sw}} = \frac{\dot{V}_{\text{sw}}}{A_{\text{c,t}}} \tag{30}$$

- **Convective heat transfer coefficient on secondary water side, α_{sw}**

The convective heat transfer coefficient on the secondary water side α_{sw} was calculated using the same correlations as that on the sewage side. Based on the calculated properties of secondary water such as k_{sw}, μ_{sw}, ρ_{sw} and $c_{p,\text{sw}}$ and secondary water velocity v_{sw}, the convective heat transfer coefficient was calculated as in Appendix C.

- **Fouling resistance on sewage side, $\alpha_{\text{ww,foul}}$**

The fouling resistance value of waste water was taken from the work of Liu et al. (2013). Thus the value of fouling resistance considered was, $\alpha_{\text{ww,foul}} = 6.7 \times 10^{-4}$ W/m^2 K.

- **Fouling resistance on secondary water side, $\alpha_{\text{sw,foul}}$**

The fouling resistance of secondary water was obtained from Towler and Sinnott (2013). Fouling resistance value of aqueous salt solution was chosen for secondary water, thus the fouling resistance value was equal to $\alpha_{\text{sw,foul}} = 2 \times 10^{-4}$ W/m^2 K.

- **Thermal conductivity of the polymer tubes, k_t**

  Thermal conductivity of HDPE tubes was considered to be 0.46 W/m K for base case simulations. To study the effect of thermal enhancement, thermal conductivity was varied from 0.46 W/m K to 1.89 W/m K.

- **Calculation of overall heat transfer coefficient, U_o**

  From the parameters calculated above, the overall heat transfer coefficient was calculated based on external area as follows,

$$\frac{1}{U_o} = \frac{1}{\alpha_{ww}} + \frac{1}{\alpha_{ww,foul}} + \frac{d_{o,t}\ ln\ (\frac{d_{o,t}}{d_{i,t}})}{2\ k_t} + \frac{d_{o,t}}{d_{i,t}} \times \frac{1}{\alpha_{sw,foul}} + \frac{d_{o,t}}{d_{i,t}} \times \frac{1}{\alpha_{sw}} \tag{31}$$

- **Heat duty per heat exchanger, $\dot{Q}_{ww,1}$**

  Since all the calculations were done on the basis of one heat exchanger, the heat duty per heat exchanger was calculated by dividing the total heat exchange duty by the number of heat exchangers.

$$\dot{Q}_{ww,1} = \frac{\dot{Q}_{ww}}{N_{hex}} \tag{32}$$

- **Calculation of LMTD**

  Based on waste water and secondary water temperatures, the LMTD was calculated as described below. The outlet temperature of waste water ($T_{ww,out}$) was assumed to be the same as that of inlet temperature ($T_{ww,in}$).

$$LMTD = \frac{(T_{ww,in} - T_{sw,out}) - (T_{ww,in} - T_{sw,in})}{ln\frac{(T_{ww,in} - T_{sw,out})}{(T_{ww,in} - T_{sw,in})}} \tag{33}$$

- **Calculation of area required for heat exchange per heat exchanger**

  Based on the value of U_o, LMTD and the heat duty per heat exchanger $\dot{Q}_{ww,1}$, the external surface area of tubes ($A_{tot,t}$) required per heat exchanger was calculated as in Equation 34.

$$A_{tot,t} = \frac{\dot{Q}_{ww,1}}{U_o \cdot LMTD} \tag{34}$$

- **Calculation of number of tubes required per heat exchanger**

  Based on the total surface area of tubes required, the number of tubes per heat exchanger was calculated.

$$N_t = \frac{A_{tot,t}}{A_{s,t}} \tag{35}$$

  If N_t was not an even integer, it was rounded off to the next nearest even integer. The number of tubes must be even to ensure that the return line can be connected from the same side as that of supply line. The number of tubes required per heat exchanger was compared with the total number of tubes that were submerged in sewage at any given time ($N_{t,sub}$) to see if it was feasible. $N_{t,sub}$ depended on tube dimensions and sewage level.

$$N_{t,sub} = \frac{P_{ch} - d_{o,t}}{w_t} + 1 \tag{36}$$

$N_{t,sub}$ was rounded to the nearest lower even integer. $N_{t,sub}$ is the total number of tubes submerged in sewage corresponding to 2 heat exchangers, thus $N_{t,sub}/2$ represents the number of tubes submerged per heat exchanger. Thus, N_t required must be less than $N_{t,sub}/2$. If the number of tubes required per heat exchanger was higher than the number of tubes submerged, then the number of tubes required was reduced to the actual number of tubes submerged. Thus if, $N_t > N_{t,sub}/2$, then

$$N_t = \frac{N_{t,sub}}{2} \tag{37}$$

Then, it that case, the total heat transfer area actually available was calculated as,

$$A_{act,t} = N_t \times A_{s,t} \tag{38}$$

Based on the actual heat transfer area $A_{act,t}$, the actual heat recovered was calculated as,

$$\dot{Q}_{ww} = U_o \times A_{act,t} \times LMTD \tag{39}$$

After the actual heat transfer possible was calculated, the mass flow of secondary water required was recalculated (from Equation 28) and from it the velocity (v_{sw}), Reynolds number (Re_{sw}), Nusselt number (Nu_{sw}) and convective heat transfer coefficient (α_{sw}) of secondary water were recalculated. Then, from the new value of α_{sw}, U_o was re-evaluated using Equation 31. This was done in an iterative manner until the difference between the U_o values of two successive iterations were less than 1%. Values such as $\dot{m}_{sw}$, $\dot{Q}_{ww}$ corresponding to the converged value of U_o were chosen for further design.

- **Pumping power required**

A pump was used for the circulation of secondary water in the waste water heat exchanger. A common HDPE header carried the total mass flow of secondary water from the 'Doelen' heating/cooling system to the waste water heat exchanger in the sewage channel. The length of this common header was considered to be approximately equal to 460 m (twice as in Myrtes). The equivalent tube length $l_{eq,t}$ of tubes in series for each heat exchanger was calculated as,

$$l_{eq,t} = N_t \times l_t + (50 \times N_{elb} \times d_{i,t}) \tag{40}$$

where 50 was the equivalent length factor ($l_{elb,eq}/d_{i,t}$ = 50) used for 180°bends. N_{elb}, the number of 180° bends were calculated as,

$$N_{elb} = \frac{N_t}{2} \tag{41}$$

Thus, using the equivalent tube length of one heat exchanger and v_{sw} and friction factor, head loss through the tubes (ΔH_t) of the waste water heat exchanger was calculated using Equation 42. For the header, mass flow rate was $m_{sw,tot}$, and based on the internal diameter of the header, secondary water velocity in the header was calculated as in Equation 30. Based on the velocity of secondary water in the header, Re number was calculated and using Re, friction factor was calculated for the header using Equation 78 or Equation 79 in Appendix C. Head loss in the header ΔH_{hd} was calculated based on Equation 42.

$$\Delta H = \left[\frac{f \times l \times v^2}{2 \times g \times d_i}\right] \tag{42}$$

The total pump power required for the secondary water flow was calculated as,

$$\dot{W}_{\text{sw, pump}} = \left[\rho_{\text{sw}} \times \dot{V}_{\text{sw,tot}} \times g \times \Delta H_{\text{hd}} + \rho_{\text{sw}} \times \dot{V}_{\text{sw}} \times g \times \Delta H_{\text{t}}\right] \times \frac{1}{\eta_{\text{pump}}} \tag{43}$$

where, η_{pump} is the efficiency of the pump. The head loss of the secondary water stream in the evaporator (in winter) and the condenser (in the summer) was negligible when compared to the head loss through header and waste water heat exchanger tubes, thus it was neglected. The head loss through the evaporator and condenser are mentioned in Table 36 in Appendix E.

- **Definition of the instantaneous COP of the system**

  In the winter,

$$COP = \frac{\dot{Q}_{\text{cond}}}{(\dot{W}_{\text{sw, pump}} + \dot{W}_{\text{comp}})} \tag{44}$$

  Calculation of the heat supplied to 'Doelen' (or condenser duty - $\dot{Q}_{\text{cond}}$) and compressor work ($\dot{W}_{\text{comp}}$) of the heat pump are described in the next section.

  In the summer,

$$COP = \frac{\dot{Q}_{\text{evap}}}{(\dot{W}_{\text{sw, pump}} + \dot{W}_{\text{comp}})} \tag{45}$$

2.2.2 Heat pump system

In the winter, exergy of heat recovered from sewage was upgraded using a heat pump between the heat recovery system and the heating network of the 'Doelen'. In the evaporator, the hot fluid was secondary water and the cold fluid was the refrigerant. In the condenser, the hot fluid was the refrigerant and the cold fluid was the water from the heating network of 'Doelen'. Propane (R290) with relatively low cost and low GWP, was chosen as the refrigerant. The condensation temperature was fixed at 55°C, while the evaporation temperature was dependent on secondary water temperature which in turn depended on sewage temperature. The high temperature heat rejected from the condenser was used in the heating network. In the summer, the heat pump was operated in reverse. Water from the chilled water network of 'Doelen' was on the hot side of the evaporator and the refrigerant was on the cold side. In the condenser, the refrigerant was the hot fluid that rejected heat to the cold secondary fluid. The exergy of heat extracted from the chilled water network of 'Doelen' was upgraded such that it could be rejected to the sewage. For the summer model, the evaporation temperature was fixed at 8°C and the condensation temperature was dependent on the sewage temperature. Thus while integrating the waste water heat exchanger with the heat pump the inputs required from the heat exchanger model to the heat pump model were the amount of heat exchanged between refrigerant and secondary water and temperature of secondary water to decide the evaporation temperature (winter) and condensation temperature (summer).

- **Winter model**

  In the winter model, temperature of the refrigerant at the outlet of the compressor was about 64°C. The refrigerant was cooled from 64°C to a sub-cooled temperature of 30°C in the condenser. Water from the 'Doelen' heating system was heated from 25°C to 53°C with a pinch of 5 K in the condenser. The secondary water temperature $T_{\text{sw,in}}$ at the outlet of the evaporator was the limiting factor for the evaporation temperature. The evaporation temperature of heat pump was set 2 K lower than $T_{\text{sw,in}}$ to prevent temperature cross-over. Heat pump calculations are described in Appendix D. From the heat pump model, parameters like compressor power ($\dot{W}_{\text{comp}}$), mass flow of refrigerant ($\dot{m}_{\text{ref}}$), and condenser duty ($\dot{Q}_{\text{cond}}$) were obtained.

- **Summer model**

  In the summer model, chilled water entered the evaporator at 14°C and it was cooled to 10°C. Thus, with a pinch of 2 K, the evaporation temperature was set at 8°C. The condensation temperature was set to be equal to $T_{\text{sw,in}}$, as described in Equation 24. The calculations of the heat pump model are provided in Appendix D. The heat pump model was used to calculate $\dot{W}_{\text{comp}}$, $\dot{m}_{\text{ref}}$ and $\dot{Q}_{\text{evap}}$.

2.3 WWSHP + ATES system

To increase the heating/cooling capacity of 'Doelen' an option considered was to integrate waste water source heat pump with ATES. In the winter, heat was recovered both from sewage and ground water of the aquifers. The waste water heat exchanger and ground water heat exchanger were placed in series with respect to secondary water flow. The amount of heat to be extracted from waste water on any given day was calculated as in the waste water source heat pump case, thus the heat extracted from ATES was in addition to that. The idea was to have an additional source of heat on days of low sewage flow or temperature. In case the total heat recovered was higher than 180 kW, the additional heat could still be used by 'Doelen' for heating. Secondary water was first heated by sewage and then further heated by ground water. Secondary water added heat to the evaporator of the heat pump which further supplied high temperature heat to the heating network of 'Doelen' through the condenser. In the summer, the main objective was to replenish the warm well with the heat that was extracted in the winter. Heat rejected from the cooling network of 'Doelen' and heat extracted from sewage were used as sources of heat to replenish the warm well.

Modeling of the ATES system was done in COMSOL. It was linked to Matlab to update injection/extraction flow rates and temperatures in accordance with the waste water source heat pump model. Since the heat recovery model was evaluated on a day basis, the COMSOL models were also run on a daily basis. Time steps of the ATES models were set to 1 day and were evaluated over winter period of 9 months and summer period of 3 months.

2.3.1 ATES model

The ATES system was modeled in a similar way as in the reference work by Bozkaya et al. (2017). The aquifer was considered to be a 2D axi-symmetric model made of porous media (sand). The aquifer was considered to be confined between two impermeable layers of clay as shown in Figure 30. The aquifer chosen for modeling is shown in Figure 32. Aquifer layer data was obtained from [2]. In Figure 32 clay layer can be seen from 10 m to 17.5 m depth, and sand layer can be seen from 17.5 m to 31.5 m. An impermeable clay layer below the sand layer was assumed to exist to make the aquifer confined. In the reference model (Bozkaya et al., 2017) used for validation of the aquifer it was seen that for an injection flow rate of 40 m^3/h and aquifer radius of 120 m, the thermal penetration depth was only 60 m. In the ATES model developed for this work, much lower injection/extraction flow rates were expected, thus the aquifer radius was chosen to be 60 m. As in the work of Bozkaya et al. (2017) the porosity of sand layer was assumed to be 0.35.

- **Conditions for Darcy's flow equation**

  The $r = 0$ m boundary was set as inlet and outlet boundary and the injection and extraction (negative sign) flow rates were imposed on it. Based on the injection/extraction flow rates, the Darcy pressure drop in porous media was calculated. The initial pressure inside the aquifer was calculated based on a water level of 31.5 m. No flow condition was set between the aquifer and the clay layers because of their impermeability. The injection and extraction flow rate values were obtained from the Matlab model that had an integration of the waste water source heat pump system and the ATES system.

- **Conditions for heat transfer through porous media equations**

  The injection and extraction temperatures were imposed at $r = 0$ m and the outer boundary was set as open boundary with a temperature of 10°C for heat flux instead of no heat flux as done by Bozkaya et al. (2017) to make the model more realistic. The initial temperature of the warm well

[2] DINOloket

was set as 18°C. The initial temperature of cold well was assumed to be the same as the ground temperature, 10°C. The clay layers were defined as solid ensuring that heat transfer was only through conduction in those layers. The aquifer layer was defined as porous media to accommodate conduction and convection of ground water. The solution from the previous iteration was used to obtain the initial and the extraction temperature.

The flow and energy equations were solved by coupling the heat transfer in porous media and Darcy's flow physics in COMSOL. The WWSHP+ATES model simulated the winter season first. The total heat extracted from the warm well was calculated at the end of winter and the summer model was simulated to replenish it. Figure 30 indicates the 2D axisymmetric model and Figure 31 indicates the quadratic meshing used. Extremely fine meshing with 12314 domain elements and 500 boundary elements were chosen for the simulations.

$$lev_{\text{ww}} = \frac{0.5 \times \dot{V}_{\text{ww}}}{\dot{V}_{\text{ww,max}}} \tag{46}$$

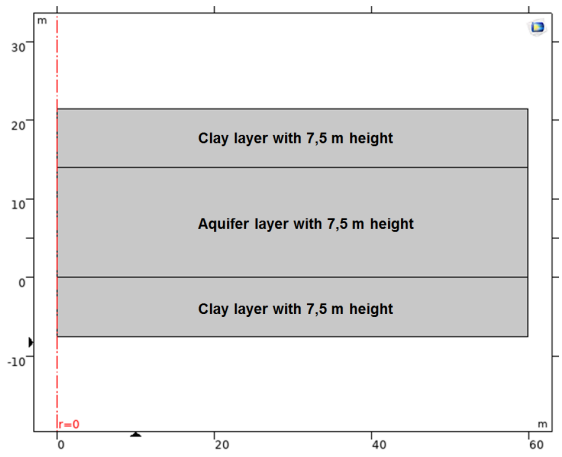

Figure 30: ATES model developed in COMSOL

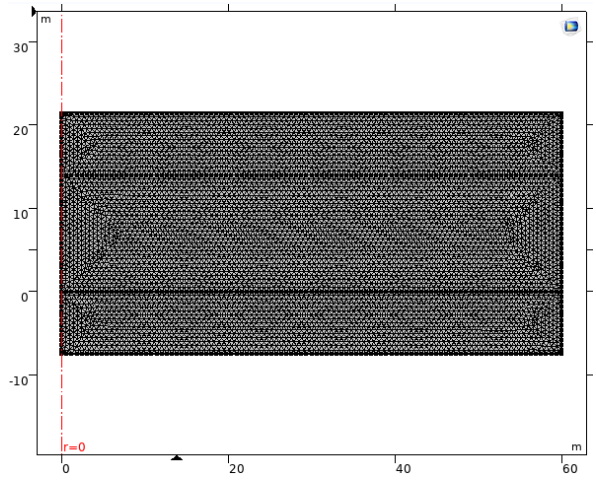

Figure 31: Meshing of the aquifer domain in COMSOL

Figure 32 provides data regarding the different aquifer layers and hydraulic conductivity value of the aquifer. The K value of the chosen aquifer is in the range of 25 to 35 m/day. Thus, the average of those values, 37.5 m/day (4.34×10^{-4} m/s) was chosen for the simulation.

Table 7: Aquifer parameters

Parameter	Value	Unit
Aquifer radius	60	m
Aquifer height	14	m
Clay layer height	7.5	m
Hydraulic conductivity	4.34×10^{-4}	m/s
Porosity	0.35	-
Initial ground temperature	10	°C

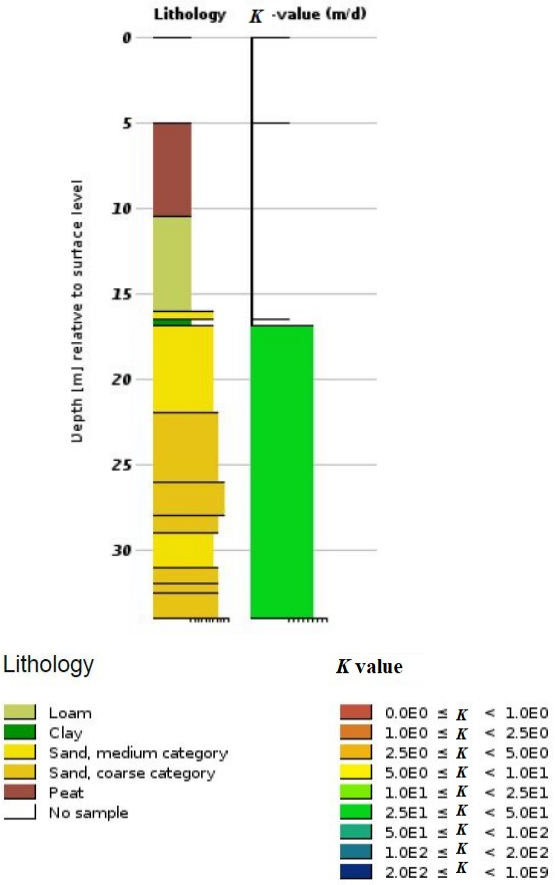

Figure 32: Aquifer lithology and hydraulic conductivity data

Note : Figure 32 was taken from [3].

- **Warm well**

  Initial temperature of warm well was set as 18°C, assuming an initial injection cycle. In the WWSHP + ATES model, winter was simulated first.

Table 8: Warm well : Initial conditions and boundary conditions

Parameter	Value	Unit
Initial temperature	18	°C
Open boundary temperature	10	°C

- **Cold well**

  Since winter was simulated first, ground water was injected at 8°C into the cold well to maintain a 10 K ΔT between the warm and the cold well.

Table 9: Cold well : Initial conditions and boundary conditions

Parameter	Value	Unit
Initial temperature	10	°C
Injection temperature	8	°C
Open boundary temperature	10	°C

[3] DINOloket

2.3.2 WWSHP + ATES : Winter

In the winter, ground water was extracted at 18°C from the warm well and after recovering heat from it, it was injected back to the cold well at 8°C. The extraction temperature of warm well varied with time due to the extraction of ground water, but the injection temperature to cold well was kept constant. Since waste water heat exchanger and the ground water heat exchanger were arranged in series as shown in Figure 33, the pre-requisite for the use of ATES was that the outlet temperature of secondary water from waste water heat exchanger ($T_{\mathrm{sw,out}}$) had to be lower than 8°C. Thus, secondary water was heated from 0°C to 7°C using waste water heat exchanger. Then the secondary water was further heated from 7°C to a temperature 2 K lower than warm well extraction temperature in the ground water heat exchanger. The hot secondary water was then sent to heat pump to supply heat to the heating network of 'Doelen'.

The waste water heat exchanger model was first simulated for the 9 months of winter based on the known secondary water temperature conditions (0°C at inlet and 7°C at outlet of waste water heat exchanger). Mass flow rate of secondary water for each of the 273 days of winter was calculated based on the calculated waste water heat exchanger duty and secondary water temperatures. Then the COMSOL model was started by Matlab. The COMSOL model was run on a daily basis for 273 days, such that the extraction and domain temperatures could be recorded. To calculate the groundwater flow rate in the ground water heat exchanger, temperatures of ground water and secondary water and mass flow of secondary water are required. The extraction temperature of warm well was obtained from the warm well temperature value of the previous iteration (18°C in the first iteration). The injection temperature to cold well was always 8°C. The secondary water temperature at the inlet of the ground water heat exchanger was always 7°C, but the outlet temperature depended on the ground water extraction temperature. From the waste water heat exchanger model, mass flow of secondary water was known, thus, ground water extraction flow rate was calculated as in Equation 49. The flowchart followed to model the WWSHP + ATES model in the winter is shown in Figure 34.

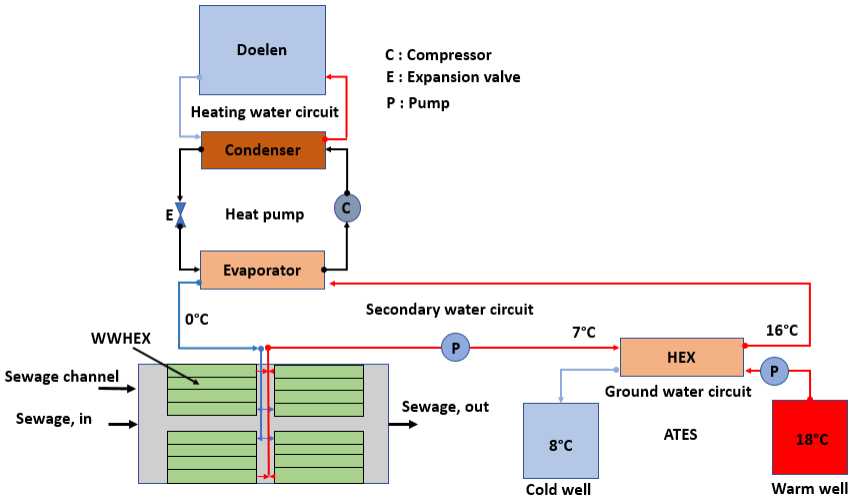

Figure 33: WWSHP + ATES : Winter model

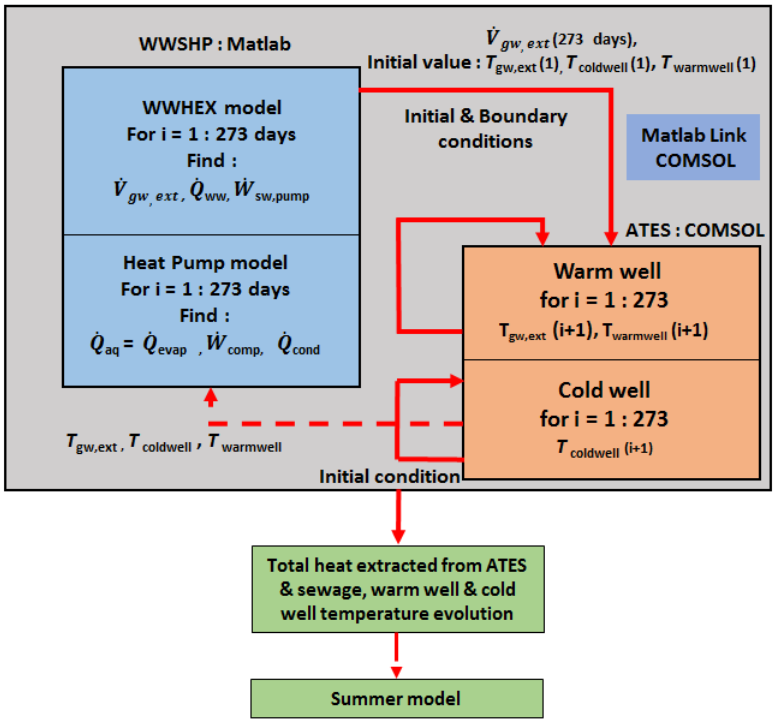

Figure 34: WWSHP + ATES Winter model : COMSOL link Matlab flow chart

Design of waste water heat exchanger was exactly the same as in the case of waste water source heat pump system except for the fact that the secondary water temperatures were not iteratively chosen. Instead, they were set to be 0°C at inlet and 7°C at the outlet of waste water heat exchanger. The equations used for the integration of waste water source heat pump system with ATES are as described below.

- **Mass flow rate of secondary water**

  Mass flow of secondary water was calculated based on the actual heat recovered from sewage ($\dot{Q}_{\mathrm{ww}}$) and secondary water temperatures in the waste water heat exchangers. $\dot{Q}_{\mathrm{ww}}$ was calculated as described in Equation 39.

$$\dot{m}_{\mathrm{sw,tot}} = \frac{\dot{Q}_{\mathrm{ww}}}{c_{p,\mathrm{sw}} \times (T_{\mathrm{sw,out}} - T_{\mathrm{sw,in}})} \tag{47}$$

  where, $T_{\mathrm{sw,in}}$ = 273.15 K and $T_{\mathrm{sw,out}}$ = 280.15 K.

- **Heat extracted from ATES**

  The value of ground water extraction temperature $T_{\mathrm{gw,ext}}$ was obtained from the previous iteration. The secondary water temperature at the exit of the ground water heat exchanger ($T_{\mathrm{sw,out2}}$) was considered to be 2 K lower than ground water extraction temperature. The secondary water outlet (from waste water heat exchanger) temperature $T_{\mathrm{sw,out}}$ was set as 7°C. Thus the heat extracted from warm well was calculated as,

$$\dot{Q}_{\mathrm{aq}} = \dot{m}_{\mathrm{sw}} \times c_{p,\mathrm{sw}} \times (T_{\mathrm{sw,out2}} - T_{\mathrm{sw,out}}) \tag{48}$$

- **Mass flow rate of ground water**

  The mass flow of ground water was calculated based on the heat extracted from ATES and the extraction and injection temperature of ground water.

$$\dot{m}_{\text{gw}} = \frac{\dot{Q}_{\text{aq}}}{c_{p,\text{gw}} \times (T_{\text{gw,ext}} - T_{\text{gw,inj}})} \tag{49}$$

  From $\dot{m}_{\text{gw}}$, the injection/extraction rate $\dot{V}_{\text{gw}}$ was calculated and used as an input in the COMSOL model.

- **Evaporator duty**

  The total heat added to the secondary water from the waste water heat exchanger ($\dot{Q}_{\text{ww}}$) and ground water heat exchanger ($\dot{Q}_{\text{aq}}$) was exchanged with the refrigerant of the heat pump in the evaporator. Thus the duty of the evaporator was calculated as,

$$\dot{Q}_{\text{evap}} = \dot{Q}_{\text{ww}} + \dot{Q}_{\text{aq}} \tag{50}$$

- **Total heat extracted**

$$Q_{\text{ext,tot}} = \sum_{1}^{273} (\dot{Q}_{\text{evap}} \times 24) \tag{51}$$

- **Secondary water and ground water pump power**

  The secondary water pump power ($\dot{W}_{\text{sw, pump}}$) was calculated using Equation 43. The ground water pump power required was calculated as follows,

$$\dot{W}_{\text{gw, pump}} = \rho_{\text{gw}} \times \dot{V}_{\text{gw}} \times g \times (\Delta H_{\text{darcy}} + \Delta H_{\text{dyn}} + H) \tag{52}$$

  where,

  - ΔH_{darcy} is the Darcy head loss in the aquifer, calculated by Equation 15
  - ΔH_{dyn} is the dynamic head loss in the ground water pipes, calculated by Equation 42. The total length of ground water pipe was chosen to be the summation of twice the aquifer radius and twice the depth at which water was injected or extracted. The head loss through the ground water heat exchanger was not considered as it was not very significant (See Table 38 in Appendix E).
  - H is the static head. The static head against which the ground water had to injected was considered to be 24.5 m. The depth to which the clay layer was present was 17.5 m and in addition to that the injection screen was assumed to be placed at mid-length of the aquifer, thus that added another 7 m to the static head. Since the water table was assumed to be at the ground surface, the total static head considered was 24.5 m.

- ***COP* of the system**

  The instanteneous COP of the system was calculated based on the total heat delivered to 'Doelen' ($\dot{Q}_{\text{cond}}$) and the total electric power required for the secondary water and ground water pumps and the compressor of the heat pump.

$$COP = \frac{\dot{Q}_{\text{cond}}}{(\dot{W}_{\text{sw, pump}} + \dot{W}_{\text{gw, pump}} + \dot{W}_{\text{comp}})} \tag{53}$$

2.3.3 WWSHP + ATES : Summer

In the summer, heat extracted from warm well in the winter was replenished by extracting ground water from cold well at around 8°C and heating it up in series using a heat pump operating in reverse and a secondary water heat exchanger. The schematic of the summer model is as shown in Figure 35. Ground water was extracted from cold well at around 8°C and it was made to pass through the condenser of the heat pump first, where it was heated to 16°C. Then it was passed through the secondary water heat exchanger so that it could be further heated to 20°C. Water in the chilled water network of 'Doelen' was cooled from 14°C to 8°C by rejecting heat in the evaporator of the heat pump. In WWSHP + ATES system, the chilled water was cooled to 8°C to obtain more heat from the heat pump so that the total replenishment of heat to the warm well was ensured. The evaporation temperature was set 2 K lower, i.e., 6°C. The condensation temperature was set as 18°C such that the ground water could be heated to 16°C. The ground water was further heated from 16°C to around 20°C using heat recovered by secondary water from waste water. Ground water was injected at 20°C to offset the reduction in temperature that occurs in the warm well due to a previous extraction cycle. The evolution of warm well and cold well temperature was recorded for each time step to update the extraction and injection temperatures of cold and warm wells respectively.

In this model, the cold well extraction was first simulated in COMSOL, it was then followed by warm well injection. The summer model was simulated for 92 days of summer (June, July and August). The design of the waste water heat exchanger was the same as in the waste water source heat pump case, except for predetermined secondary water temperatures. The secondary water was heated from 17°C to a temperature 1 K lower than waste water temperature in the waste water heat exchanger. A temperature difference of 1 K was maintained between the secondary water and ground water in the secondary water heat exchanger. Based on the total heat extracted in the winter, the daily quantity of required heat injection to warm well was calculated. The heat extracted from sewage was known, thus the difference in the total heat to be injected to warm well and the heat extracted from sewage was calculated to find the heat to be rejected by the condenser. Thus, the total replenishment of heat to warm well was always ensured. The flowchart followed to develop the WWSHP + ATES model is shown in Figure 36.

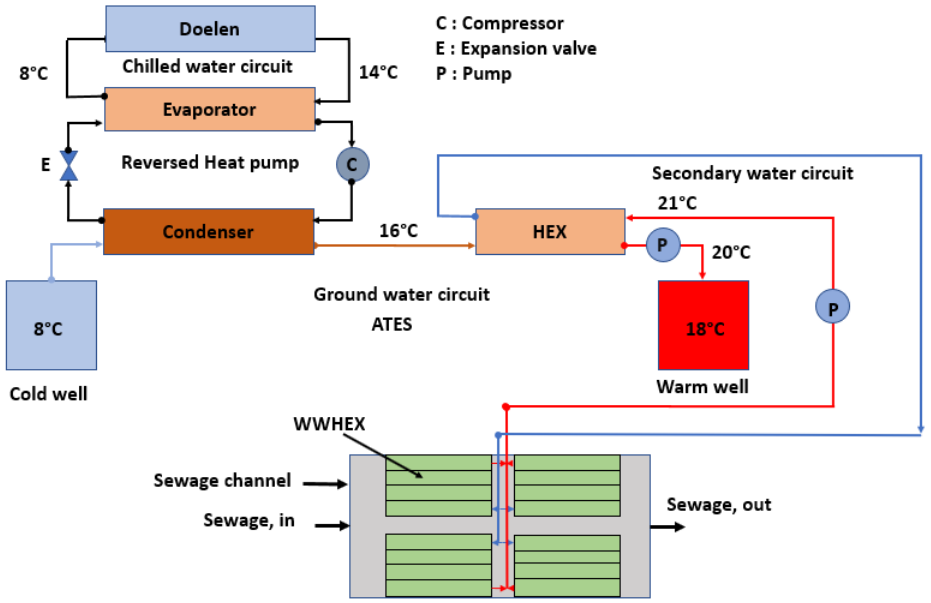

Figure 35: WWSHP + ATES : Summer model

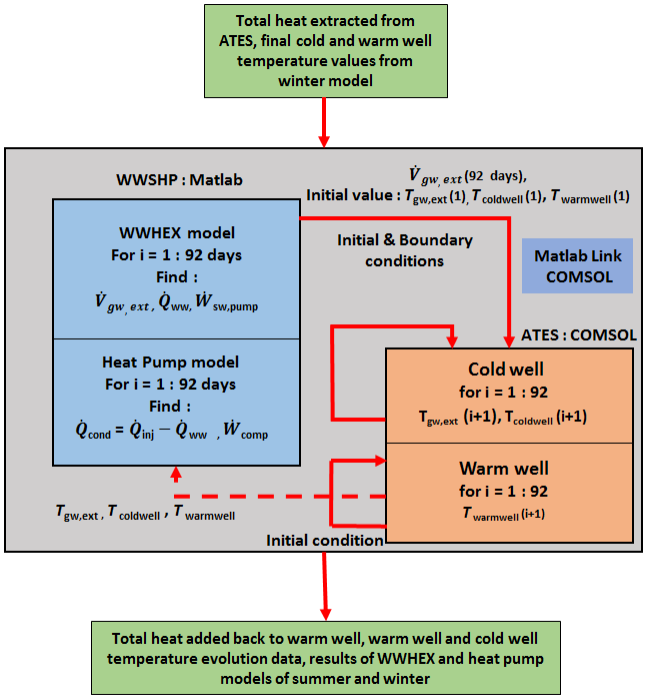

Figure 36: WWSHP + ATES Summer model : COMSOL link Matlab Flow chart

The following equations were used in the summer model,

- **Mass flow rate of secondary water**

  Mass flow rate of secondary water ($\dot{m}_{\text{sw,tot}}$) was calculated as in Equation 47.

- **Heat to be injected**

  The rate at which heat was to be injected to the warm well was calculated based on the total heat extracted from the warm well in the winter ($Q_{\text{ext,tot}}$ is defined in Equation 51) and the number of days of summer (92 days).

$$\dot{Q}_{\text{inj}} = \frac{Q_{\text{ext,tot}}}{92 \times 24} \tag{54}$$

- **Heat to be rejected by condenser**

  Heat to be rejected by the condenser was calculated by finding the difference between the heat that has to be injected to the warm well ($\dot{Q}_{\text{inj}}$) and the actual heat recovered from sewage ($\dot{Q}_{\text{ww}}$).

$$\dot{Q}_{\text{cond}} = \dot{Q}_{\text{inj}} - \dot{Q}_{\text{ww}} \tag{55}$$

  Based on $\dot{Q}_{\text{cond}}$, the mass flow of refrigerant $\dot{m}_{\text{ref}}$ was calculated and from that the heat extracted from the chilled water network of 'Doelen' was calculated ($\dot{Q}_{\text{evap}}$).

- **Mass flow rate of ground water**

  Mass flow of ground water ($\dot{m}_{\text{gw}}$) was calculated from the total heat injected to the warm well and the increase in temperature of ground water from cold well ($T_{\text{gw, ext}}$) to warm well ($T_{\text{gw, inj}}$).

$$\dot{m}_{\text{gw}} = \frac{\dot{Q}_{\text{inj}}}{(c_{p,\text{gw}} \times (T_{\text{gw,inj}} - T_{\text{gw,ext}}))} \tag{56}$$

From $\dot{m}_{\text{gw}}$, the injection/extraction rate $\dot{V}_{\text{gw}}$ was calculated and used as an input in the COMSOL model.

- **Secondary water and ground water pump power**

  $\dot{W}_{\text{sw, pump}}$ and $\dot{W}_{\text{gw, pump}}$ were calculated as mentioned in the winter model (Equation 43 and Equation 52).

- **COP of the system**

  Since the objective of the summer model was to produce cooling effect in the 'Doelen', the COP of the system was defined as,

$$COP = \frac{\dot{Q}_{\text{evap}}}{(\dot{W}_{\text{sw, pump}} + \dot{W}_{\text{comp}})} \tag{57}$$

3 Results

3.1 Validation of models

Waste water source heat pump model was validated by comparing its results with the experimental and simulation results of the Myrtes project. The ATES model was validated by comparing the results obtained with those of the model developed by Bozkaya et al. (2017).

3.1.1 Waste water source heat pump model

Input parameters for the waste water source heat pump model validation were collected from measurements made at the installation site of the Myrtes project. The input parameters are listed in Table 10. The dimensions of the sewage channel used in the Myrtes project were not available, hence the dimensions of the sewage channel in Rotterdam were used for the validation case as well.

Table 10: Input parameters from the installed WWSHP of Myrtes

Parameter	Value
HEX Type	Multi-row tube
Tube material	HDPE
k_{t}, (W/m K)	0.5
$d_{\mathrm{i,t}}$ (mm)	32
thk_{t} (mm)	2.13
l_{t} (m)	6
Exposed area	50%
Refrigerant	R410A
Secondary fluid	MEG
Sewage flow (m^3/h)	5 - 60
Sewage temperature (°C)	6 - 18
Pumping distance (m)	230

In Table 10, exposed area refers to the area of the tube exposed to sewage and which is available for heat exchange. These data were taken from the heat recovery model developed by Spriet and Hendrick (2017). Sewage flow, temperature and sewage heat recovery data were monitored at the Myrtes test facility in Brussels, Belgium. The flow was found to vary between 5 m^3/h to 60 m^3/h, and the corresponding sewage level was found to vary between 5 cm to 30 cm. Measured sewage temperature was in the range of 6°C to 18°C. It was seen in the experimental data that the heat recovered from the sewage was found to vary between 2.5 to 5.5 kW, while the heat pump delivered 3.2 to 7 kW of heating power. COP calculated based on experimental values was found to vary between 3.7 to 5.

Authors Spriet and Hendrick (2017), in their work developed a waste water source heat pump model using the experimental input data (sewage flow and temperature and ambient temperature) to evaluate the potential of heat recovery from sewage for future scenarios. According to their simulation, an average of 6.3 kW of heating power was delivered by the heat pump and the system operated with a COP of 3.5.

For the validation case, sewage flow was varied from 5 m^3/h to 60 m^3/h, and the corresponding sewage level in the channel was varied from 5 cm to 30 cm. From the sewage level and the sewage channel dimensions of 'Doelen', flow velocity and number of tubes submerged in sewage flow were calculated. The number of tubes completely submerged in sewage flow was thus the limiting factor on the maximum heat exchange between sewage and secondary water. Variation of heat recovery from sewage with the preset variation in sewage level and temperature is depicted in Figure 37.

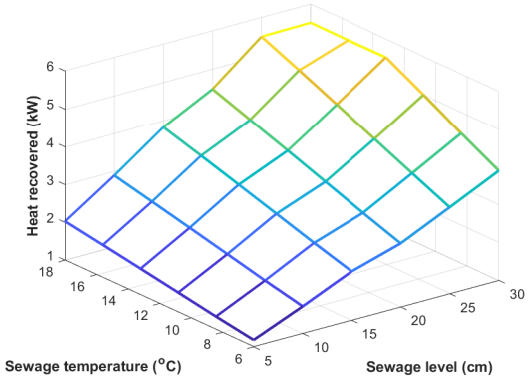

Figure 37: Heat recovery performance of the model developed in this work

Figure 37 confirms that the model behaves in accordance with the theory. The heat recovery increased with increase in sewage level and sewage temperature. Maximum heat (5.5 kW) was recovered when sewage flow and temperature were both maximum. Heat recovered from sewage was found to vary between 1.2 kW to 5.5 kW, while the heat pump delivered 2.7 to 7.4 kW through the condenser. The system COP was found to be 3.9. Parameters corresponding to maximum heat recovery were compared between this work and the Myrtes project. The comparison is in Table 11.

Table 11: WWSHP model validation with measured values of WWSHP installation of the Myrtes project

Parameter	Myrtes exp.	This work
Heat recovered (kW)	5.5	5.5
Heat delivered by heat pump (kW)	7	7.4
Heat exchange area (m^2)	10.3	15.8
COP	5	3.9
Number of tubes	30	46

It can be seen from Table 11 that the maximum heat recovery values for the model developed in this work and Myrtes project were the same. Lower condenser duty (heat delivered) of the Myrtes installation was possibly because of lower isentropic efficiency value of the installed compressor. It can be seen that the heat exchanger developed in this work required 5.5 m^2 more heat exchange area than the installed heat exchanger of Myrtes project to recover 5.5 kW. Each 6 m tube with an outside diameter of 36.27 mm and 50% exposed area provides 0.34 m^2 area, thus an additional 5.5 m^2 would imply 16 more tubes. It can be seen in Table 11 that this model required 46 tubes while the Myrtes facility had just 30 tubes. In Table 12, the performance characteristics of this model, the installed system at Brussels and the results of its model are compared.

Table 12: Comparison of system performance of this model with Myrtes project

Parameter	Myrtes installation	Myrtes model	This work
Heat recovered (kW)	2.5 - 5.5	NA	1.2 - 5.5
Heat delivered (kW)	3.2 - 7	6.3	2.7 - 7.4
COP	3.7 - 5	3.5	3.9

The lower bound of heat recovery value of this model and the measured data were different. The difference in channel dimensions of 'Doelen' and 'Myrtes', which affects the number of tubes submerged in sewage flow at any given point of time, was considered to be the reason for the difference in lower bounds of heat recovery values. COP value calculated in this model was in the range of measured COP, but it was higher than the COP of Myrtes model.

3.1.2 ATES model

Aquifer models developed in COMSOL were validated using the results from the work of Bozkaya et al. (2017). In the reference model, the warm and cold wells were simulated for one injection season considering the maximum injection volume of both the wells. The conditions used for validation of each of the wells are provided in Table 13 and Table 14. The temperature distribution profiles of warm well and cold well obtained after one injection cycle were compared with the results of the reference model.

- **Warm well**

  The maximum injection volume of ground water into the warm well was 176,000 m^3 in one season. For an injection flow rate of 40 m^3/h, the simulation time was calculated to be 4400 h.

  Table 13: Injection parameters of the warm well in the reference model (Bozkaya et al., 2017)

Parameter	Value	Unit
Injection volume	176,000	m^3
Injection flow rate	40	m^3/h
Injection period	4400	h
Simulation time step	1	h
Initial temperature	12.5	°C
Injection temperature	16	°C
Aquifer height	60	m
Aquifer radius	120	m
Clay layer height	5	m

  Based on the conditions mentioned in Table 13, the following temperature profile (Figure 39) was obtained. It is important to note that in the reference plot (Figure 38), additional aquifer layers are shown at the top and bottom of 5 m thick clay layers marked by dotted lines, where temperature is not plotted. The region of interest in the reference temperature profile is thus only between -57.5 m at the top to -127.5 m at the bottom.

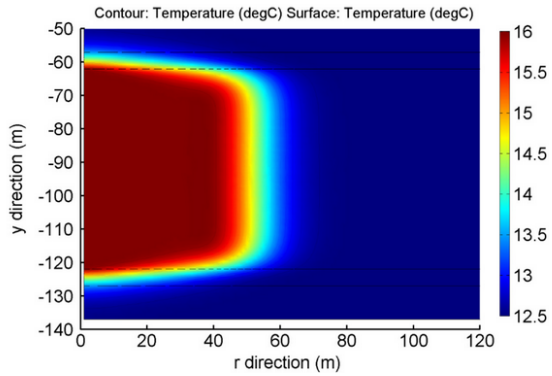

Figure 38: Warm well temperature profile from literature (Bozkaya et al., 2017)

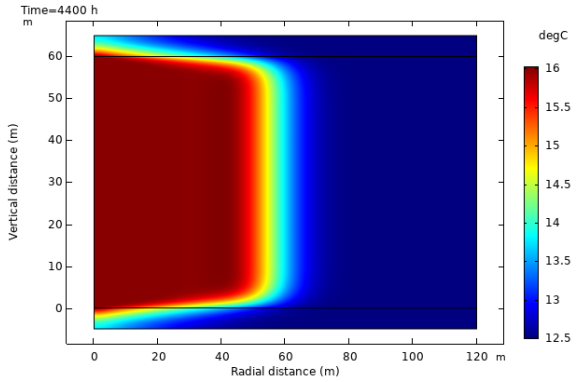

Figure 39: Warm well temperature profile obtained

  In the reference temperature profile on the left, it can be seen that the thermal penetration depth is close to 60 m, which is also the case in this work. It can also be seen that the shape of temperature profiles are similar.

- **Cold well**

  The maximum injection volume of ground water into the cold well was 57,000 m^3 in one season. Similar to the warm well, the injection time was calculated to be 1425 h based on a flow of 40 m^3/h.

Table 14: Injection parameters of the cold well in the reference model (Bozkaya et al., 2017)

Parameter	Value	Unit
Injection volume	57,000	m^3
Injection flow rate	40	m^3/h
Injection period	1425	h
Simulation time step	1	h
Initial temperature	11.5	°C
Injection temperature	8	°C
Aquifer radius	120	m
Clay layer height	5	m
Aquifer height	20	m

From the parameters listed in Table 14, after 1425 h of injection of ground water at 8°C, the temperature profile obtained is as shown in Figure 41.

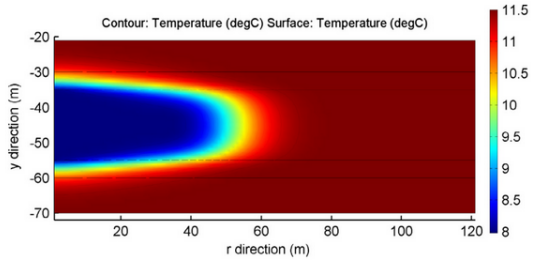

Figure 40: Cold well temperature profile from literature (Bozkaya et al., 2017)

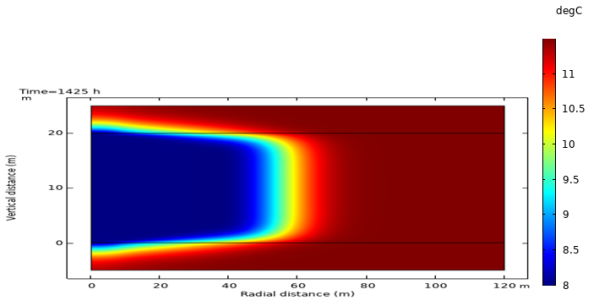

Figure 41: Cold well temperature profile obtained

Thermal penetration depth in the reference model (Figure 40) was found to be close to 60 m, which was the same in this work as well, but a difference in the shape of the temperature profiles was observed. It appears as if more heat transfer occurred between the clay layer and the aquifer layer in the reference model (Figure 40) than in the model developed in this work (Figure 41).

3.2 WWSHP system

In this section, the results of the simulation of waste water source heat pump system for winter and summer conditions are provided. The dimensions of the tubes used in waste water heat exchanger were optimized first. Then based on the optimized dimensions, winter and summer situations were simulated.

3.2.1 Winter model

- **Optimization of waste water heat exchanger tube dimensions**

  The winter model was simulated for 6 combinations of tube lengths and diameters. Standard HDPE tube lengths of 12 m and 30 m and tube inner diameters of 17 mm, 29 mm and 58 mm were chosen for simulations. To understand the effect of tube length and diameter on heat recovery and system performance, winter model was simulated for month of February which had the coldest day of the year. COP of the system (Figure 42) and heat recovered from sewage (Figure 43) on different days of February are plotted. It can be seen in Figure 42 that the smaller diameter options resulted in lower COP values. This was because of the fact that larger diameters lead to lower pressure drop, hence lower pump power required. The lowest COP value was observed for the combination of l_t = 30 m and $d_{i,t}$ = 17 mm while the highest COP was observed for $d_{i,t}$ = 58 mm options. Smaller tube diameters resulted in more heat recovery due to higher secondary water velocity (hence higher U_o).

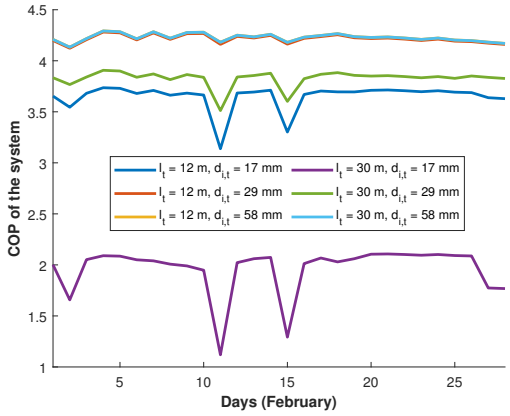

Figure 42: Optimization : Effect of tube dimensions on system COP

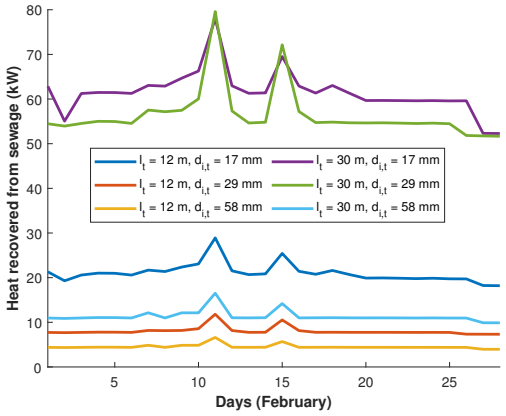

Figure 43: Optimization : Effect of tube dimensions heat recovered from sewage

It can be seen from Figure 43 that the highest heat recovered from sewage was for l_t = 30 m and $d_{i,t}$ = 17 mm. The lowest heat recovered was for l_t = 12 m and $d_{i,t}$ = 58 mm combination. For COP it was the other way around. The winter model was evaluated for all the winter months (September to December - January to May) to find the optimal heat exchanger tube dimensions. Table 15 provides seasonal values of COP, heat recovered from sewage, total electrical energy required to run the pump and the compressor along with the cost comparison. The cost column includes the cost of the waste water heat exchanger and the cost of electricity. Calculation of the cost of heat exchanger is explained in Equation 75 in Appendix A. The cost of electricity was considered to be 50.7 €/MWh (Greunsven and Derks, 2018). The system performance was measured as the amount of heat delivered to 'Doelen' (Q_{cond}) per unit cost (kWh/€).

Table 15: Optimization : Seasonal (winter) performance values of different tube dimension combinations

Dimensions		Q_{cond}	Q_{ww}	W_{elec}	N_t	**Cost (€)**			**kWh/€**	COP
l_t **(m)**	$d_{i,t}$ **(mm)**	**MWh**				**WWHEX**	W_{elec}	**Total**		
12	17	236	181	66	200	396	3346	3742	63	3.6
	29	**131**	**103**	**30**	**128**	**415**	**1521**	**1936**	**68**	**4.5**
	58	43	34	9	64	403	456	859	50	4.6
30	17	535	405	331	200	989	16782	17771	30	1.6
	29	**486**	**374**	**126**	**128**	**1037**	**6388**	**7425**	**65**	**3.9**
	58	188	148	41	64	1007	2079	3085	61	4.6

From Table 15 it was clear that the best two options were $d_{i,t}$ = 29 mm, l_t = 12 m and $d_{i,t}$ = 29 mm, l_t = 30 m. The 12 m option delivered 68 kWh/€, while the 30 m option delivered 65 kWh/€ which was only 4.6% lower. Thus, to make a choice between l_t = 12 m and l_t = 30 m, a comparison between the actual heat recovered and the required heat exchange with sewage was compared as shown in Figure 44. It was observed that the heat recovered in the case of l_t = 12 m option was much lower than what was necessary (Figure 44 (a)), while it was much better in the case of l_t = 30 m (Figure 44 (d)). Thus, making use of just one heat exchanger with l_t = 12 m was not sufficient to recover the required amount of heat. Considering that l_t = 12 m option was 3.8 times less expensive than l_t = 30 m option, 3 and 4 units of l_t = 12 m heat exchangers were evaluated to see if more heat could be recovered. For 3 and 4 units, the heat recovered exceeded the demand sometimes but was lower when the demand was actually higher (Figure 44(b) and Figure 44(c)). Difference between the required heat from sewage vs actual heat recovery is plotted for all the four cases as shown in Figure 44(e). When the heat recovered was higher than or equal to what was required, the difference is indicated as zero. Clearly, most of the time, the difference between required and actual heat recovery for l_t = 30 m option was the lowest. Not only that, the system complexity and overall costs would be much higher if 3 or 4 heat exchangers with 12 m tubes are installed. The second best option in terms of difference between actual and required heat recovery was 4 heat exchangers with l_t = 12 m tubes. But the cost of the heat exchangers, plus the cost of electricity for the l_t = 12 m option with 4 heat exchangers, went up to €7744 as opposed to the €7425 for one unit l_t = 30 m. Combining one l_t = 30 m heat exchanger with one l_t = 12 m heat exchanger would make the system more expensive and complex. Thus, l_t = 30 m and $d_{i,t}$ = 29 mm were chosen as the optimized tube dimensions.

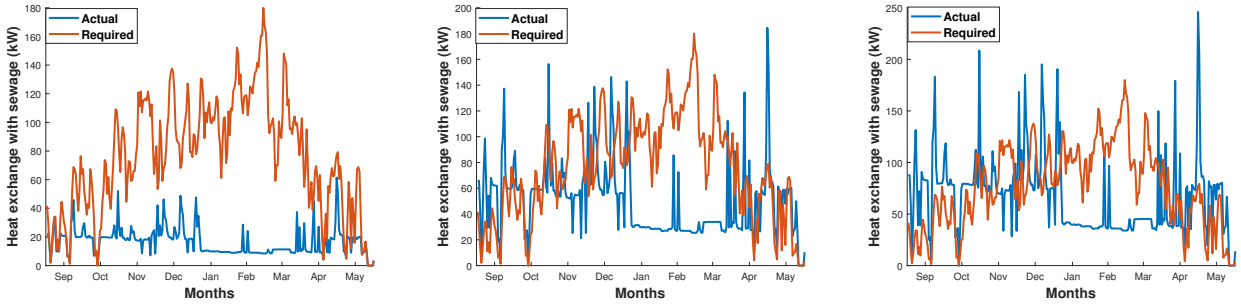

(a) l_t = 12 m, $d_{i,t}$ = 29 mm (1 unit)

(b) l_t = 12 m, $d_{i,t}$ = 29 mm (3 units)

(c) l_t = 12 m, $d_{i,t}$ = 29 mm (4 units)

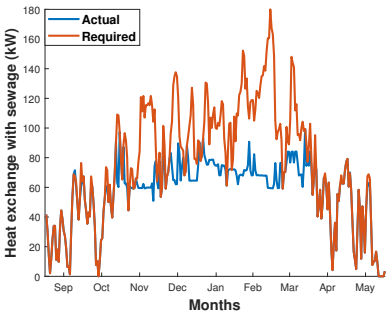

(d) l_t = 30 m, $d_{i,t}$ = 29 mm (1 unit)

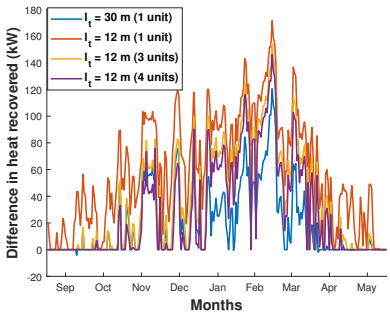

(e) Difference between required and actual heat recovery from sewage for all the 4 options

Figure 44: Optimization : Effect of tube dimensions and number of heat exchanger units on heat recovered from sewage (1 unit consists of 4 WWHEX connected in parallel)

- **Choice of polymer for waste water heat exchanger**

  The effect of waste water heat exchanger tube material on heat recovery and system performance was studied to ascertain relative performances. Each polymer had a different thermal conductivity value and each polymer tube required different thickness based on its material strength (calculation in Appendix A, Equation 73). Table 16 provides the results of the simulations carried out for different polymers to study the effect of tube material. The operating pressure of the closed secondary water piping system for thickness calculation was chosen based on the maximum pressure drop through the tubes.

Table 16: Optimization : Effect of waste water heat exchanger tube material on heat recovery

Polymer	k	thk_t	Rate	Q_{cond}	Q_{ww}	W_{elec}	Cost €		Total cost	kWh/€
	W/m K	mm	€/kg	MWh			WWHEX	W_{elec}	€	
PS	**0.14**	**0.50**	**0.90**	**530**	**407**	**141**	**513**	**7149**	**7661**	**69.2**
LDPE	0.30	2.00	0.57	331	257	80	1243	4031	5273	62.8
HDPE	0.46	0.85	0.54	632	483	192	474	9734	10209	61.9
PC	0.20	0.35	1.10	638	487	201	519	10165	10685	59.7
PPS	0.30	0.32	1.60	653	497	216	777	10941	11718	55.7

It is clear from Table 16 that PS had the best system performance with 69.2 kWh of heat delivered per unit cost. Due to its higher yield strength than LDPE or HDPE, tube thickness of 0.5 mm was sufficient to withstand the operating pressure. The heat recovered was 407 MWh which was lower than what was recovered by HDPE, PC & PPS tubes because of low thermal conductivity value. Considering the uncertainty in manufacturability and availability of PS tubes with 0.5 mm, the system performance was studied for a standard tube thickness value of 1.8 mm. Thus, for the constant tube thickness value of 1.8 mm, effect of thermal conductivity on system performance and economics was studied.

Table 17: Effect of polymer k_t on system performance and economics

Polymer	k	Rate	Q_{cond}	Q_{ww}	W_{elec}	Cost €		Total cost	kWh/€
	W/m K	€/kg	MWh			WWHEX	W_{elec}	€	
HDPE	**0.46**	**0.54**	**486**	**374**	**126**	**1037**	**6388**	**7425**	**65.5**
LDPE	0.30	0.57	361	280	88	1111	4462	5573	64.7
PS	0.14	0.90	183	143	41	1926	2094	4020	45.5
PC	0.20	1.10	264	205	61	2803	3113	5916	44.6
PPS	0.30	1.60	361	280	88	4591	4462	9052	39.9

Table 17 indicates that HDPE is the best choice of polymer when the tube thickness is 1.8 mm. Not only did it recover the most heat, the heat recovery was also the most economic. Although LDPE was the next closest, its thickness cannot actually be chosen as 1.8 mm as the minimum thickness necessary is 2 mm as in Table 16. Thus, HDPE was chosen as the tube material for the rest of the analysis.

- **Optimization : Effect of thermal enhancement of polymers on heat recovery**

  The effect of thermal enhancement of different polymers on the performance of waste water source heat pump is provided in Table 18. The heat recovered from sewage and the electrical power required was the highest for k_t = 1.89 W/m K.

Table 18: Winter model : Effect of 'k_t' values on system performance

Matrix	Filler	Filler	k_t	Q_{cond}	Q_{ww}	W_{elec}	Cost €		Total cost	kWh/€
		(%)	W/m K	MWh			WWHEX	W_{elec}	€	
PPS	SHB	0	0.30	361	280	88	**4591***	4462	9053	39.9
		10	**1.83**	**650**	**495**	**211**		**10698**	**15289**	**42.5**
		30	**1.89**	**650**	**495**	**211**		**10698**	**15289**	**42.5**
PE	Graphite	**10**	**0.65**	**573**	**439**	**134**	**572***	**6794**	**7366**	**77.8**
		30	**1.8**	**650**	**495**	**157**		**7960**	**8532**	**76.2**
LDPE	AlN	0	0.30	361	280	88	**1111***	4462	5573	64.8
		30	**1.08**	**637**	**487**	192		**9734**	**10845**	**58.7**
PS	Graphite	10	0.25	315	245	75	**1926***	**3803**	**5729**	**55.0**
		30	**0.9**	**624**	**477**	**182**		**9227**	**11153**	**55.9**
HDPE	-	0	0.46	486	374	126	1037*	6388	7425	65.5

Note :

- Cost of PE is 0.31 €/kg [4] and ρ of PE is 920 kg/m^3 (T'Joen et al., 2009).
- * - Cost of fillers and the additional cost of adding them to polymers was not known. Hence the cost of HEX was considered to be the cost of the heat exchanger without any filler.

Table 18 illustrates the effect of thermal enhancement of different polymers on the performance of the WWSHP system. For the same number of tubes, tube dimensions and heat demand, the heat supplied to the 'Doelen' per unit cost (heat exchanger + electricity) was compared to find the best combination. The total heat demand in winter was 495 MWh. This demand was met by PPS + SHB and PE + Graphite. Among those two options, PE + Graphite was more economic as the system supplied 76.2 kWh/€, while the WWSHP system with PPS + SHB heat exchangers supplied 42.5 kWh/€ to 'Doelen'. There is a huge margin for increase in the total cost of PE + Graphite option despite the addition of cost of fillers. PE with 10% graphite filler is the best choice among all the alternatives, but to meet the required heat demand PE with 30% is the best choice .

- **Winter model - Tube and heat exchanger details**

  The winter and summer WWSHP models were simulated with the tube properties mentioned in Table 19. Four heat exchangers were considered as explained in the modeling section.

Table 19: Simulation parameters of WWSHP Winter model

Parameter	Value	Unit
l_t	30	m
$d_{i,t}$	29	mm
thk_t	1.8	mm
k_t	0.46	W/m K
N_{hex}	4	-

  - **Stream temperatures**

    Based on different sewage temperature values, secondary water inlet and outlet temperatures were found to optimize system COP and heat recovery as described in the modeling section. Based on secondary water inlet (to waste water heat exchanger) temperature, heat pump evaporation temperature was calculated (2 K lower). Condensation and evaporation temperature of

[4] New Media Publisher

the heat pump, sewage inlet and outlet temperatures and secondary water temperatures for the winter model are plotted in Figure 45. In the figure, secondary water temperatures indicated are at the inlet and outlet of waste water heat exchanger. It can be seen from Figure 45 that the optimum value COP of the system was calculated by the model to be at secondary water $\Delta T \approx 10$ K. No change in sewage temperature can be seen. Based on these stream temperatures, the winter model was evaluated and the results obtained are described below.

– **Heat recovered from sewage**

The variation of heat recovered from sewage ($\dot{Q}_{ww}$) with time is plotted in Figure 46. It can be seen that the maximum heat recovered from sewage went up to a 100 kW. At times of zero heat demand, heat recovered from sewage was naturally zero, meaning that the waste water source heat pump was not operational on those days. It can be seen in Figure 28 that the demand is zero around mid - October and end of May which is also where the heat recovered from sewage is zero.

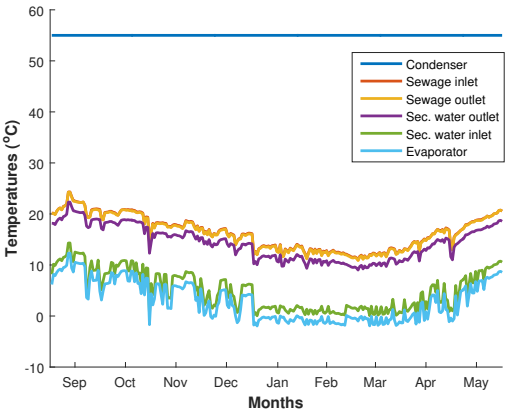

Figure 45: WWSHP Winter model : Temperatures of different streams

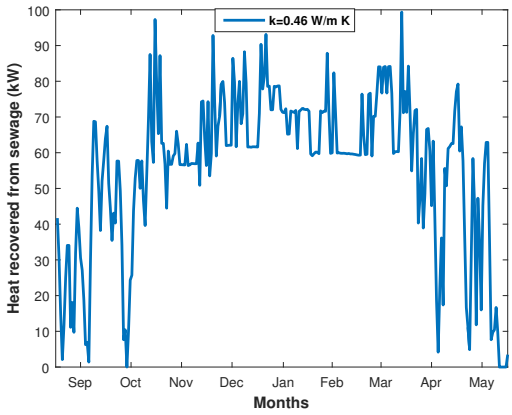

Figure 46: WWSHP Winter model : Heat recovered from sewage

– **Required vs Actual heat recovered from sewage**

Figure 47 shows the difference between the heat recovery required and the actual heat recovered from sewage. On the days with either low sewage level or low sewage temperatures, the actual heat recovered from sewage went down. It can be seen in Figure 47 that the difference between required and actual is large between mid-November till almost the end of March. Although sewage level in these months was not significantly lower than other months, sewage temperature was lower than other months. Thus, the difference in the required and actual heat recovery can be attributed to low sewage temperatures. The maximum heat recovered at any instant was also limited by the sewage level which affected the number of tubes submerged in sewage flow.

– **Number of tubes required for heat exchange vs actual number of tubes submerged in sewage flow**

It can be seen in Figure 48 that the number of tubes necessary to recover the required heat was often higher than the number of tubes actually submerged in sewage flow. Thus, the actual heat recovered was more often lower than the heat to be recovered from sewage. In some cases, the number of tubes submerged in sewage flow was higher than what was required, in those cases the model only counted the tubes actually required to estimate the heat recovered. In reality, flow can be switched off in one of the heat exchangers if the excess heat is not required. The maximum number of 29 mm tubes that can be placed on one side was calculated to be 64, which implies 32 tubes per heat exchanger. Thus, if the number of submerged tubes are close to 32 higher than what is required, then the secondary water flow to one of the heat exchangers can be stopped.

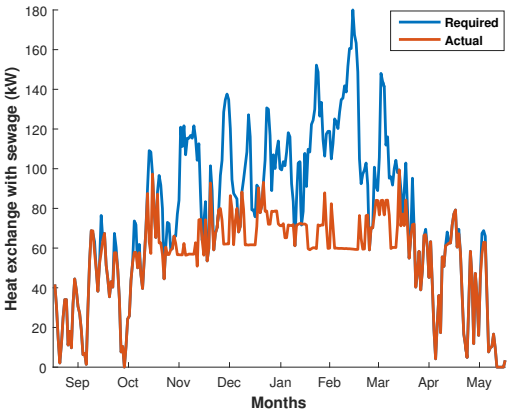

Figure 47: WWSHP Winter model : Heat recovery required vs actual heat recovered

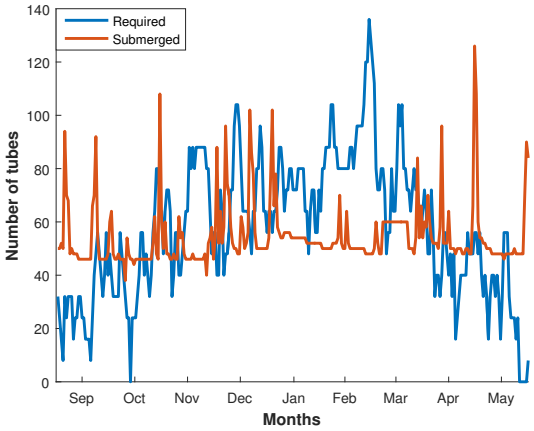

Figure 48: WWSHP Winter model : Number of tubes required vs the actual number of tubes submerged in sewage flow

– **Instantaneous COP of the system**

The instantaneous COP of the system was found to vary between a maximum of 5.5 to a minimum of 2.9. Discontinuities in the plot in Figure 49 were due to no heat recovery which meant that the heat pump was not operational. When more heat was recovered from sewage (Figure 46), COP of the system went down. This was attributed to increase in secondary mass flow (Figure 50) due to increase in heat recovery requirement. Increase in secondary water mass flow resulted in an increase in pump power. Furthermore, higher heat recovery increased the compressor power due to increase in refrigerant flow. Refer to Figure 77 and Figure 78 in Appendix E to see the variation in compressor and pump power with time.

– **Secondary water flow required**

The mass flow of secondary water was found to vary between 0 to 3.1 kg/s. It varied linearly with the heat to be recovered from sewage at any given time. The secondary water required to recover the defined quantity of heat is plotted in Figure 50

– **U_o value of the heat exchanger**

The highest value of U_o attained in the waste water heat exchanger was 174 W/m^2 K in the winter. The average U_o attained was 149 W/m^2 K.

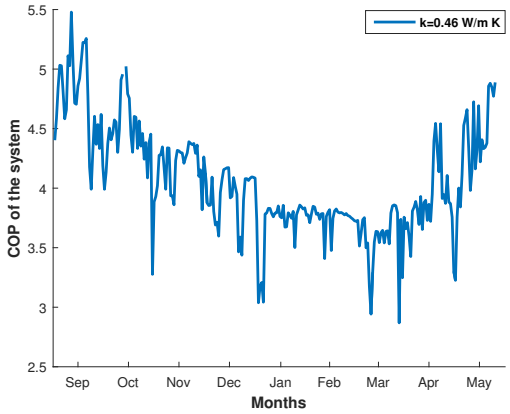

Figure 49: WWSHP Winter model : COP of the system

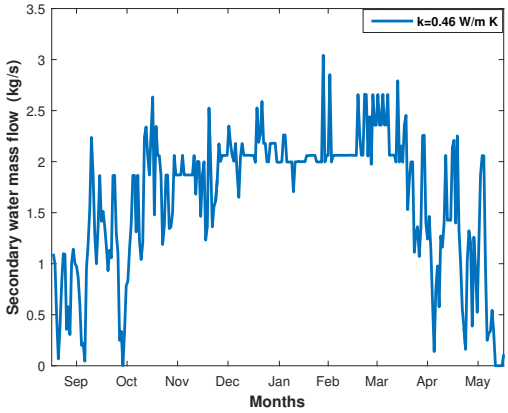

Figure 50: WWSHP Winter model : Secondary water mass flow required

- **Heat exchanger parameters**

Table 20: WWSHP Winter model : Heat exchanger parameters

Number of heat exchangers	4
Total length (m)	60
Total number of tubes	128
Heat exchange area (m^2)	48.5×4
Maximum secondary water flow (kg/s)	3.1
Maximum sewage flow (kg/s)	606
Maximum heat exchange (kW)	100
Average Δp_{sw} (bar)	9.7
Capacity in kW/m^2	≈ 1

- **Effect of thermal conductivity**

  The effect of thermal enhancement of polymers on heat recovery and system performance was studied. Waste water source heat pump system behaviour when PE with 10% and 30% graphite filler was used as the heat exchanger tube material is described in detail in this section. With 10% graphite filler, the k_t value of PE is 0.65 W/m K and with 30% filler, k_t is 1.8 W/m K.

  - **Effect on heat recovery**

    As expected, increase in thermal conductivity of heat exchanger tubes resulted in increase in heat recovery from sewage. For k_t = 0.65 W/m K, the maximum value of heat recovered was 126 kW while for k_t = 1.8 W/m K, it was 152 kW. Thus, 21% increase in heat recovery was seen. Refer to Figure 51 to see the heat recovery trend.

  - **Effect on instantaneous system COP**

    As seen before, more heat exchange through the waste water heat exchanger demanded more secondary water flow and indirectly more refrigerant flow. Both of these effects led to increase in pump and compressor power. Thus, increase in thermal conductivity led to decrease in system COP. Average COP for k_t = 0.65 W/m K was 3.9 while it was 3.6 for k_t = 1.8 W/m K. Variation of instantaneous COP of the system is plotted in Figure 52.

  - **Effect of number of tubes required for heat exchange**

    Clearly, increase in thermal conductivity of heat exchanger tubes led to higher U_o, which reduced the heat exchange area required which led to reduction in the number of tubes required. Figure 53 describes the effect of k_t on number of tubes required. The maximum number of tubes required reduced from 104 to 56 upon thermal enhancement. Thus, a 46% reduction in number of tubes required was seen.

  - **Effect on U_o of the heat exchanger**

    The U_o value of the heat exchanger increased from an average value of 186 W/m^2K to 296 W/m^2K upon thermal enhancement of PE. Thus, the U_o value increased by 57%. Variation of U_o with time is plotted in Figure 54.

- **Parameters of the winter model**

  Table 21 indicates the installation capacity required for the different equipment of the system. The dimensions, cost and other parameters of the different equipment are provided in Appendix E.

Table 21: Maximum capacities of different equipment of the WWSHP system

Equipment	Capacity (kW)	
	k_t = 0.46	k_t = 1.89
WWHEX	100	152
Evaporator	100	152
Condenser	132	201
Compressor	33	50
Pump	13	70

Note : k_t in Table 21 is in W/m K.

- **Thermal enhancement of PE with graphite**

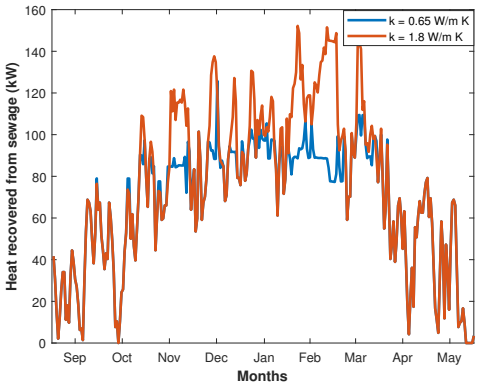

Figure 51: WWSHP Winter model : Effect of thermal enhancement of PE with Graphite on heat recovered

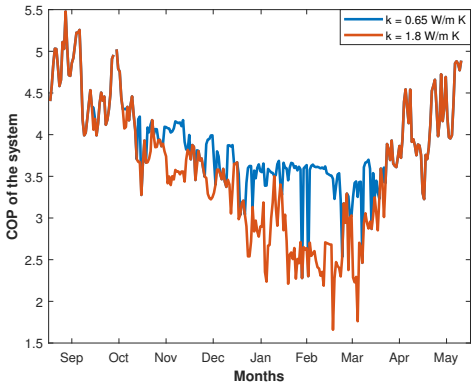

Figure 52: WWSHP Winter model : Effect of thermal enhancement of PE with Graphite on system COP

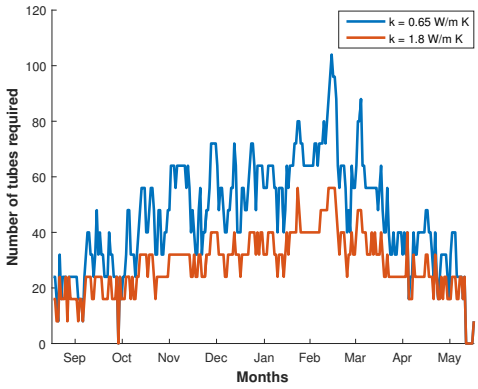

Figure 53: WWSHP Winter model : Effect of thermal enhancement of PE with Graphite on number of tubes required

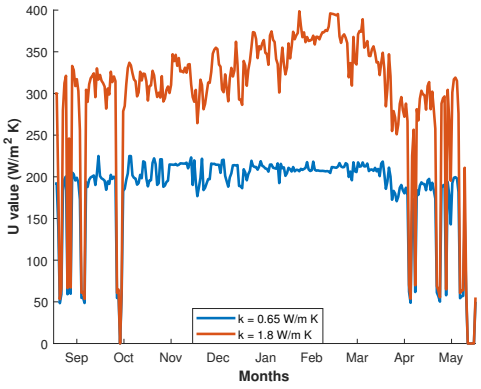

Figure 54: WWSHP Winter model : Effect of thermal enhancement of PE with Graphite on U value

3.2.2 Summer model

In the summer model, the evaporation temperature was fixed at 8°C, but the condensation temperature was a function of waste water temperature as explained in the modeling section. To find the optimum con-

densation temperature, the condensation temperature was varied from 10 K above sewage temperature to 50 K above sewage temperature. The effect of varying the condensation on various aspects of heat recovery is described first. As explained in the modeling section, the heat exchanger tube dimensions for the summer model were the optimized tube dimensions of the winter model.

- **Sewage temperature and condensation temperature**

  Sewage temperature in the summer varied between 19°C to 21.5°C (see Figure 55). The condenser temperature sets chosen were 10 K to 50 K (in steps of 10) higher than sewage temperature (Figure 56).

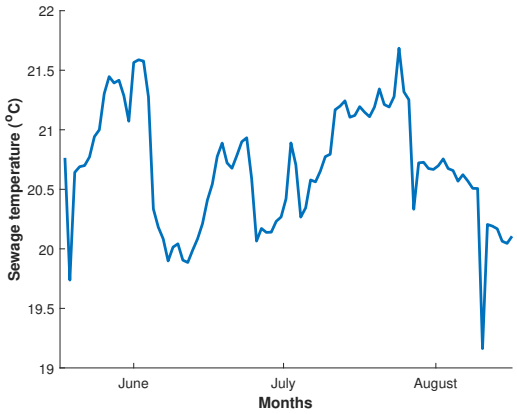

Figure 55: WWSHP Summer model : Sewage temperature

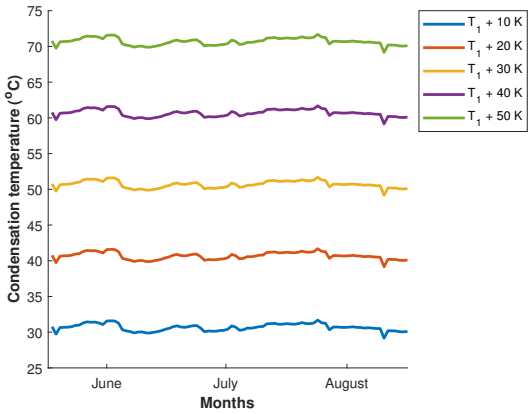

Figure 56: WWSHP Summer model : Condenser temperature options

- **Effect of condensation temperature on heat rejected to sewage**

  In Figure 57, the blue curve marked 'Required' was the required amount of heat that had to be rejected to the sewage to utilize the waste water heat exchanger's potential to exchange 180 kW. From Figure 57, it is clear that higher condensation temperatures lead to higher heat rejection to the sewage. The difference between 'Required' and what is actually rejected reduced with increase in condensation temperature.

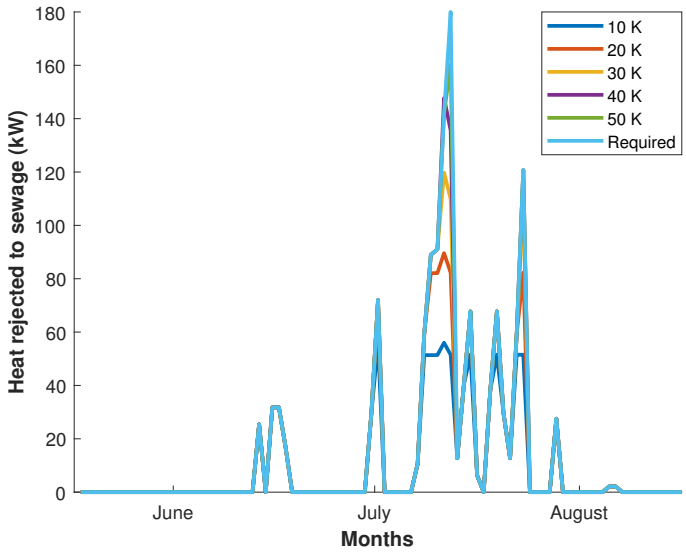

Figure 57: WWSHP Summer model : Effect of condenser temperature on heat rejection to sewage

- **Effect of condensation temperature on COP and mass flow of secondary water**

  As in the case of the winter model, more heat exchange led to increase in secondary water flow (Figure 59), which led to increase in compressor (indirectly) and pump work, which reduced the COP of the system. Thus, it can be seen that the highest COP is for $\Delta T = 10$ K (Figure 58).

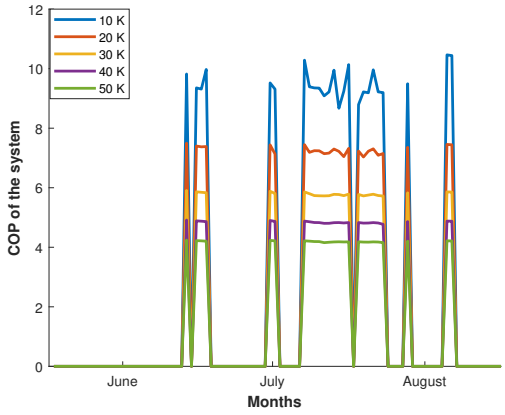

Figure 58: WWSHP Summer model : Effect of condenser temperature on COP

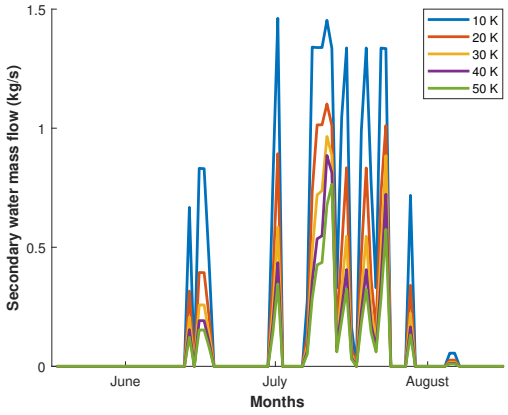

Figure 59: WWSHP Summer model : Effect of condenser temperature on sec. water mass flow

- **Choice of condenser temperature**

  The condenser temperature was chosen on the basis of the amount of heat rejected to sewage. Higher condenser temperatures led to more heat rejection to sewage but at the cost of electrical power. Thus, the temperature at which the heat rejected to sewage was closest to what was required and yet the power consumption was not significantly higher, was chosen. Total heat to be rejected to sewage in the summer was 30.4 MWh. The total heat rejected to sewage for different condenser temperatures is provided in Table 22. It was clear from the table that the increase in heat rejected to the sewage was not as drastic as it was till T_{cond} - T_{ww} = 20 K. The COP of the system decreased, compressor power consumption increased while the difference between the required heat exchange and actual heat exchange reduced with increase in condensation temperature. The reduction in ΔQ was drastic from T_{cond} - T_{ww} = 10 K to 20 K. After that the reduction was much more gradual. Thus, T_{cond} = T_{ww} + 20 K was chosen for the summer model.

Table 22: WWSHP Summer model : Effect of condenser temperature on heat extracted from 'Doelen'

T_{cond} - T_{ww} (K)	Q_{cond} (MWh)	W_{comp} (MWh)	ΔQ (MWh)	COP
10	20.2	1.8	10.2	9.3
20	25.5	3.0	4.9	7.2
30	27.9	4.1	2.5	5.8
40	29.5	5.0	0.9	4.8
50	29.9	5.8	0.5	4.2

Note : In Table 22, $\Delta Q = Q - Q_{\text{cond}}$, where $Q = 30.4$ MWh is the required heat rejection to the sewage.

- **Summer model characteristics**

  - **Stream temperatures**

    Figure 60 shows all the temperatures of different streams of the summer model. It can be seen that there was negligible change in sewage temperature even after heat was rejected to it. The

evaporation temperature of the heat pump was set as 8°C and the condensation temperature was close to 40°C.

– **Heat rejected to sewage**
Maximum value of heat rejected to sewage was 90 kW. The variation of heat rejection to sewage is plotted in Figure 61.

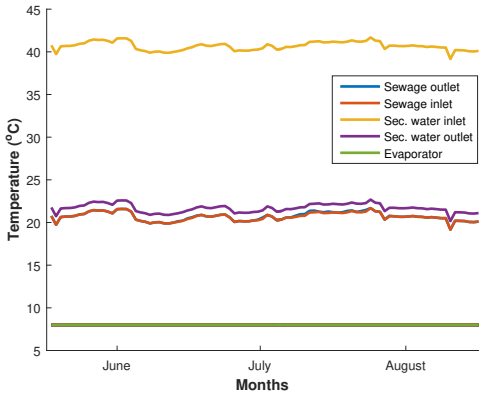

Figure 60: WWSHP Summer model : Temperatures of different streams

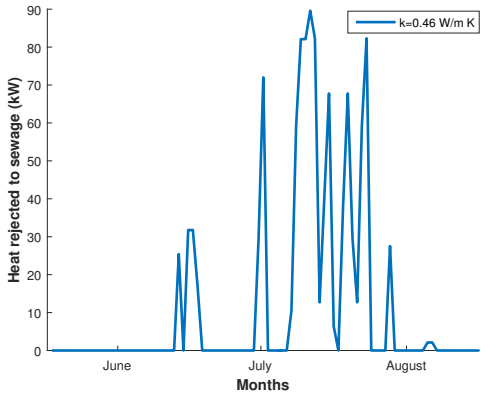

Figure 61: WWSHP Summer model : Heat rejected to sewage in the summer

– **Number of tubes required for heat rejection**
It can be seen from Figure 62 that most of the times the number of tubes submerged in sewage flow were generally higher than what was required. But at peak load, 104 tubes were required for heat exchange, and only about 52 tubes were submerged.

– ***COP* of the system**
The instantaneous COP of the system was found to vary between a minimum value of 5.9 to a maximum of 7.5, excluding the zero values obtained when the heat pump was not operational (see Figure 63).

– **U_o value of the heat exchanger**
The maximum U_o value attained in the summer was 177 W/m^2 K which is similar to what was obtained in the winter (174 W/m^2 K). The average value of U_o attained was 143 W/m^2 K.

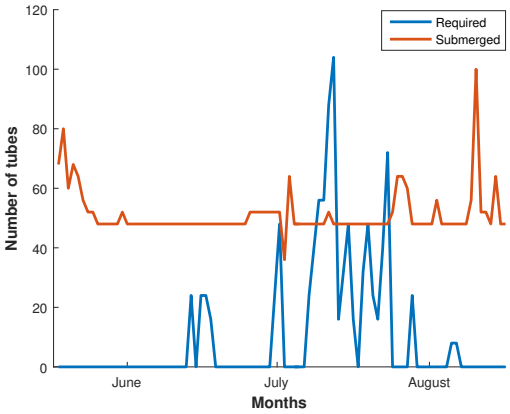

Figure 62: WWSHP Summer model : Number of tubes required vs actually submerged in sewage flow

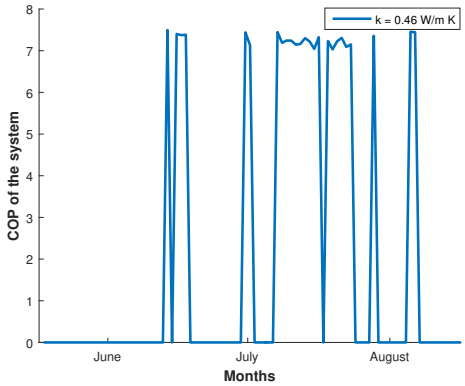

Figure 63: WWSHP Summer model : COP of the system

– **Effect of thermal conductivity**
Similar to the winter model, the effect of thermal enhancement of the polymer tubes used in the waste water heat exchanger was studied. In this model, just the base case with HDPE and no filler was compared with k_t = 1.89 W/m K. Significant difference was not observed since the heat pump was not operational for the majority of the times and the number of tubes submerged in sewage flow were low most of the times.

Table 23: WWSHP Summer model : Effect of k_t value on system performance

k_t	Q_{evap}	Q_{cond}	W_{comp}	$W_{sw,pump}$	COP
(W/m K)	(MWh)				
0.46	22.5	25.5	3.0	0.08	7.3
1.89	26.8	30.4	3.6	0.31	6.9

Increase in k_t from 0.46 to 1.89 W/m K resulted in an increase in U_o value from 143 W/m^2 K to 290 W/m^2 K which was almost twice.

- **Parameters of the summer model**
Table 24 indicates the maximum capacities of the different components of the WWSHP system required for installation.

Table 24: Maximum capacities of different equipment of the WWSHP system

Equipment	Capacity (kW)	
	k_t = 0.46	k_t = 1.89
WWHEX	90	180
Condenser	90	180
Evaporator	79	158
Compressor	11	22
Pump	0.4	5

Note : k_t in Table 24 is in W/m K.

3.2.3 Summary of the WWSHP system

A comparison of WWSHP system performance in the winter and summer is provided in Table 25. Clearly, increase in thermal conductivity of the polymer tubes enhanced heat recovery in the winter much more than in the summer. The electrical energy consumption was higher in the winter due to longer period of operation (9 months) and more heat recovery. Seasonal COP value of summer was higher than winter for both the cases (of thermal conductivity). The increase in U_o in both the cases with increase in k_t from 0.46 W/m K to 1.89 W/m K was almost two times the initial values.

Table 25: Summary of WWSHP system performance in the winter and summer

Model	k_t	U_o	Q_{cond}	Q_{evap}	W_{elec}	Cost (€)			kWh/€	COP
	(W/m K)	(W/m^2 K)	(MWh)			WWHEX	W_{elec}	Total		
Winter	0.46	149	**486**	374	126	1037*	6388	7425	65.5	3.9
Summer		143	26	**23**	3		152	1189	19.3	7.3
Winter	1.89	296	**650**	495	211		10698	11735	55.4	3.1
Summer		290	30	**27**	4.0		203	1240	21.8	6.9

Note - * indicates that the cost of WWHEX does not include the cost of filler and their inclusion in the polymers

The system performance was measured in terms of kWh heat supplied or removed from or to 'Doelen' respectively per € spent on the waste water heat exchanger and electricity. The system performance was higher for the winter system than the summer system. It was interesting to note that the performance of the winter system decreased from 65.5 kWh/€ to 55.4 kWh/€ when k_t was increased. This implied that higher k_t although improved heat recovery, led to a higher increase in electrical power requirement.

In the winter, for a 34% increase in heat delivered to 'Doelen' (from 486 MWh to 650 MWh) due to thermal enhancement of polymer tubes, the increase in the cost of heat supply was by 58%. In the summer, thermal enhancement of polymer tubes led to 4% increase in cost of heat removal from the 'Doelen' with an increase in the amount of heat removed from 'Doelen' by 17%. Thus, more heat exchange from the waste water heat exchanger appeared to be more beneficial in the summer than in the winter.

3.3 WWSHP + ATES model

3.3.1 Winter model

- **Warm well extraction temperature and cold well temperature evolution**

  Ground water extraction temperature decreased from 18°C to 13.7°C in a span of 9 months. The initial temperature of the cold well was 10°C. Due to injection of ground water into the cold well at 8°C, the average cold well temperature went down to 8.8°C in a span of 9 months.

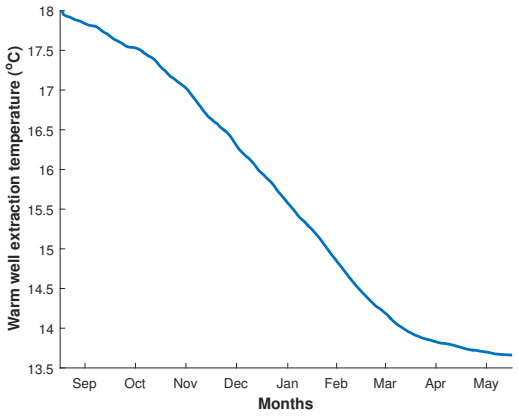

Figure 64: WWSHP + ATES Winter model : Warm well extraction temperature

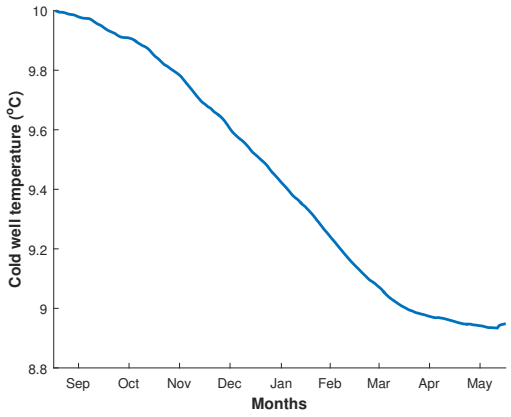

Figure 65: WWSHP + ATES Winter model : Cold well temperature

- **Heat extracted from sewage and aquifer**

  The maximum heat recovered from sewage was 139 kW, and from the aquifer it was 145 kW. The heat extracted from the aquifer gradually decreased after January due to reduction in extraction temperature (Figure 64). Secondary water was heated by sewage from 0°C to 7°C in the waste water heat exchanger, then it was heated from 7°C to a temperature 2 K lower than warm well extraction temperature. The quantity of heat recovered from sewage depended on the calculated heat rejection duty. The initial trends in both the plots in Figure 66 and 67 were similar due to similar ΔT values across both the heat exchangers. Later, the ΔT across the ground water heat exchanger reduced due to reduction in extraction temperature.

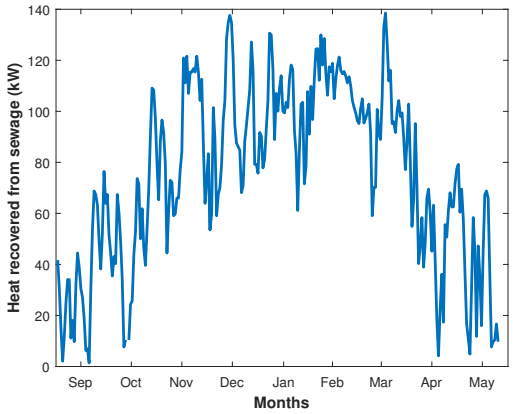

Figure 66: WWSHP + ATES Winter model : Heat recovered from sewage

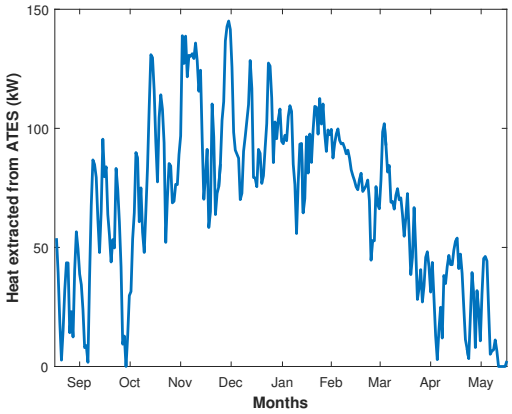

Figure 67: WWSHP + ATES Winter model : Heat extracted from aquifer

- **Ground water extraction rate**

  Ground water extraction flow rate was calculated based on the ΔT_{sw} that had to be achieved in the ground water heat exchanger. Thus, as the ground water extraction temperature dropped, the amount of heat that could be extracted from the aquifer dropped, which led to a decrease in the groundwater extraction rate. Thus, the trend of extraction rate in Figure 68 was the same as the trend of heat extraction from aquifer (Figure 67).

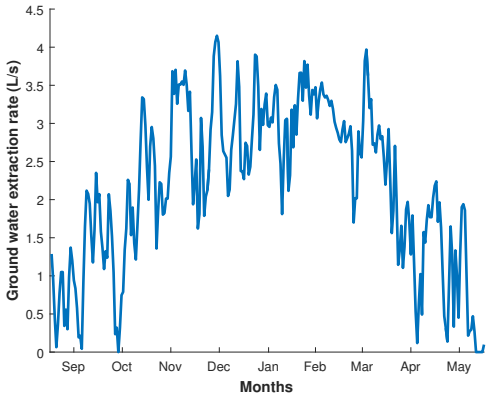

Figure 68: WWSHP + ATES Winter model : Ground water extraction rate

- **Secondary water temperatures**

  Figure 69 shows the variation of secondary water temperatures at different points of the system. At the inlet and outlet of the waste water heat exchanger, the secondary water temperatures were 0°C and 7°C. At the outlet of the groundwater heat exchanger, the secondary water temperature was 2 K lower than warm well extraction temperature. Thus, due to reduction in ΔT_{sw} across the ground water heat exchanger, the heat extracted from ground water reduced with time.

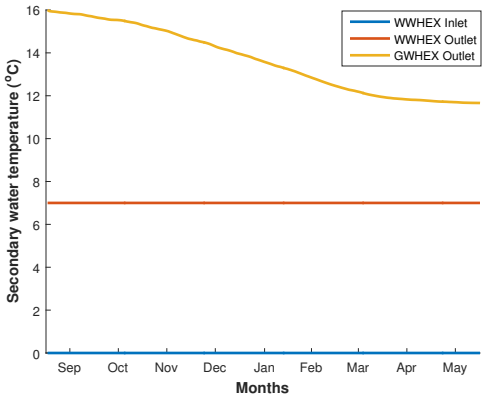

Figure 69: WWSHP + ATES Winter model : Secondary water temperatures

- **Instantaneous COP of the system**

  The instantaneous COP of the system was found to vary between a maximum of 3.9 and a minimum of 2. Like in the case of the WWSHP model, higher heat recovery led to lower COP. As explained before this was due to increase in mass flow of secondary water (to recover more heat) which led to higher pump and compressor power consumption.

- **Effect of thermal conductivity of polymer tubes on system performance**

  Effect of increase in thermal conductivity of polymer tubes of the waste water heat exchanger on the overall performance of the WWSHP + ATES system was studied by considering the lowest (0.46 W/m K) and the highest k_t (1.89 W/m K) values of the tube.

Table 26: WWSHP + ATES Winter model : Effect of k_t value on system performance

k_t	Q_{ww}	Q_{aq}	Q_{evap}	Q_{cond}	W_{comp}	$W_{sw,pump}$	$W_{gw,pump}$	COP
(W/m K)	(MWh)							
0.46	481	453	934	1244	309	150	4	2.7
1.89	498	464	962	1280	318	196	4	2.5

From Table 26 it is clear that increase in thermal conductivity of polymer tubes did not affect the system performance much. The heat extracted from sewage only increased from 481 MWh to 498 MWh at the expense of 46 MWh increase in secondary water pump power. The limit in temperature rise of secondary water in the WWSHP + ATES model was the reason for the limitation in the amount of heat recovered from sewage. Due to increase in k_t more heat was recovered from sewage, but since ΔT_{sw} was fixed, the mass flow of secondary water increased much more. Thus the secondary water pump power increased.

- **Parameters of the winter model**

  Table 27 indicates the maximum capacities of different equipment of the WWSHP + ATES system. For k_t = 0.46 W/m K, the maximum heat recovered from sewage was 139 kW and the corresponding maximum heat extracted from aquifer was 145 kW. But, when 180 kW was extracted from the waste water for k_t = 1.89 W/m K, it was seen that only 139 kW was extracted from the aquifer. On a different day, 145 kW was still recovered from the aquifer for the k_t = 1.89 W/m K case, but not at the same time that 180 kW was recovered from the sewage. Thus, although the maximum capacity of the ground water heat exchanger mentioned in Table 27 is 145 kW, the maximum evaporator duty is not equal to 180 + 145 kW. The maximum evaporator duty was obtained when 180 kW was recovered from the sewage and 139 kW was recovered from the aquifer.

Table 27: Maximum capacities of different equipment of the WWSHP + ATES system

Parameters	Capacity (kW)	
Equipment	k_t = 0.46	k_t = 1.89
WWHEX	139	180
Ground water HEX	145	145
Evaporator	284	319
Condenser	376	424
Compressor	92	99
Sec. water pump	93	195

3.3.2 Summer model

Results of the WWHEX + ATES summer model are presented in this section.

- **Cold well extraction temperature and warm well temperature evolution**

  The cold well extraction temperature increased from 8.8°C to 9.4°C in the summer due to inflow of ground water from the regions outside the thermal penetration depth. Injection of hot ground water into the warm well increased its average temperature from 13.7°C to 15.9°C. Thus, at the end of one year, the ΔT between the two wells reduced from 8°C to 6.5°C. The temperature profiles were linear due to constant rate of injection and extraction from warm and cold wells respectively.

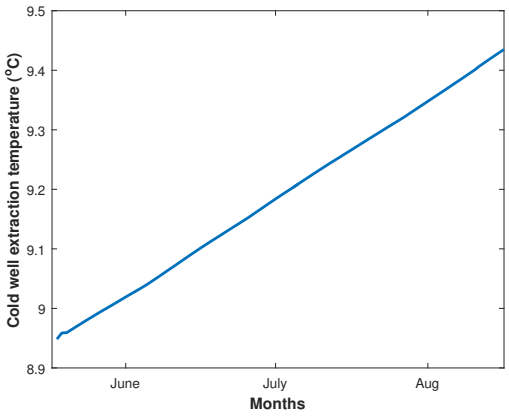

Figure 70: WWSHP + ATES Summer model : Cold well extraction temperature

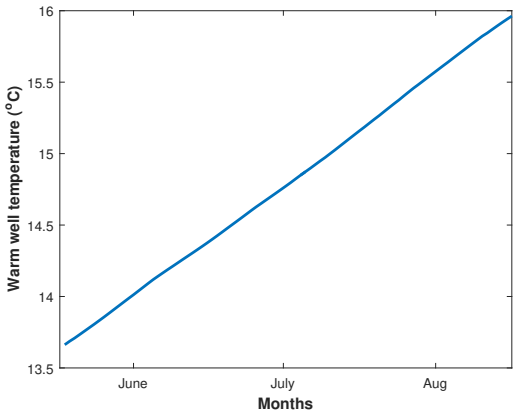

Figure 71: WWSHP + ATES Summer model : Warm well temperature

- **Heat extracted from condenser and sewage**

  The heat to be injected into the warm well to maintain thermal balance was obtained from the condenser of the heat pump and from sewage. Heat extracted from the condenser was much larger than what was extracted from the sewage. The chilled water from the Doelen's cooling network was cooled from 14°C to 8°C in the evaporator, which provided large quantities of heat. The amount of heat recovered from sewage was low due to a small ΔT across the waste water heat exchanger. Thus, majority of the heat required to replenish the warm well came from the condenser of the heat pump.

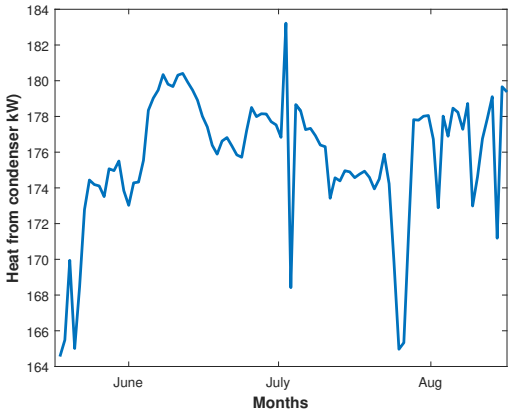

Figure 72: WWSHP + ATES Summer model : Heat extracted from condenser

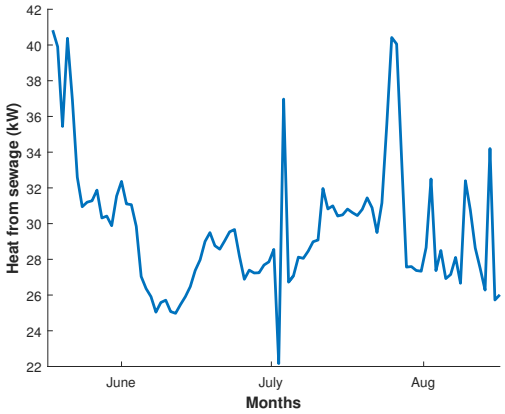

Figure 73: WWSHP + ATES Summer model : Heat extracted from sewage

- **Secondary water mass flow and temperatures**

  Figure 75 indicates the secondary water temperatures at the inlet and outlet of the waste water heat exchanger. The inlet temperature was fixed at 17°C, and the outlet temperature was 1 K lower than the waste water temperature. Figure 74 indicates the mass flow of secondary water. It can be seen that the point at which the secondary water outlet temperature was the lowest, was also the point where the mass flow of secondary water was the highest. This was to ensure that the required amount of heat was recovered. The secondary water mass flow varied from 1.9 kg/s to 6.5 kg/s.

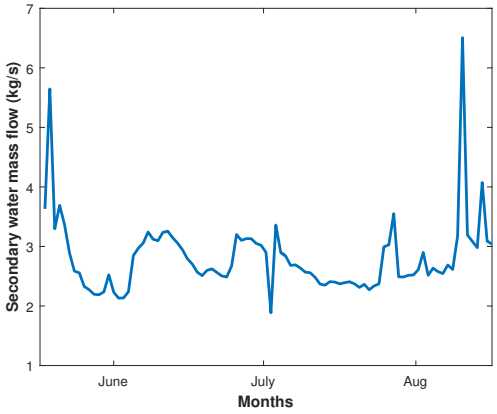

Figure 74: WWSHP + ATES Summer model : Secondary water mass flow

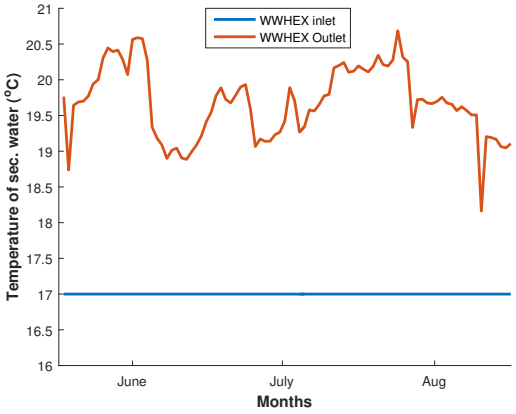

Figure 75: WWSHP + ATES Summer model : Secondary water temperatures

- ***COP* of the system**

  The COP values in the summer model were higher due to large heat extraction from condenser at the cost of low compressor power consumption. The compressor power consumption was low due to a small temperature lift across it from 6°C to 18°C. In the winter the temperature lift was 57°C, thus the compressor power consumption was significantly higher in the winter, which reduced the COP.

- **Effect of thermal conductivity of polymer tubes on system performance**

  Similar to the winter model the effect of increasing the thermal conductivity of polymer tubes was studied for the lowest and highest k_t values.

Table 28: WWSHP + ATES Summer model : Effect of k_t value on system performance

k_t	Q_{cond}	Q_{ww}	Q_{tot}	Q_{evap}	W_{comp}	$W_{sw,pump}$	$W_{gw,pump}$	COP
(W/m K)	(MWh)							
0.46	388	65	453	368	20	16	4	9.2
1.89	334	130	464	318	17	161	4	1.7

As expected, the increase in thermal conductivity of the polymer tubes of the waste water heat exchanger led to increase in heat recovery from sewage (by two times), which in turn reduced the amount of heat to be extracted from the condenser Table 28. Increase in heat extraction from sewage led to increase in secondary water mass flow, which resulted in increase in electricity consumption and reduction in the system COP.

- **Parameters of the WWSHP + ATES system**

  Table 29 enlists the maximum capacities of the different equipment used in the WWSHP + ATES system. The capacities of most of the equipment are smaller than that of the winter model, except for the secondary water pump rating for the k_t = 0.46 W/m K case. The installation of these equipment must be based on the maximum capacities among the winter and summer systems, since the same equipment are used in both the seasons.

Table 29: Maximum capacities of different equipment of the WWSHP+ATES system

Parameters	Capacity (kW)	
Equipment	k_t = 0.46	k_t = 1.89
Evaporator	174	170
Condenser	183	179
WWHEX	41	75
Ground water HEX	41	75
Compressor	9	9
Sec. water pump	119	127

3.3.3 Summary of WWSHP + ATES System

The system performance in winter was measured as the total heat supplied to the 'Doelen' (Q_{cond}) per unit cost of the investment made on the waste water heat exchanger and the ground water heat exchanger in addition to the cost of electricity. In summer, the performance was measured based on the amount of heat removed from the 'Doelen' (Q_{evap}). Since the cost of the heat pump is a common factor in both this and the WWSHP system, it was not considered for the analysis. The cost estimation of the ground water heat exchanger is described in Table 38 in Appendix E.

Table 30: Summary of WWSHP + ATES system performance in the winter and summer

Model	k_t	Q_{cond}	Q_{evap}	Q_{ww}	Q_{aq}	W_{elec}	Cost (€)			kWh/€	COP
		(MWh)					HEX	W_{elec}	Total		
Winter	0.46	1244	934	481	453	463	12937	23474	36411	34.2	2.7
Summer		388	368	65	453	40		2028	14965	24.6	9.2
Winter	1.89	1280	962	498	464	518		26263	39200	32.7	2.5
Summer		335	318	130	464	182		9227	22164	14.3	1.7

It is clear from Table 30 that the performance of the winter model (kWh/€) was better than the performance of the summer model for both the k_t values. It can also be seen from the table that the total quantity heat extracted from the aquifer, Q_{aq} in the winter was exactly equal to the total heat injected back to the aquifer in the summer. The system COP of the summer model was higher than the winter model for k_t = 0.46 W/m K, but the COP went down when k_t was 1.89 W/m K. The COP of the summer model decreased due to more heat recovery from waste water (due to higher k_t) which increased the secondary water pump work significantly.

Comparison of WWSHP + ATES with WWSHP system

When the system performance (kWh/€) of the WWSHP + ATES system was compared with that of the WWSHP system, it was clear that the WWSHP system always performed better in winter. In the summer, for lower thermal conductivity (k_t = 0.46 W/m K) of the polymer tubes, the WWSHP + ATES system performed better. This was due to the fact that the condenser in the WWSHP + ATES system was designed to reject more heat to ensure complete refilling of the warm well of the aquifer and hence the low thermal conductivity of the polymer tubes was compensated. Table 31 and Table 32 provide a comparison between the systems proposed.

Table 31: Comparison of WWSHP and WWSHP + ATES system for winter

Parameter	k_t = 0.46 W/m K			k_t = 1.89 W/m K		
	WWSHP	**WWSHP + ATES**	Δ	**WWSHP**	**WWSHP + ATES**	Δ
Q_{cond} (MWh)	486	1244	+ 758	650	1280	+ 630
HEX cost (€)	1037	12937	+11900	1037	12937	+11900
Electricity cost (€)	6388	23474	+17086	10698	26263	+12565
kWh/€	65.6	34.2	-31.4	55.4	32.7	-22.7

Table 32: Comparison of WWSHP and WWSHP + ATES system for summer

Parameter	k_t = 0.46 W/m K			k_t = 1.89 W/m K		
	WWSHP	**WWSHP + ATES**	Δ	**WWSHP**	**WWSHP + ATES**	Δ
Q_{evap} (MWh)	23	368	+345	27	318	+291
HEX cost (€)	1037	12937	+11900	1037	12937	+11900
Electricity cost (€)	152	2028	+1876	203	9227	+9024
kWh/€	19.3	24.6	-5.3	21.8	14.3	-7.5

In the winter, recovering heat from the aquifer increased the amount of heat supplied to 'Doelen' by a significant amount (759 MWh and 630 MWh) for both of k_t = 0.46 and 1.89 W/m K. Similar effect was seen in summer where the heat removed from 'Doelen' increased by 345 MWh and and 291 MWh for k_t = 0.46 and 1.89 W/m K respectively. WWSHP + ATES system performed better without the thermal enhancement of the tubes of the waste water heat exchanger. WWSHP system performed better with thermally enhanced tubes in the summer.

4 Conclusions and Recommendations

4.1 Conclusions

- **Optimized tube dimensions of the waste water heat exchanger**

  The optimized dimensions of the HDPE tubes were found to be l_t = 30 m and $d_{i,t}$ = 29 mm. Since the sewage level in 2018 was close to 0.1 m throughout the year, the required ΔT of the secondary water stream could only be achieved with a tube length of 30 m. It was seen that the difference between the required heat recovery from the sewage and actual heat recovery was the lowest for the tubes with l_t = 30 m and $d_{i,t}$ = 29 mm (Figure 44). The performance of the WWSHP system was actually found to be better with l_t = 12 m and $d_{i,t}$ = 29 mm tubes, but the necessary heat was not recovered from the sewage. Thus, for sewage channels with higher sewage level, smaller tube lengths of waste water heat exchanger might be a better option.

- **Best choice of polymer for the waste water heat exchanger tubes**

  HDPE with a thermal conductivity of value of 0.46 W/m K and price of 0.54 €/kg was found to be the best choice for the material of the waste water heat exchanger. The waste water source heat pump system delivered about 65 kWh of heat per € to the 'Doelen' in the winter and removed 19 kWh of heat per € from the 'Doelen' in the summer when HDPE tubes without any thermal enhancement were used.

- **Effect of tube thickness on heat recovery from waste water**

  Polymers with higher yield strength can withstand the operating pressure with thin tube walls. Thinner tube walls lead to better U_o values. Thus, it was seen that WWSHP system with PS that has low thermal conductivity (k_t = 0.14 W/m K) delivered 69 kWh/€ while WWSHP system with HDPE that has higher thermal conductivity (k_t = 0.46 W/m K) recovered 62 kWh/€. Thus reducing the thickness of the polymer tubes has significant effect on system performance.

- **Best polymer and filler combination**

  PE with 10% graphite filler was found to be the best polymer and filler combination based on the amount of heat exchanged with sewage per unit cost. For more heat recovery, PE with 30% was a better choice. The thermal conductivity of PE increased to 1.8 W/m K when it was filled with 30% graphite. This enhancement resulted in much higher heat recovery from sewage. With 30% graphite filler, the waste water heat exchanger recovered 495 MWh from the sewage in the winter as opposed to the 374 MWh recovered by the HDPE tubes without any enhancement. Thus the heat recovered from sewage increased by 121 MWh upon thermal enhancement, indicating enormous potential.

- **WWSHP system performance**

  In the winter, the WWSHP system delivered 66 kWh/€ to the 'Doelen' when the waste water heat exchanger had HDPE tubes with no fillers and the total heat delivered to the 'Doelen' was 486 MWh. The total heat delivered to the 'Doelen' increased to 650 MWh when k_t was increased to 1.89 W/m K. The increase in heat recovery also led to increase in power consumption, thus the system performance reduced to 55 kWh/€.

  In the summer, the WWSHP system removed 23 MWh of heat from the 'Doelen', and the performance factor was 19 kWh/€. Upon using tubes with k_t = 1.89 W/m K in the waste water heat exchanger, the heat removed from the 'Doelen' went up to 27 MWh, but it was at 22 kWh/€. The heat rejected to sewage in the summer increased from 26 MWh to 30 MWh upon thermal enhancement, which was not as significant as the winter case. The seasonal COP of the system was higher in the summer (6.9 - 7.3) than in the winter (3.1 - 3.9).

- **WWSHP + ATES system performance**

  Due to recovery of heat from the aquifer and the waste water, the total heat supplied to the 'Doelen' in the winter went up to 1244 MWh in the WWSHP + ATES system. But this heat was more expensive as the system only delivered 34 kWh/€. The cost of electricity and the cost heat exchangers were also higher in this case. Increase in k_t to 1.89 W/m K, did not affect the heat recovery significantly as the temperature rise across the waste water heat exchanger was fixed and the mass flow of secondary water was dictated by the amount of heat extracted from the ATES. The system delivered 1280 MWh to the 'Doelen' in the winter upon thermal enhancement at the rate of 33 kWh/€. Thus, thermal enhancement was not that beneficial for the winter model of the WWSHP + ATES system.

  In the summer, the thermal enhancement of the polymer tubes of the waste water heat exchanger resulted in an increase in the heat recovered from sewage from 65 MWh to 130 MWh. But this reduced the system performance from 25 kWh/€ to 14 kWh/€. When more heat was recovered from the waste water heat exchanger, the secondary water pump work increased significantly. Recovering more heat from the condenser of the heat pump not only increased the cooling effect in the 'Doelen', but also costed lesser electricity due to a small temperature lift across the compressor of the heat pump. Thus, the performance of the WWSHP + ATES system was better with waste water heat exchanger that had HDPE tubes with no thermal enhancement in both the summer and the winter.

  The economic performance factor (kWh/€) for the WWSHP system with normal HDPE tubes was 66 kWh/€ in the winter and 19 kWh/€ in the summer. For the WWSHP + ATES system, the performance factor was 34 kWh/€ in the winter and 25 kWh/€ in the summer. Thus, use of WWSHP + ATES system would be justified only if large amount heating and cooling loads are to be handled by the system. The WWSHP + ATES system consists of an additional ground water heat exchanger and a ground water pump. All these equipment add to the system complexity and costs. Thus, only if the ATES system is already being used for the heating and cooling of nearby buildings or or a different part of the 'Doelen', integrating that system with waste water source heat pump system would be advisable.

4.2 Recommendations

- The waste water source heat pump model can be extended based on predictive models to optimize heat recovery for any sewage channel dimensions, sewage flows and temperatures.

- Effect on system performance and system economics if direct and indirect waste water heat exchangers are used can be quantitatively studied. (See Page 11 for definition)

- Experimental studies can be performed to determine the effect of using different types of fillers and their orientation on the thermal conductivity of polymers.

Appendices

A Dimensions of channel and tubes

A.1 Sewage channel dimensions

Calculations of sewage channel dimensions are provided in this section. Refer to Figure 19 for the labelling of the dimensions.

- **Slant height of the channel**

  The slant height of the channel was calculated from the dimensions, l_5 and l_1 and the known angle between the horizontal and the slant edges (30°).

$$l_2 = l_3 = \frac{l_5 - l_1}{2 \cdot cos\ \ 30^\circ} = 0.58\ \ \text{m} \tag{58}$$

- **Height of the trapezoidal part of the channel**

  The height of the trapezoidal part of the channel was found out by using the slant height l_2 and the angle that the slant edge makes with the horizontal (30°).

$$l_4 = l_2 \times sin\ \ 30^\circ = 0.29\ \ \text{m} \tag{59}$$

- **Height of the rectangular part of the channel**

  When sewage level, lev_{ww} 0.5 m,

$$l_6 = l_7 = 0.5 - l_4 = 0.21\ \ \text{m} \tag{60}$$

  When sewage level is, $0.29\ \ \text{m} < lev_{\text{ww}} > 0.5\ \ \text{m}$,

$$l_6 = l_7 = lev_{\text{ww}} - l_4 \tag{61}$$

  When the sewage level is less than $l_4 = 0.29$ m, there would be no rectangular part. There would only be a trapezoidal part whose height l_2, l_3 and top side l_5 would be functions of the sewage level. In that case, l_5 is calculated by linearizing the increase in l_5 from 0.5 m at lev_{ww} = 0 to $l_5 = 1.5$ m at lev_{ww} = 0.29 m,

$$l_5 = \frac{1.5 + 0.5 \times \dfrac{0.29 - lev_{\text{ww}}}{lev_{\text{ww}}}}{1 + \dfrac{0.29 - lev_{\text{ww}}}{lev_{\text{ww}}}} \tag{62}$$

  From l_5, slant heights l_2, l_3 and vertical height l_4 are calculated as shown in Equation 58 and Equation 59.

- **Perimeter of the channel in flow area**

$$P_{\text{tot,ch}} = l_1 + l_2 + l_3 + l_6 + l_7 + l_5 \tag{63}$$

- **Perimeter of the channel available for heat exchangers**

$$P_{\text{ch}} = l_1 + l_2 + l_3 + l_6 + l_7 \tag{64}$$

- **Cross sectional area of flow in the channel**

$$A_{\text{c,ch}} = \frac{1}{2} \times (l_2 + l_3) \times l_4 \;\; + \;\; (l_6 \times l_5) \tag{65}$$

Note : If $lev_{\text{ww}} < 0.29$ m, $l_6 = l_7 = 0$ and $l_4 = lev_{\text{ww}}$ and l_5, l_2 and l_3 are functions of lev_{ww} as described above (Equation 62).

- **Hydraulic diameter of the channel**

$$d_{\text{hyd,ch}} = \frac{4 \times A_{\text{c,ch}}}{P_{\text{tot,ch}}} \tag{66}$$

- **Hydraulic radius of the channel**

$$r_{\text{hyd,ch}} = \frac{A_{\text{c,ch}}}{P_{\text{tot,ch}}} \tag{67}$$

A.2 Heat exchanger tube dimensions

Based on the chosen internal diameter ($d_{\text{i,t}}$) and length (l_{t}) of polymer tubes, the following tube dimensions were calculated.

- **Outer diameter of the tubes, $d_{\text{o,t}}$**

$$d_{\text{o,t}} = d_{\text{i,t}} + 2 \times thk_{\text{t}} \tag{68}$$

where, thk_{t} is tube thickness.

- **Hydraulic diameter of the tubes, $d_{\text{hyd,t}}$**

$$d_{\text{hyd,t}} = d_{\text{i,t}} \tag{69}$$

- **Cross-sectional area of each tube, $A_{\text{c,t}}$**

$$A_{\text{c,t}} = \frac{\pi \times {d_{\text{i,t}}}^2}{4} \tag{70}$$

- **Surface area of tubes available for heat transfer, $A_{\text{s,t}}$**

Since the tubes of the heat exchanger were considered to be placed on the sewage channel, it was approximated that about 50% of the total surface area of the tubes would be available for heat transfer. Thus, the area of tubes available for heat transfer was calculated by multiplying the total surface area by a factor of 0.5.

$$A_{\text{s,t}} = 0.5 \times \pi \times d_{\text{o,t}} \times l_{\text{t}} \tag{71}$$

- **Pitch of tube arrangement, w_{t}**

To accommodate more tubes and enhance heat exchange area, the pitch of tube arrangement was chosen to be equal to the outer diameter of the tube.

$$w_{\text{t}} = d_{\text{o,t}} \tag{72}$$

- **Required tube thickness**

  The thickness of the tube (thk_{t}) required to withstand the operating pressure p (with a safety factor of 1.5) and allowable stress σ (YTS) was calculated as follows.

$$thk_{\mathrm{t}} = \frac{p \times d_{\mathrm{o,t}}}{2 \times \sigma} \tag{73}$$

- **Weight of tubes**

  Total weight of all the tubes was calculated as,

$$Weight_{\mathrm{t}} = \pi \times \frac{({d_{\mathrm{o,t}}}^2 - {d_{\mathrm{i,t}}}^2)}{4} \times l_{\mathrm{t}} \times N_{\mathrm{t}} \times \rho_{\mathrm{t}} \tag{74}$$

- **Cost of heat exchanger**

  It was assumed that the cost of heat exchanger would be 3 times the cost of the polymer based on general heat exchanger cost estimations. The cost of polymer ($rate_{\mathrm{poly}}$) was available in per kg basis.

$$Cost_{\mathrm{hex}} = 3 \times Weight_{\mathrm{t}} \times rate_{\mathrm{poly}} \tag{75}$$

B Polymer and Secondary water properties

B.1 Polymer properties

Table 33: Mechanical and thermal properties of polymers (T'Joen et al., 2009)

Properties	HDPE	PPS	LDPE	PC	PS
k, W/m K	**0.46**	**0.3**	**0.3**	**0.2**	**0.14**
Cost (€/kg)	**0.54**	**1.60**	**0.57**	**1.1**	**0.90**
YTS, MPa	**25.9**	**68.9**	**10.8**	**62**	**43.9**
ρ (kg/m^3)	957	1290	923	1260	1050
c_p, J/kg K	1900	-	2200	1200	2100

Note : Prices of polymers are as of February 2019 and were obtained from [5]. Properties of some polymers were obtained from [6].

B.2 Secondary water property coefficients

Table 34 provides values of coefficients ($C_{i,j}$) required to calculate the properties of ethylene glycol mixture at different temperatures. For each property, ρ, c_p, k and μ, values of coefficients $C_{0,0}$, $C_{0,1}$, $C_{0,2}$....$C_{i,j}$ are given in the respective rows marked with values of i and j. Equation 25 was used to find property values at different secondary water temperatures.

Table 34: Values of coefficients for ethylene glycol property calculation (Melinder, 2010)

i	j	ρ	c_p	k	μ
0	0	$1.04\times10^{+3}$	$3.64\times10^{+3}$	4.46×10^{-1}	6.16×10^{-1}
0	1	-5.16×10^{-1}	$3.80\times10^{+0}$	7.97×10^{-4}	-2.61×10^{-2}
0	2	-2.35×10^{-3}	-7.69×10^{-3}	-1.63×10^{-7}	1.89×10^{-4}
0	3	4.59×10^{-6}	-4.94×10^{-5}	-3.00×10^{-9}	-9.16×10^{-7}
1	0	$-1.40\times10^{+0}$	$2.26\times10^{+1}$	4.26×10^{-3}	-2.36×10^{-2}
1	1	6.15×10^{-3}	-1.21×10^{-1}	1.35×10^{-5}	1.16×10^{-4}
1	2	-3.75×10^{-5}	1.89×10^{-4}	-8.94×10^{-8}	-1.06×10^{-6}
1	3	5.28×10^{-8}	7.31×10^{-7}	1.53×10^{-10}	1.69×10^{-8}
2	0	-1.58×10^{-2}	1.17×10^{-1}	8.07×10^{-5}	-3.63×10^{-4}
2	1	1.90×10^{-4}	-2.68×10^{-3}	3.34×10^{-7}	2.27×10^{-6}
2	2	-1.99×10^{-6}	2.25×10^{-5}	-9.48×10^{-9}	-3.21×10^{-8}
2	3	7.56×10^{-9}	-3.11×10^{-9}	3.79×10^{-12}	-4.01×10^{-10}
3	0	-4.47×10^{-5}	-1.22×10^{-2}	1.92×10^{-6}	-2.61×10^{-5}
3	1	3.51×10^{-6}	-3.56×10^{-5}	2.01×10^{-8}	1.15×10^{-7}
3	2	-4.17×10^{-8}	7.86×10^{-7}	-2.19×10^{-10}	-1.27×10^{-9}
4	0	-3.72×10^{-5}	3.05×10^{-4}	1.16×10^{-7}	-2.54×10^{-7}
4	1	-1.02×10^{-8}	-8.15×10^{-8}	4.04×10^{-10}	3.51×10^{-9}
5	0	-1.19×10^{-6}	1.93×10^{-5}	2.83×10^{-9}	1.14×10^{-8}

[5] New Media Publisher
[6] MatWeb

C Convective heat transfer coefficient

The convective heat transfer coefficients on sewage side and secondary water side were calculated using the same correlation, approximating flow through the closed sewage channel to be flow through tubes. The following expressions were taken from Towler and Sinnott (2013)

- **Reynolds number**

$$Re = \frac{\rho \cdot v \cdot d_{\text{hyd}}}{\mu} \tag{76}$$

- **Prandtl number**

$$Pr = \frac{\mu \cdot c_p}{k} \tag{77}$$

- **Friction factor**

  For turbulent flow ($4 \times 10^4 < Re < 10^6$) Petuchov's formula was used to calculate the friction factor

$$f = (0.79 \cdot \log(Re) - 1.64)^{-2} \tag{78}$$

  For laminar flow the following expression was used to evaluate the friction factor,

$$f = 64/Re \tag{79}$$

- **Nusselt number**

  To calculate the Nusselt number for turbulent flow ($3000 < Re < 10^6$) Gnielinski's correlation was used for more accuracy.

$$Nu = \frac{(f/8) \cdot (Re - 1000) \cdot Pr}{1 + 12.7 \cdot (f/8)^{1/2} \cdot (Pr^{2/3} - 1)} \tag{80}$$

  For laminar flow ($Re_{\text{ww}} \leq 2300$), Nusselt number was calculated using the following correlation.

$$Nu = 3.66 + \frac{0.065 \cdot (d_{\text{hyd}}/l) \cdot Re \cdot Pr}{1 + 0.04 \cdot [(d_{\text{hyd}}/l)^{1/2} \cdot Re \cdot Pr]^{2/3}} \tag{81}$$

  Convective heat transfer coefficient

  The convective heat transfer coefficient on the sewage side was calculated as,

$$\alpha = \frac{Nu \cdot k}{d_{\text{hyd}}} \tag{82}$$

D Heat pump calculations

The equations used for the calculations of the heat pump system are provided in this section. The different heat pump models used in WWSHP and WWSHP + ATES systems are described. Refer to Figure 76 for the nodes referred to in the explanation. Modeling of the heat pump was different in the summer and winter.

D.1 Winter model

- **Condensation temperature and pressure**

  The condensation temperature (T_{cond}) was set at 55°C in the winter model, and the corresponding condensation pressure (p_{cond}) was found at saturated vapor condition of quality = 1.

- **Evaporation temperature and pressure**

  The evaporation temperature (T_{evap}) was set 2 K lower than the secondary water outlet temperature ($T_{\text{sw,in}}$ in waste water heat exchanger) in the evaporator. The evaporation pressure (p_{evap}) was calculated at saturated vapor condition of quality = 1.

- **Condenser outlet, expansion valve inlet - Node 3**

  Water from the heating network entered the condenser at 25°C, and temperature of the refrigerant at the exit of the condenser (T_3) was set 5 K higher than water. Thus, $T_3 = 30°\text{C}$. Enthalpy at the exit of the condenser, (h_3) was calculated at p_{cond} and T_3. This enthalpy corresponds to sub-cooled state. At the point of saturation, enthalpy $h_{3,\text{sat}}$ was calculated at T_{cond} and quality = 0.

- **Expansion valve outlet, evaporator inlet - Node 4**

  As the expansion valve is isenthalpic, the enthalpy at the inlet of the evaporator h_4 is equal to the enthalpy at the exit of the condenser. Thus, $h_4 = h_3$.

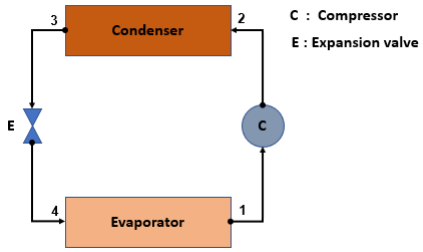

Figure 76: Heat pump model

- **Evaporator outlet, compressor inlet - Node 1**

  Enthalpy (h_1) and entropy (s_1) at the outlet of the evaporator were calculated at T_{evap} and quality = 1.

- **Compressor outlet, condenser inlet - Node 2**

  - **Entropy - s_2**
    Ideal entropy at the outlet of the compressor, $s_2 = s_1$
  - **Enthalpy - h_2**
    To calculate h_2, the isentropic enthalpy ($h_{2,\text{is}}$) was calculated first. $h_{2,\text{is}}$ was calculated based on condenser pressure (p_{cond}) and entropy (s_2). Then, h_2 was calculated based on isentropic efficiency (η_{is}) as follows,

$$h_2 = h_1 + \frac{(h_{2,\text{is}} - h_1)}{\eta_{\text{is}}} \tag{83}$$

For the calculations, $\eta_{\text{is}} = 0.7$

- **Enthalpy - $h_{2,\text{sat}}$**
  The enthalpy of refrigerant in the condenser at vapor saturation point was calculated at T_{cond} and quality = 1.
- **Mass flow of refrigerant, $\dot{m}_{\text{r}}$**
  Mass flow of the refrigerant was calculated from the difference in enthalpy across the evaporator. The actual heat recovered from sewage ($\dot{Q}_{\text{ww}}$) was equal to the evaporator duty ($\dot{Q}_{\text{evap}}$).

$$\dot{m}_{\text{ref}} = \frac{\dot{Q}_{\text{evap}}}{(h_1 - h_4)} \tag{84}$$

- **Power consumption of the compressor, $\dot{P}_{\text{comp}}$**
  Power required by the compressor to upgrade heat from low to high temperature was calculated from the enthalpy difference across the compressor and the mass flow of the refrigerant.

$$\dot{W}_{\text{comp}} = \dot{m}_{\text{ref}} \times (h_2 - h_1) \tag{85}$$

- **Condenser duty or the heat supplied to the building, $\dot{Q}_{\text{cond}}$**

  The heat supplied to the building was calculated from the enthalpy difference across the condenser as in Equation 86.

$$\dot{Q}_{\text{cond}} = \dot{m}_{\text{ref}} \times (h_2 - h_3) \tag{86}$$

- **Temperature of water at the outlet of condenser**

  Hot water to be produced for the heating network of 'Doelen' entered the condenser at 25 °C. At this point the refrigerant temperature was set at $T_3 = 30$ °C. The increase in temperature of water was linear from 25°C to 51.5°C. Decrease in temperature of the refrigerant occurred in three stages, in the first stage it was linear from 64°C to 55°C. In the second stage, which was in the two-phase state, the temperature was constant at 55°C. In the last stage, the temperature decreased linearly from 55°C to 30°C. The pinch point was identified at the point of $T_{\text{cond}} = 55$°C and quality = 1. At this point the temperature of the water was set as 50°C, thus ensuring a pinch of 5 K. The mass flow of water '$\dot{m}_{\text{w}}$' required in the condenser was calculated based on the heat required to raise the temperature of water from 25°C to 50°C. From the pinch point setting it was clear that the point where the temperature of water was 50°C, the enthalpy of refrigerant was $h_{2,\text{sat}}$ and at the inlet point of water ($T_{\text{w,in}}$ = 25°C), the enthalpy of refrigerant is h_3. Thus, using these points $\dot{m}_{\text{w}}$ was calculated as follows,

$$\dot{m}_{\text{w}} = \frac{\dot{m}_{\text{ref}} \times (h_{2,\text{sat}} - h_3)}{c_{p,\text{w}} \times (50 - 25)} \tag{87}$$

D.2 Summer model

In the summer, the heat pump was operated in reverse. The property calculation at various points is described below.

- **Condensation temperature and pressure**
  At (T_{cond}) and quality = 1, p_{cond} was calculated.

- **Evaporation temperature and pressure**

  The evaporation temperature (T_{evap}) was set as 8°C. The evaporation pressure (p_{evap}) was calculated at quality, quality = 1.

- **Evaporator outlet, compressor inlet - Node 1**

  Enthalpy (h_1) and entropy (s_1) at the outlet of the evaporator were calculated at T_{evap} and quality = 1.

- **Compressor outlet, condenser inlet - Node 2**

  - **Entropy - s_2**

    Ideal entropy at compressor outlet, $s_2 = s_1$

  - **Enthalpy - h_2**

    To calculate h_2, the isentropic enthalpy ($h_{2,\text{is}}$) was calculated based on condenser pressure (p_{cond}) and entropy (s_2). h_2 was calculated as in Equation 83.

  - **Condenser outlet, expansion valve inlet - Node 3**

    Condenser outlet enthalpy (h_3) was evaluated at T_{cond} and quality = 0.

  - **Expansion valve outlet, evaporator inlet - Node 4**

    Due to isenthalpic expansion in the expansion valve, enthalpy at the inlet of the evaporator $h_4 = h_3$.

  - **Mass flow of refrigerant, $\dot{m}_{\text{ref}}$**

    Mass flow of the refrigerant was calculated from the difference in enthalpy across the condenser and the total heat rejected to the sewage. As explained before, the actual heat rejected to sewage ($\dot{Q}_{\text{ww}}$) was considered to be equal to ($\dot{Q}_{\text{cond}}$).

$$\dot{m}_{\text{ref}} = \frac{\dot{Q}_{\text{cond}}}{(h_2 - h_3)} \tag{88}$$

  - **Power required by the compressor, $\dot{W}_{\text{comp}}$**

    Power required by the compressor to upgrade heat from low to high temperature was calculated from the enthalpy difference across the compressor

$$\dot{W}_{\text{comp}} = \dot{m}_{\text{ref}} \times (h_2 - h_1) \tag{89}$$

  - **Evaporator duty or the heat removed from the building, $\dot{Q}_{\text{evap}}$**

    The heat removed from the building was calculated from the enthalpy difference across the condenser as in Equation 90.

$$\dot{Q}_{\text{evap}} = \dot{m}_{\text{ref}} \times (h_1 - h_4) \tag{90}$$

E Additional Results

In this part of the appendix, all the additional graphs and results are provided for better understanding.

E.1 WWSHP system

– **Pump and compressor power required**
It can be seen from Figure 77 and Figure 78 that compressor power was much higher than pump power on most days, indicating that COP of the system was more dependent on compressor than on the secondary water pump.

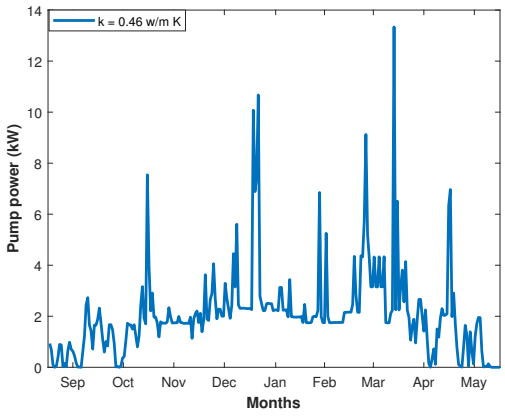

Figure 77: WWSHP Winter model : Sec. water pump power

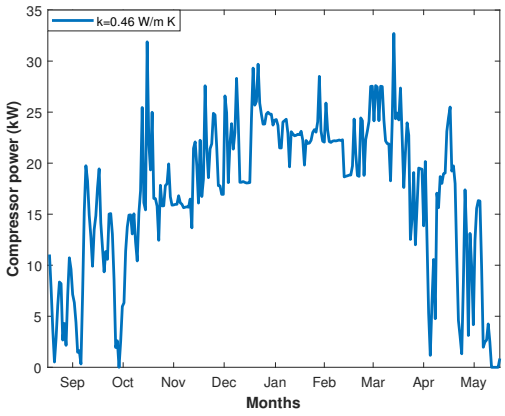

Figure 78: WWSHP Winter model : Compressor power

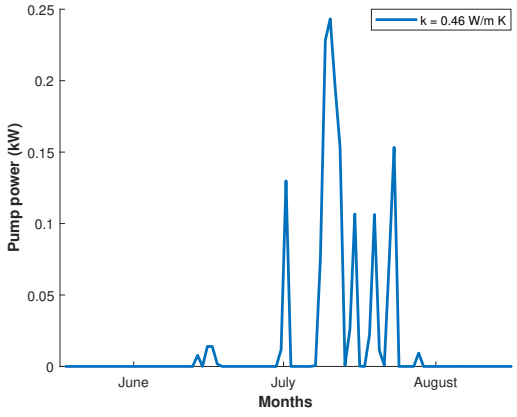

Figure 79: WWSHP Summer model : Sec. water pump power

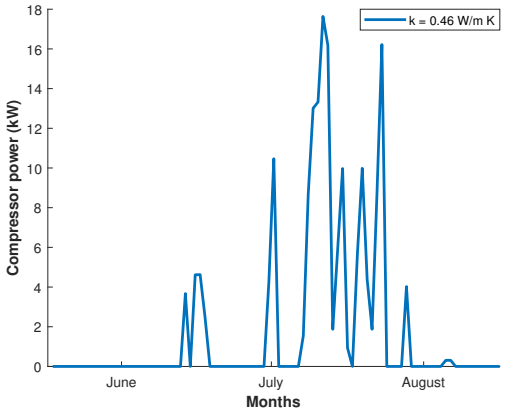

Figure 80: WWSHP Summer model : Compressor power

– **Increase in pump and compressor power due to thermal enhancement of polymer**
It can be seen that higher heat recovery necessitates the requirement of more pump and compressor power as in Figure 81 and Figure 82.

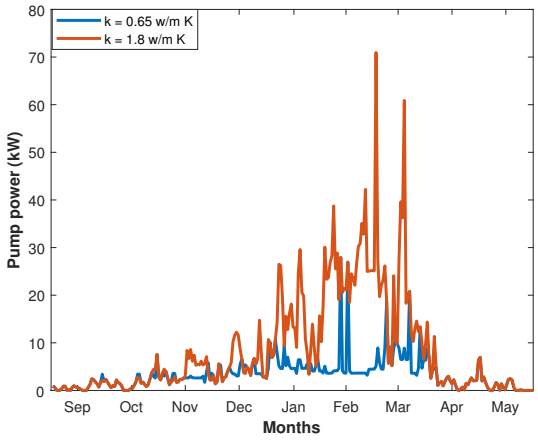

Figure 81: WWSHP Winter model : Increase in sec. water pump power due to increase in k_t of PE

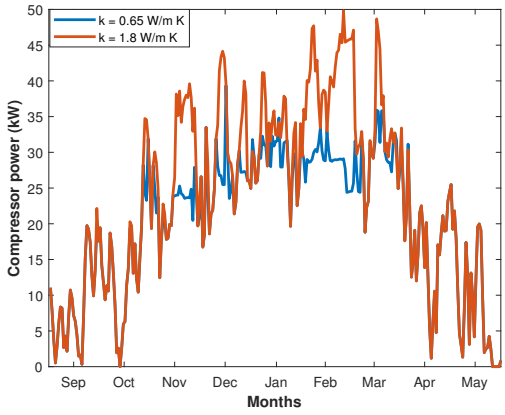

Figure 82: WWSHP Winter model : Increase in compressor power due to increase in k_t of PE

– **Increase in secondary water mass flow due thermal enhancement**
Increase in thermal conductivity of the polymer tubes enabled more heat recovery which in turn resulted in higher secondary water mass flow. This can be seen in Figure 83.

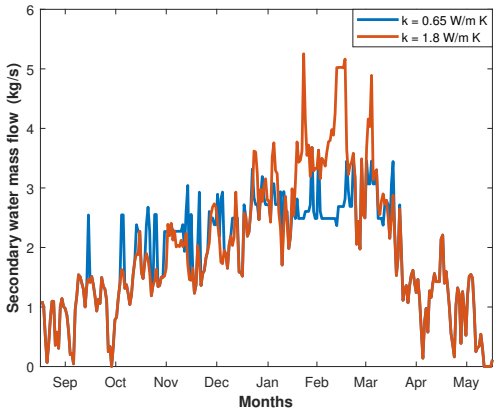

Figure 83: WWSHP Winter model : Effect of thermal enhancement of PE with Graphite on secondary water mass flow

E.2 Design and cost estimation of plate heat exchangers

The plate heat exchangers required for the evaporator, condenser and the ground water heat exchanger were designed in accordance with the design principles provided in Chapter 19 of Towler and Sinnott (2013). The design is not explained in detail, but the parameters used for the design are provided in Table 35 and Table 37. Results of the design such as plate size, pressure drop and cost are provided in Table 36 and Table 38. The cost estimation procedure is described in E.3.

Table 35: Input parameters for the design of maximum capacity plate HEX of the WWSHP model

Condenser				Evaporator			
Data	k_t = 0.46	k_t = 1.89	Unit	Data	k_t = 0.46	k_t = 1.89	Unit
$\dot{Q}$	132	201	kW	$\dot{Q}$	100	152	kW
$T_{w,in}$	25	25	°C	$T_{sw,in}$	12	12	°C
$T_{w,out}$	53	53	°C	$T_{sw,out}$	2	2	°C
$T_{ref,in}$	64	64	°C	$T_{ref,in}$	0	0	°C
$T_{ref,out}$	30	30	°C	$T_{ref,out}$	0	0	°C
$\dot{m}_w$	1.1	1.7	kg/s	$\dot{m}_{sw}$	2.8	4.3	kg/s
$\dot{m}_{ref}$	0.3	0.5	kg/s	$\dot{m}_{ref}$	0.3	0.5	kg/s

Table 36: Plate HEX designed for the maximum capacity requirements of the WWSHP model

Condenser			Evaporator		
Data	k_t = 0.46	k_t = 1.89	Data	k_t = 0.46	k_t = 1.89
Plate length	192 mm	300 mm	Plate length	335 mm	593 mm
Plate width	64 mm	100 mm	Plate width	112 mm	198 mm
Δp_w	913 Pa	1.6 kPa	Δp_{sw}	3.6 kPa	4.9 kPa
Δp_{ref}	0.33 Pa	0.88 Pa	Δp_{ref}	≈0 Pa	≈0 Pa
No. of plates	30	30	No. of plates	30	30
Cost	1500 €	1830 €	Cost	1883 €	2438 €

Table 37: Input parameters for the design of maximum capacity plate HEX of the WWSHP+ATES model

Condenser				Evaporator				Ground water HEX			
Data	k_t = 0.46	k_t = 1.89	Unit	Data	k_t = 0.46	k_t = 1.89	Unit	Data	k_t = 0.46	k_t = 1.89	Unit
$\dot{Q}$	376	424	kW	$\dot{Q}$	284	319	kW	$\dot{Q}$	145	145	kW
$T_{w,in}$	25	25	°C	$T_{sw,in}$	14	14	°C	$T_{sw,in}$	7	7	°C
$T_{w,out}$	53	53	°C	$T_{sw,out}$	0	0	°C	$T_{sw,out}$	14	14	°C
$T_{ref,in}$	64	64	°C	$T_{ref,in}$	-2	-2	°C	$T_{gw,in}$	16	16	°C
$T_{ref,out}$	30	30	°C	$T_{ref,out}$	-2	-2	°C	$T_{gw,out}$	8	8	°C
$\dot{m}_w$	3.2	3.6	kg/s	$\dot{m}_{sw}$	5.5	7.2	kg/s	$\dot{m}_{sw}$	5.5	5.5	kg/s
$\dot{m}_{ref}$	1	1.1	kg/s	$\dot{m}_{ref}$	1	1.1	kg/s	$\dot{m}_{gw}$	4.3	4.3	kg/s

Table 38: Plate HEX designed for the maximum capacity requirements of the WWSHP + ATES model

Condenser			Evaporator			Ground water HEX		
Data	k_t = 0.46	k_t = 1.89	Data	k_t = 0.46	k_t = 1.89	Data	k_t = 0.46	k_t = 1.89
Plate length	563 mm	820 mm	Plate length	985 mm	1104 mm	Plate length	1800 mm	1800 mm
Plate width	188 mm	273	Plate width	328 mm	368 mm	Width	600 mm	600 mm
Δp_w	2.5 kPa	2.3 kPa	Δp_{sw}	5.2 kPa	6.1 kPa	Δp_{sw}	1.1 kPa	1.1 kPa
Δp_{ref}	3.4 Pa	4 Pa	Δp_{ref}	0.1 Pa	0.2 Pa	Δp_{gw}	636 Pa	636 Pa
No. of plates	30	30	No. of plates	30	30	No. of plates	60	60
Cost	2360 €	3150 €	Cost	3797 €	4330 €	Cost	11900 €	11900 €

Note : The values of k_t mentioned in the tables above are all in W/m K.

E.3 Cost estimation

The capital cost estimation of different equipment was done using Equation 91. The equation, the estimation method and the values required for the estimation were all taken from Chapter 7 of Towler and Sinnott (2013).

$$Cost = 0.88 \times (L + M \times X^n) \tag{91}$$

- The values of L, M, and n for different equipment are provided in Table 39.
- X is the sizing factor that depends on the equipment. For a plate HEX X is the heat exchange area in m^2.
- The $Cost$ obtained from Equation 91 was in United States Dollars. The conversion factor from United States Dollar to Euro was taken to be 1 United States Dollar = 0.88 Euro.

Table 39: Parameters used for cost estimation of equipment (Towler and Sinnott, 2013)

Equipment	L	M	n
Plate HEX	1600	210	0.95

Table 40: Estimated costs of different heat exchangers of the WWSHP system

Equipment	k_t = 0.46	k_t = 1.89
	Cost (€)	
Evaporator	1883	2438
Condenser	1500	1830
Total	**3383**	**4268**

Table 41: Estimated costs of different heat exchangers of the WWSHP + ATES system

Equipment	k_t = 0.46	k_t = 1.89
	Cost (€)	
Evaporator	3797	4330
Condenser	2360	3150
Ground water HEX	11900	11900
Total	**18057**	**19380**

References

Basar Bozkaya, Rongling Li, Timilehin Labeodan, Rick Kramer, and Wim Zeiler. Development and evaluation of a building integrated aquifer thermal storage model. *Applied Thermal Engineering*, 126:620–629, 2017. doi: 10.1016/j.applthermaleng.2017.07.195.

F. W. Chapin, H. D. Chapin, and P. R. Armstrong. A waste water heat exchanger for laundromats-technical and behavioral considerations. *Journal of Heat Recovery Systems*, 4(2):93–100, 1984. doi: 10.1016/0198-7593(84)90013-4.

Xiangjie Chen, Yuehong Su, David Reay, and Saffa Riffat. Recent research developments in polymer heat exchangers - A review. *Renewable and Sustainable Energy Reviews*, 60:1367–1386, 2016. doi: 10.1016/j.rser.2016.03.024.

Sara Simona Cipolla and Marco Maglionico. Heat recovery from urban wastewater: Analysis of the variability of flow rate and temperature in the sewer of Bologna, Italy. In *Energy Procedia*, pages 288–297, 2014. doi: 10.1016/j.egypro.2014.01.031.

Oguzhan Culha, Huseyin Gunerhan, Emrah Biyik, Orhan Ekren, and Arif Hepbasli. Heat exchanger applications in wastewater source heat pumps for buildings: A key review. *Energy and Buildings*, 104:215–232, 2015. doi: 10.1016/j.enbuild.2015.07.013.

DINOloket. Subsurface models. URL https://www.dinoloket.nl/en/subsurface-models.

Jos Frijns, Jan Hofman, and Maarten Nederlof. The potential of (waste)water as energy carrier. *Energy Conversion and Management*, 65:357–363, 2013. doi: 10.1016/j.enconman.2012.08.023.

N. Funamizu, M. Iida, Y. Sakakura, and T. Takakuwa. Reuse of heat energy in wastewater: implementation examples in Japan. *Water Science and Technology*, 43(10):277–285, 2001. doi: 10.2166/wst.2001.0640. URL https://doi.org/10.2166/wst.2001.0640.

H. Ghaebi, M. N. Bahadori, and M. H. Saidi. Performance analysis and parametric study of thermal energy storage in an aquifer coupled with a heat pump and solar collectors, for a residential complex in Tehran, Iran. *Applied Thermal Engineering*, 62:156–170, 2014. doi: 10.1016/j.applthermaleng.2013.09.037.

Joost Greunsven and Maria Derks. Tennet - Annual Market Update. page 3, 2018. URL https://www.tennet.eu/fileadmin/user_upload/Company/Publications/Technical_Publications/Dutch/Annual_Market_Update_2018_-_Final.pdf.

Arif Hepbasli, Emrah Biyik, Orhan Ekren, Huseyin Gunerhan, and Mustafa Araz. A key review of wastewater source heat pump (WWSHP) systems. *Energy Conversion and Management*, 88:700–722, 2014. doi: 10.1016/j.enconman.2014.08.065.

Jan Hofman, Roberta Hofman-Caris, Maarten Nederlof, Jos Frijns, and Mark van Loosdrecht. Water and energy as inseparable twins for sustainable solutions. *Water science and technology*, 63(1):88–92, 2011. doi: 10.2166/wst.2011.013.

Afrin Roja Jahir Hussain, Abbas A. Alahyari, Scott A. Eastman, Catherine Thibaud-Erkey, Stephen Johnston, and Margaret J. Sobkowicz. Review of polymers for heat exchanger applications: Factors concerning thermal conductivity. *Applied Thermal Engineering*, 113:1118–1127, 2017. doi: 10.1016/j.applthermaleng.2016.11.041.

Jongchan Kim, Youngmin Lee, Woon Sang Yoon, Jae Soo Jeon, Min-Ho Koo, and Youngseuk Keehm. Numerical modeling of aquifer thermal energy storage system. *Energy*, 35(12):4955–4965, 12 2010. ISSN 0360-5442. doi: 10.1016/J.ENERGY.2010.08.029. URL https://www.sciencedirect.com/science/article/abs/pii/S0360544210004652.

Zhibin Liu, Liangdong Ma, and Jili Zhang. Application of a heat pump system using untreated urban sewage as a heat source. *Applied Thermal Engineering*, 62:747–757, 2013. doi: 10.1016/j.applthermaleng.2013.08.048.

MatWeb. The Online Materials Information Resource. URL http://www.matweb.com/search/datasheet.aspx?matguid=482765fad3b443169ec28fb6f9606660&ckck=1.

Ake Melinder. *Properties of secondary working fluids for indirect systems*. International Institute of Refrigeration, 2010. ISBN 978-91-7178-707-1.

M Menkveld and L.W.M Beurskens. *Renewable heating and cooling in the Netherlands*. 2009. ISBN ECN-B–09-013. URL https://publications.ecn.nl/ECN-B--09-013.

New Media Publisher. Raw Materials and Prices. URL https://plasticker.de/preise/preise_monat_single_en.php.

Kees Roest, Jan Hofman, and Mark van Loosdrecht. De Nederlandse watercyclus kan energie opleveren. *H2O*, 47(25/26):47–51, 2010.

Jan Spriet and P Hendrick. Wastewater as a Heat Source for Individual Residence Heating: A Techno-economic Feasibility Study in the Brussels Capital Region. *Journal of Sustainable Development of Energy, Water and Environment Systems*, 5:289–308, 2017. doi: 10.13044/j.sdewes.d5.0148.

C. T'Joen, Y. Park, Q. Wang, A. Sommers, X. Han, and A. Jacobi. A review on polymer heat exchangers for HVAC&R applications. *International Journal of Refrigeration*, 32:763–779, 2009. doi: 10.1016/j.ijrefrig.2008.11.008.

Gavin Towler and Ray K. Sinnott. *Chemical Engineering Design - Principles, Practice and Economics of Plant and Process Design (2nd Edition). Elsevier.* Elsevier, 2nd edition, 2013. URL https://app.knovel.com/hotlink/toc/id:kpCEDPPEP4/chemical-engineering/chemical-engineering.

Jan Peter Van Der Hoek, Heleen De Fooij, and André Struker. Wastewater as a resource: Strategies to recover resources from Amsterdam's wastewater. *Resources, Conservation and Recycling*, 113:53–64, 2016. doi: 10.1016/j.resconrec.2016.05.012.

Oskar Wanner, Vassileios Panagiotidis, Peter Clavadetscher, and Hansruedi Siegrist. Effect of heat recovery from raw wastewater on nitrification and nitrogen removal in activated sludge plants. *Water Research*, 39(19):4725–4734, 11 2005. doi: 10.1016/J.WATRES.2005.09.026. URL https://www.sciencedirect.com/science/article/abs/pii/S0043135405005403.

Liu Yang, Haiyan Yan, and Joseph C. Lam. Thermal comfort and building energy consumption implications - A review. *Applied Energy*, 115:164–173, 2014. doi: 10.1016/j.apenergy.2013.10.062.